CONVERGENCE ANALYSIS OF YEE-FDTD SCHEMES FOR 3D MAXWELL'S EQUATIONS IN LINEAR DISPERSIVE MEDIA

PUTTHA SAKKAPLANGKUL AND VRUSHALI A. BOKIL

Abstract. In this paper, we develop and analyze finite difference methods for the 3D Maxwell's equations in the time domain in three different types of linear dispersive media described as Debye, Lorentz and cold plasma. These methods are constructed by extending the Yee-Finite Difference Time Domain (FDTD) method to linear dispersive materials. We analyze the stability criterion for the FDTD schemes by using the energy method. Based on energy identities for the continuous models, we derive discrete energy estimates for the FDTD schemes for the three dispersive models. We also prove the convergence of the FDTD schemes with perfect electric conducting boundary conditions, which describes the second order accuracy of the methods in both time and space. The discrete divergence-free conditions of the FDTD schemes are studied. Lastly, numerical examples are given to demonstrate and confirm our results.

Key words. Maxwell's equations, Debye, Lorentz, cold plasma dispersive media, Yee scheme, FDTD method, energy decay, convergence analysis.

1. Introduction

The finite difference time domain (FDTD) method by Kane Yee [50] is a numerical technique for discretizing the time-dependent Maxwell's equations in computational electromagnetics and has been widely used in engineering, physics and computational mathematics [47, 50]. Electromagnetic wave propagation in a material is described by the three dimensional (3D) Maxwell's equations, modeling the evolution in space and time of the electric and magnetic fields, along with constitutive laws, relations between electric and magnetic fluxes and fields, that describe the response of the material to the propagating fields.

The FDTD method was first proposed for a linear dielectric (e.g., free space) by K. S. Yee [50] in 1966, and is also referred to as the (classical) Yee scheme or the Yee-FDTD method. The Yee scheme, as originally constructed, is an explicit scheme for the discretization of the 3D Maxwell's equations on structured staggered space-time grids. The staggered discretization results in a second order accurate method. The classical Yee scheme has been theoretically analyzed for stability and dispersion error [47], convergence analysis and error estimates [40, 41], and has been extended to discretize Maxwell's equations with constitutive laws describing electromagnetic wave propagation in a variety of materials [47].

In this paper, we focus on constitutive laws that do not include any magnetic effects, i.e. the magnetic constitutive law is the same as that in free space (linear dielectric). Previous work in this area includes extension of the Yee scheme to conductive media [47], linear dispersive media [4, 10, 14, 26, 27, 28, 38, 43] using constitutive laws that include models such as the Debye model for orientational polarization [16, 28], Lorentz model for electronic polarization [26, 42], cold plasma model [14, 51, 52] and the Cole-Cole [10, 13] model. In nonlinear optics, nonlinear dispersive models in 1D for the Kerr and Raman effects have been constructed and discretized within this FDTD approach [5, 20, 25]. There is a large literature

on the construction of Yee type FDTD schemes for other applications including in metamaterials [21, 34], micromagnetics [1, 45], plasmas [15, 39], among others. The classical Yee scheme for a linear dielectric, and many of its extensions, leads to a conditionally stable second order accurate scheme. The scheme may no longer be fully explicit for some constitutive laws, and other complications can arise [5]. In addition, there are extensions of the Yee schemes to higher than second order [5, 6] and to extensions on unstructured meshes [17].

One of the areas in which the Yee scheme has been relatively less studied is convergence analysis, while there are several papers on dispersion analysis of the Yee and Yee type schemes. In our recent work [7], we presented Yee schemes and their convergence analysis for the 2D Maxwell's equations in Debye and Lorentz (linear) dispersive media. The Yee scheme for both media was proved to be conditionally stable under the same stability condition as the classical Yee scheme. We proved that the proposed Yee scheme in both media is of second order convergent in time and space by the energy method.

In this paper, we extend the convergence of Yee schemes for linear dispersive media in two spatial dimensions to 3D. We consider three types of models for linear dispersive materials; the (single pole) Debye model for orientational polarization (Maxwell-Debye), the (single pole) Lorentz (Maxwell-Lorentz) and the isotropic cold plasma (Maxwell-Cold Plasma) model. We focus on the construction and analysis of the finite difference time domain methods based on the staggered Yee grids for 3D Maxwell's equations in these three linearly dispersive media. We show that our fully discrete schemes are conditionally stable via the energy method, and convergent with second order accuracy. Moreover, we use the energy technique to analyze the discrete divergence for the discrete Maxwell's equations in dispersive media. The energy method is a powerful method used on both the continuous PDEs and discrete finite difference methods by defining an energy associated with the solution and then showing that the energy is non-increasing. Recently, the energy technique has been applied for analyzing stability and convergence properties of the Yee scheme in various dispersive media, applied in operator splitting FDTD methods [8, 9, 11, 18, 49, 35, 36], finite element methods (FEM) and discontinuous Galerkin (DG) methods (for example see [22, 29, 30, 31, 32, 33, 37, 48] and references therein).

We present numerical experiments to illustrate our theoretical results by constructing exact solutions for Maxwell's equations in these linearly dispersive media: Debye, Lorentz and Cold plasma. We also investigate the discrete divergence properties of electric and magnetic flux densities for these dispersive media. Our analysis shows that the numerical divergence satisfies discrete versions of the continuous Gauss's laws for the 3D Maxwell's equations in dispersive media.

This paper is organized as follows. In Section 2, we present the 3D Maxwell's equations in three types of linearly dispersive media (Debye, Lorentz and isotropic cold plasma) and then present their corresponding weak formulations. In addition, we present energy decay results for these dispersive models that are available in the literature [7, 31]. Section 3 details the staggered discretization in space and time. The stability, discrete energy estimates and convergence analysis, including the analysis of the discrete divergence property are presented in Sections 4, 5 and 6. Numerical experiments demonstrating our theoretical results are presented in Section 7. We provide concluding remarks in Section 8.

2. Maxwell's Equations in Dispersive Dielectrics

Let $\Omega \subset \mathbb{R}^3$ be an open bounded domain. Let $T > 0$ be given. The time dependent three dimensional (3D) Maxwell's equations on $\Omega \times [0, T]$ in a charge and source free vacuum are a system of vector PDEs governing the evolution in space and time of the electric field $\mathbf{E}$ and the magnetic field $\mathbf{H}$, which are given as follows:

On $\Omega \times (0, T]$ we have

$$(1a) \qquad \frac{\partial \mathbf{B}}{\partial t} + \mathbf{curl}\ \mathbf{E} = \mathbf{0},$$

$$(1b) \qquad \frac{\partial \mathbf{D}}{\partial t} - \mathbf{curl}\ \mathbf{H} = \mathbf{0},$$

$$(1c) \qquad \mathbf{div}\ \mathbf{D} = \mathbf{0} = \mathbf{div}\ \mathbf{B},$$

along with initial conditions

$$(1d) \qquad \mathbf{D}(\mathbf{x}, 0) = \mathbf{D}_0(\mathbf{x});\ \mathbf{B}(\mathbf{x}, 0) = \mathbf{B}_0(\mathbf{x}),\ \text{on } \Omega$$

where $\mathbf{D}$ is the electric flux density, $\mathbf{B}$ is the magnetic flux density, $\mathbf{D}_0$ and $\mathbf{B}_0$ are initial conditions on the electric field and the magnetic field, respectively. All fields in (1) are 3D vector fields with components that are functions of position $\mathbf{x} = (x, y, z)^T \in \Omega$ and time $t \in [0, T]$, i.e., every vector field $\mathbf{V}(\mathbf{x}, t) := (V_x(\mathbf{x}, t), V_y(\mathbf{x}, t), V_z(\mathbf{x}, t))^T$. The 3D operators, **curl** and **div**, are vector curl and divergence operators respectively, operating on vector fields.

The boundary condition in this paper is assumed to be the perfect electric conductor (PEC) boundary condition given as

$$(2) \qquad \mathbf{n} \times \mathbf{E} = \mathbf{0},\ \text{on } \partial\Omega,$$

where the vector $\mathbf{n}$ is the outward unit normal vector to $\partial\Omega$.

Both the electric and magnetic flux densities are related to the electric and magnetic fields through the constitutive relations on $\Omega \times [0, T]$. The constitutive relations for a dispersive medium are given as

$$(3a) \qquad \mathbf{D} = \epsilon_0 \epsilon_\infty \mathbf{E} + \mathbf{P},$$

$$(3b) \qquad \mathbf{B} = \mu_0 \mathbf{H},$$

where ϵ_0 is the electric permittivity of free space, μ_0 is the magnetic permeability of free space, and $c_0 = 1/\sqrt{\epsilon_0 \mu_0}$ is the speed of light in vacuum. We note that the magnetic constitutive law is the same as that in vacuum; thus we neglect magnetic effects. The vector field $\mathbf{P}$ is the electric (macroscopic) polarization field, and ϵ_∞ is the permittivity at infinite frequency. The (linear, isotropic) vector polarization field $\mathbf{P}$ in the constitutive relation (3a) is defined as a convolution in time with the electric field given as

$$(4) \qquad \mathbf{P}(\mathbf{x}; t) = \int_0^t g(\mathbf{x}; t - s) \mathbf{E}(\mathbf{x}; s) ds,$$

where g is the linear susceptibility kernel (or the dielectric response function) of the dispersive medium [4, 7] which is a function of space and time. Equation (4) describes the non-instantaneous (delayed or retarded) response of the dispersive material [2]. The system of equations (1), (2), (3), and (4), fully describe the propagation of an electromagnetic field in a linear, isotropic, dispersive medium.

In this paper, we focus on three of the most common models for linear dispersive materials. These are, the Debye model for orientational polarization which describes relaxation processes and is used to model polar materials [16, 43, 16, 28]; the Lorentz

model [42] for electronic polarization which describes resonance phenomenon at the atomic level [43, 26, 42]; and the isotropic cold plasma model for the absorption and propagation of electromagnetic waves in non-magnetized materials [46, 44, 32]. Next, we describe these three models.

2.1. Maxwell-Debye Model and Energy Estimates. In this section, we consider the case of the single-pole Debye dispersive model for orientational polarization [28, 7, 53]. The linear susceptibility kernel g, defined in (4), takes on the form

$$(5) \qquad g(\mathbf{x}; t) = \frac{\epsilon_0 \epsilon_\infty (\epsilon_q - 1)}{\tau} e^{-t/\tau}, \ \mathbf{x} \in \Omega,$$

in which ϵ_s is the static relative permittivity and $\epsilon_q := \epsilon_s/\epsilon_\infty$ is the ratio of static to infinite permittivities. The parameter τ is the relaxation time of the medium. All parameters τ, ϵ_∞, and ϵ_s are assumed to be constant within the medium. We also have the physical conditions $\epsilon_s > \epsilon_\infty$, i.e., $\epsilon_q > 1$, and $\tau > 0$.

The time convolution in (4) for $\mathbf{P}$ with the susceptibility g given in (5) can be converted into an ordinary differential equation (ODE) for the time evolution of the polarization, given as

$$(6) \qquad \tau \frac{\partial \mathbf{P}}{\partial t} + \mathbf{P} = \epsilon_0 \epsilon_\infty (\epsilon_q - 1)\mathbf{E}.$$

Combining the ODE in (6) with Maxwell's equations (1) and the constitutive laws (3), we arrive at the 3D Maxwell-Debye model in the form of three first order vector differential equations:

3D Maxwell-Debye Model:

$$(7a) \qquad \frac{\partial \mathbf{H}}{\partial t} = -\frac{1}{\mu_0} \operatorname{\mathbf{curl}} \mathbf{E},$$

$$(7b) \qquad \frac{\partial \mathbf{E}}{\partial t} = \frac{1}{\epsilon_0 \epsilon_\infty} \operatorname{\mathbf{curl}} \mathbf{H} - \frac{(\epsilon_q - 1)}{\tau} \mathbf{E} + \frac{1}{\epsilon_0 \epsilon_\infty \tau} \mathbf{P},$$

$$(7c) \qquad \frac{\partial \mathbf{P}}{\partial t} = \frac{\epsilon_0 \epsilon_\infty (\epsilon_q - 1)}{\tau} \mathbf{E} - \frac{1}{\tau} \mathbf{P}.$$

We assume the PEC boundary condition (2) on $\partial\Omega$ and the initial conditions (1d), along with homogeneous initial conditions for the polarization, in the domain $\Omega \subset \mathbb{R}^3$.

To show that the system (7) is well-posed, we construct a weak formulation. We first define the following two functional spaces:

$$(8a) \qquad \mathbf{H}(\operatorname{\mathbf{curl}}, \Omega) = \{\mathbf{u} \in \left(L^2(\Omega)\right)^3 \mid \operatorname{\mathbf{curl}} \mathbf{u} \in \left(L^2(\Omega)\right)^3\},$$

$$(8b) \qquad \mathbf{H}_0(\operatorname{\mathbf{curl}}, \Omega) = \{\mathbf{u} \in \mathbf{H}(\operatorname{\mathbf{curl}}, \Omega) \mid \mathbf{n} \times \mathbf{u} = \mathbf{0} \text{ on } \partial\Omega\}.$$

Let $(\cdot, \cdot)$ denote the L^2 inner products and $\|\cdot\|_2$ denote the corresponding norm. The weak formulation for the 3D Maxwell-Debye system can be constructed as follows (see also [7]). Multiplying equation (7a), equation (7b), and equation (7c) by test functions $\mu_0 \mathbf{v} \in \left(L^2(\Omega)\right)^3$, $\epsilon_0 \epsilon_\infty \mathbf{u} \in \mathbf{H}_0(\operatorname{\mathbf{curl}}, \Omega)$, and $\frac{1}{\epsilon_0 \epsilon_\infty (\epsilon_q - 1)} \mathbf{w} \in \left(L^2(\Omega)\right)^3$, respectively, and then integrating over the domain $\Omega \subset \mathbb{R}^3$ and finally applying Green's formula for the **curl** operator

$$(9) \qquad (\operatorname{\mathbf{curl}} \mathbf{H}, \mathbf{u}) = (\mathbf{H}, \operatorname{\mathbf{curl}} \mathbf{u}), \ \forall \mathbf{u} \in \mathbf{H}_0(\operatorname{\mathbf{curl}}, \Omega),$$

the weak formulation for the 3D Maxwell-Debye system of equations (7) is:

3D Maxwell-Debye Variational Formulation: Find $\mathbf{E} \in C(0, T; \mathbf{H}_0(\mathbf{curl}, \Omega)) \cap C^1(0, T; (L^2(\Omega))^3)$, and $\mathbf{H}, \mathbf{P} \in C^1(0, T; (L^2(\Omega))^3)$ such that

(10a) $\qquad \left(\mu_0 \dfrac{\partial \mathbf{H}}{\partial t}, \mathbf{v} \right) = (-\mathbf{curl}\, \mathbf{E}, \mathbf{v}), \mathbf{v} \in (L^2(\Omega))^3,$

(10b) $\qquad \left(\epsilon_0 \epsilon_\infty \dfrac{\partial \mathbf{E}}{\partial t}, \mathbf{u} \right) = (\mathbf{H}, \mathbf{curl}\, \mathbf{u}) - \left(\dfrac{\epsilon_0 \epsilon_\infty (\epsilon_q - 1)}{\tau} \mathbf{E}, \mathbf{u} \right) + \left(\dfrac{1}{\tau} \mathbf{P}, \mathbf{u} \right),$
$$\mathbf{u} \in \mathbf{H}_0(\mathbf{curl}, \Omega),$$

(10c)
$$\left(\dfrac{1}{\epsilon_0 \epsilon_\infty (\epsilon_q - 1)} \dfrac{\partial \mathbf{P}}{\partial t}, \mathbf{w} \right) = \left(\dfrac{1}{\tau} \mathbf{E}, \mathbf{w} \right) - \left(\dfrac{1}{\epsilon_0 \epsilon_\infty (\epsilon_q - 1)\tau} \mathbf{P}, \mathbf{w} \right), \mathbf{w} \in (L^2(\Omega))^3.$$

The Maxwell-Debye model exhibits energy decay, as stated in the theorem below.

Theorem 2.1 (**Maxwell-Debye Energy Decay**). *Let* $\Omega \subset \mathbb{R}^3$ *and suppose that the solutions of the weak formulation* (10) *for the 3D Maxwell-Debye system of equations* (7) *satisfy the regularity conditions* $\mathbf{E} \in C(0, T; \mathbf{H}_0(\mathbf{curl}, \Omega)) \cap C^1(0, T; (L^2(\Omega))^3)$, *and* $\mathbf{H}, \mathbf{P} \in C^1(0, T; (L^2(\Omega))^3)$ *along with the PEC boundary conditions* (2). *Then the system exhibits energy decay,*

(11) $\qquad\qquad\qquad\qquad \mathcal{E}_D(t) \leq \mathcal{E}_D(0), \quad \forall t \geq 0,$

where the energy $\mathcal{E}_D(t)$ *is defined by*

(12) $\qquad \mathcal{E}_D(t) = \left(\mu_0 \left\| \mathbf{H}(t) \right\|_2^2 + \epsilon_0 \epsilon_\infty \left\| \mathbf{E}(t) \right\|_2^2 + \dfrac{1}{\epsilon_0 \epsilon_\infty (\epsilon_q - 1)} \left\| \mathbf{P}(t) \right\|_2^2 \right)^{\frac{1}{2}}.$

Proof. See [7, 29, 31]. $\qquad\qquad\qquad\qquad\qquad\qquad\qquad\qquad\qquad\qquad\qquad \square$

2.2. Maxwell-Lorentz Model and Energy Estimates. The second model for a dispersive medium that we consider is the single pole Lorentz model for electronic polarization. The susceptibility kernel function for the Lorentz model (see [28, 7, 53]) is given as

(13) $\qquad\qquad\qquad\qquad g(\mathbf{x}; t) = \dfrac{\epsilon_0 \omega_p^2}{\nu_0} \mathrm{e}^{-t\lambda} \sin(\nu_0 t),$

where ω_0 is the resonance frequency of the medium, $\lambda := \dfrac{1}{2\tau}$ is a damping frequency with $\frac{1}{\tau}$ the damping constant, the plasma frequency is $\omega_p := \omega_0 \sqrt{\epsilon_s - \epsilon_\infty}$, and $\nu_0 := \sqrt{\omega_0^2 - \lambda^2}$.

The time convolution for the electric polarization $\mathbf{P}$ with the susceptibility (13) can be converted to a second order ODE in the form [27, 53]

(14) $\qquad\qquad\qquad \dfrac{\partial^2 \mathbf{P}}{\partial t^2} + \dfrac{1}{\tau} \dfrac{\partial \mathbf{P}}{\partial t} + \omega_0^2 \mathbf{P} = \epsilon_0 \omega_p{}^2 \mathbf{E}.$

We define a new vector field, $\mathbf{J} = \dfrac{\partial \mathbf{P}}{\partial t}$, the polarization current density. With this definition, combining the ODE in (14) with Maxwell's equations (1) and the constitutive laws (3), we arrive at the 3D Maxwell-Lorentz model written as

3D Maxwell-Lorentz Model:

$$
(15a) \qquad \frac{\partial \mathbf{H}}{\partial t} = -\frac{1}{\mu_0} \operatorname{curl} \mathbf{E},
$$

$$
(15b) \qquad \frac{\partial \mathbf{E}}{\partial t} = \frac{1}{\epsilon_0 \epsilon_\infty} \operatorname{curl} \mathbf{H} - \frac{1}{\epsilon_0 \epsilon_\infty} \mathbf{J},
$$

$$
(15c) \qquad \frac{\partial \mathbf{J}}{\partial t} = -\frac{1}{\tau} \mathbf{J} - \omega_0^2 \mathbf{P} + \epsilon_0 \omega_p{}^2 \mathbf{E},
$$

$$
(15d) \qquad \frac{\partial \mathbf{P}}{\partial t} = \mathbf{J}.
$$

We assume the PEC boundary conditions (2) on $\partial\Omega$ and the initial conditions (1d), along with homogeneous initial conditions for $\mathbf{P}$ and $\mathbf{J}$, in the domain $\Omega \subset \mathbb{R}^3$. To show that the system (15) is well-posed, we construct a weak formulation as follows:

3D Maxwell-Lorentz Variational Formulation:
Find $\mathbf{E} \in C(0, T; \mathbf{H}_0(\mathbf{curl}, \Omega)) \cap C^1(0, T; (L^2(\Omega))^3)$, $\mathbf{P}, \mathbf{J}, \mathbf{H} \in C^1(0, T; (L^2(\Omega))^3)$ such that

$$
(16a) \qquad \left(\mu_0 \frac{\partial \mathbf{H}}{\partial t}, \mathbf{v} \right) = -\left(\operatorname{curl} \mathbf{E}, \mathbf{v} \right), \ \forall \mathbf{v} \in \left(L^2(\Omega) \right)^3,
$$

$$
(16b) \qquad \left(\epsilon_0 \epsilon_\infty \frac{\partial \mathbf{E}}{\partial t}, \mathbf{u} \right) = (\mathbf{H}, \operatorname{curl} \mathbf{u}) - (\mathbf{J}, \mathbf{u}), \ \forall \mathbf{u} \in \mathbf{H}_0(\mathbf{curl}, \Omega),
$$

$$
(16c) \qquad \left(\frac{1}{\epsilon_0 \omega_p{}^2} \frac{\partial \mathbf{J}}{\partial t}, \mathbf{w} \right) = -\left(\frac{1}{\epsilon_0 \omega_p{}^2 \tau} \mathbf{J}, \mathbf{w} \right) - \left(\frac{1}{\epsilon_0 \epsilon_\infty (\epsilon_q - 1)} \mathbf{P}, \mathbf{w} \right)
$$
$$
+ (\mathbf{E}, \mathbf{w}), \quad \forall \mathbf{w} \in \left(L^2(\Omega) \right)^3,
$$

$$
(16d) \qquad \left(\frac{1}{\epsilon_0 \epsilon_\infty (\epsilon_q - 1)} \frac{\partial \mathbf{P}}{\partial t}, \mathbf{q} \right) = \left(\frac{1}{\epsilon_0 \epsilon_\infty (\epsilon_q - 1)} \mathbf{J}, \mathbf{q} \right), \ \forall \mathbf{q} \in \left(L^2(\Omega) \right)^3.
$$

The Maxwell-Lorentz model exhibits energy decay, as stated in the theorem below (also see [31]).

Theorem 2.2 (Maxwell-Lorentz Energy Decay). *Let $\Omega \subset \mathbb{R}^3$ and suppose that the solutions of the weak formulation (16) for the Maxwell-Lorentz system of equations (15) satisfy the regularity conditions $\mathbf{E} \in C(0, T; \mathbf{H}_0(\mathbf{curl}, \Omega)) \cap C^1(0, T;$ $(L^2(\Omega))^3)$, $\mathbf{P}, \mathbf{J}, \mathbf{H} \in C^1(0, T; (L^2(\Omega))^3)$, along with the PEC boundary conditions (2). Then the system exhibits energy decay,*

$$
(17) \qquad \mathcal{E}_L(t) \le \mathcal{E}_L(0), \quad \forall \, t \ge 0,
$$

where the energy $\mathcal{E}_L(t)$ is defined by

$$
(18)
$$

$$
\mathcal{E}_L(t) = \left(\mu_0 \left\| \mathbf{H}(t) \right\|_2^2 + \epsilon_0 \epsilon_\infty \left\| \mathbf{E}(t) \right\|_2^2 + \frac{1}{\epsilon_0 \epsilon_\infty (\epsilon_q - 1)} \left\| \mathbf{P}(t) \right\|_2^2 + \frac{1}{\epsilon_0 \omega_p{}^2} \left\| \mathbf{J}(t) \right\|_2^2 \right)^{\frac{1}{2}}.
$$

Proof. See [7, 31]. □

2.3. Maxwell-Cold Plasma: Model and Energy Estimates. The cold plasma model is used to describe the propagation and absorption of electromagnetic waves in isotropic non-magnetized cold plasma [46, 32]. The susceptibility kernel function in isotropic cold plasma (see [53]) is given by

$$
(19) \qquad g(\mathbf{x}; t) = \frac{\epsilon_0 \omega_p^2}{\nu_c} (1 - \mathrm{e}^{-t\nu_c}),
$$

where ω_p is the plasma frequency of the medium, and ν_c is the collision frequency.

The time convolution for the electric polarization $\mathbf{P}$ with the susceptibility (19) in the isotropic cold plasma model can be converted to a second order ODE in the form [24, 23, 53]

$$(20) \qquad \frac{\partial^2 \mathbf{P}}{\partial t^2} + \nu_c \frac{\partial \mathbf{P}}{\partial t} = \epsilon_0 \omega_p^2 \mathbf{E}.$$

By defining the polarization current density $\frac{\partial \mathbf{P}}{\partial t} = \mathbf{J}$, as before, we can rewrite this system as a first order ODE

$$(21) \qquad \frac{\partial \mathbf{J}}{\partial t} = -\nu_c \mathbf{J} + \epsilon_0 \omega_p^2 \mathbf{E}.$$

The plasma model is a special case of the Lorentz model (15) with zero resonance frequency. The 3D Maxwell-Cold Plasma equations of the non-magnetized cold plasma are

3D Maxwell-Cold Plasma Model:

$$(22a) \qquad \frac{\partial \mathbf{H}}{\partial t} = -\frac{1}{\mu_0} \, \mathbf{curl} \, \mathbf{E},$$

$$(22b) \qquad \frac{\partial \mathbf{E}}{\partial t} = \frac{1}{\epsilon_0 \epsilon_\infty} \mathbf{curl} \, \mathbf{H} - \frac{1}{\epsilon_0 \epsilon_\infty} \mathbf{J},$$

$$(22c) \qquad \frac{\partial \mathbf{J}}{\partial t} = -\nu_c \mathbf{J} + \epsilon_0 \omega_p^2 \mathbf{E}.$$

We note that, we do not need to include the polarization $\mathbf{P}$ in this model, rather just the polarization current density $\mathbf{J}$. Similar to the Debye and the Lorentz case, the weak formulation for the Maxwell cold plasma system (22) reads

3D Maxwell-Cold Plasma Variational Formulation:
Find $\mathbf{E} \in C(0, T; \mathbf{H}_0(\mathbf{curl}, \Omega)) \cap C^1(0, T; (L^2(\Omega))^3)$, $\mathbf{J}, \mathbf{H} \in C^1(0, T; (L^2(\Omega))^3)$, such that

$$(23a) \qquad \left(\mu_0 \frac{\partial \mathbf{H}}{\partial t}, \mathbf{v} \right) = -\left(\mathbf{curl} \, \mathbf{E}, \mathbf{v} \right), \ \forall \mathbf{v} \in \left(L^2(\Omega) \right)^3,$$

$$(23b) \qquad \left(\epsilon_0 \epsilon_\infty \frac{\partial \mathbf{E}}{\partial t}, \mathbf{u} \right) = (\mathbf{H}, \mathbf{curl} \, \mathbf{u}) - (\mathbf{J}, \mathbf{u}), \ \forall \mathbf{u} \in \mathbf{H}_0(\mathbf{curl}, \Omega),$$

$$(23c) \qquad \left(\frac{1}{\epsilon_0 \omega_p^2} \frac{\partial \mathbf{J}}{\partial t}, \mathbf{w} \right) = -\left(\frac{\nu_c}{\epsilon_0 \omega_p^2} \mathbf{J}, \mathbf{w} \right) + (\mathbf{E}, \mathbf{w}), \quad \forall \mathbf{w} \in \left(L^2(\Omega) \right)^3.$$

The Maxwell-Cold Plasma model exhibits energy decay, as stated in the theorem below.

Theorem 2.3 (Maxwell-Cold Plasma Energy Decay). *Let $\Omega \subset \mathbb{R}^3$ and suppose that the solutions of the weak formulation (23) for the Maxwell-Cold Plasma system of equations (22) satisfy the regularity conditions $\mathbf{E} \in C(0, T; \mathbf{H}_0(\mathbf{curl}, \Omega)) \cap C^1(0, T; (L^2(\Omega))^3)$, $\mathbf{J} \in C^1(0, T; (L^2(\Omega))^3)$, and $\mathbf{H} \in C^1(0, T; (L^2(\Omega))^3)$ along with the PEC boundary conditions (2). Then the system exhibits energy decay,*

$$(24) \qquad \mathcal{E}_C(t) \leq \mathcal{E}_C(0), \quad \forall \, t \geq 0,$$

where the energy $\mathcal{E}_C(t)$ is defined by

$$(25) \qquad \mathcal{E}_C(t) = \left(\mu_0 \left\| \mathbf{H}(t) \right\|_2^2 + \epsilon_0 \epsilon_\infty \left\| \mathbf{E}(t) \right\|_2^2 + \frac{1}{\epsilon_0 \omega_p^2} \left\| \mathbf{J}(t) \right\|_2^2 \right)^{\frac{1}{2}}.$$

Proof. See [31]. $\qquad\qquad\qquad\qquad\qquad\qquad\qquad\qquad\qquad\qquad\qquad\qquad\qquad\qquad \square$

3. Discretization on Staggered Grids

In this section, we define spatial and temporal discretization in a standard way (see for e.g. [3, 5, 7, 9, 11]) to obtain a staggered grid in space-time that we will call a Yee grid or mesh. Here we consider a cubic spatial domain $\Omega = [0,a] \times [0,b] \times [0,c] \subset \mathbb{R}^3$ for $a,b,c > 0$ and time interval $[0,T]$ with $T > 0$. Let I, J, K and N be positive integers such that $I = a/\triangle x$, $J = b/\triangle y$, $K = c/\triangle z$, and $N = T/\triangle t$ where $\triangle x, \triangle y$ and $\triangle z$ are spatial step sizes along the $x, y,$ and z direction, respectively, and $\triangle t$ is the time step size. Let $\ell, j, k, n \in \mathbb{N}$. We define grid points in the t, x, y, z directions as

$$t^n = n \triangle t, \quad t^{n+\frac{1}{2}} = \left(n + \frac{1}{2}\right)\triangle t, \quad n = 0,1,2,...,N-1, \quad t^N = N\triangle t = T,$$

$$x_\ell = \ell \triangle x, \quad x_{\ell+\frac{1}{2}} = \left(\ell + \frac{1}{2}\right)\triangle x, \quad \ell = 0,1,2,...,I-1, \quad x_I = I\triangle x = a,$$

$$y_j = j\triangle y, \quad y_{j+\frac{1}{2}} = \left(j + \frac{1}{2}\right)\triangle y, \quad j = 0,1,2,...,J-1, \quad y_J = J\triangle y = b,$$

$$z_k = k\triangle z, \quad z_{k+\frac{1}{2}} = \left(k + \frac{1}{2}\right)\triangle z, \quad k = 0,1,2,...,K-1, \quad z_K = K\triangle z = c.$$

To derive some of our results, we will sometimes consider the special case $\Delta x = \Delta y = \Delta z = h$. In any case, we consistently use the notation $U_h(t)$ for an appropriate grid function which approximates a smooth scalar field components $u(\mathbf{x},t)$ on a Yee grid. We represent the discrete electric and magnetic vector field grid functions by, $\mathbf{E}_h$ and $\mathbf{H}_h$, respectively. For components of fields related to the electric field, i.e., $F_{\kappa,h}$ where $F \in \{E, P, J\}$ and $\kappa \in \{x,y,z\}$, we define the set of spatial grid points on which these fields are discretized as follows:

(26a) $\Omega_h^{E_x} := \left\{ \left(x_{\ell+\frac{1}{2}}, y_j, z_k\right) \,\middle|\, 0 \leq \ell \leq I-1, 0 \leq j \leq J, 0 \leq k \leq K \right\},$

(26b) $\Omega_h^{E_y} := \left\{ \left(x_\ell, y_{j+\frac{1}{2}}, z_k\right) \,\middle|\, 0 \leq \ell \leq I, 0 \leq j \leq J-1, 0 \leq k \leq K \right\},$

(26c) $\Omega_h^{E_z} := \left\{ \left(x_\ell, y_j, z_{k+\frac{1}{2}}\right) \,\middle|\, 0 \leq \ell \leq I, 0 \leq j \leq J, 0 \leq k \leq K-1 \right\}.$

For magnetic field components, $H_{\kappa,h}$, the sets of spatial grid points on which these fields are discretized are

(27a) $\Omega_h^{H_x} := \left\{ \left(x_\ell, y_{j+\frac{1}{2}}, z_{k+\frac{1}{2}}\right) \,\middle|\, 0 \leq \ell \leq I, 0 \leq j \leq J-1, 0 \leq k \leq K-1 \right\},$

(27b) $\Omega_h^{H_y} := \left\{ \left(x_{\ell+\frac{1}{2}}, y_j, z_{j+\frac{1}{2}}\right) \,\middle|\, 0 \leq \ell \leq I-1, 0 \leq j \leq J, 0 \leq k \leq K-1 \right\},$

(27c) $\Omega_h^{H_z} := \left\{ \left(x_{\ell+\frac{1}{2}}, y_{j+\frac{1}{2}}, z_k\right) \,\middle|\, 0 \leq \ell \leq I-1, 0 \leq j \leq J-1, 0 \leq k \leq K \right\}.$

Thus, all x components of $\mathbf{E}_h$ (and $\mathbf{P}_h$ and $\mathbf{J}_h$) are discretized at grid points on $\Omega_h^{E_x}$ and collectively form the *set of degrees of freedom* (DoF) of $E_{x,h}$, given as $\{E_{x,h_{\ell+\frac{1}{2},j,k}}, \left(x_{\ell+\frac{1}{2}}, y_j, z_k\right) \in \Omega_h^{E_x}\}$. Similarly y components are discretized on $\Omega_h^{E_y}$, and z components on $\Omega_h^{E_z}$. All x components of $\mathbf{H}_h$ are discretized on $\Omega_h^{H_x}$, y components on $\Omega_h^{H_y}$, and z components on $\Omega_h^{H_z}$. We denote $\Omega_h^{\mathbf{E}} := \Omega_h^{E_x} \times \Omega_h^{E_y} \times \Omega_h^{E_z}$ and $\Omega_h^{\mathbf{H}} = \Omega_h^{H_x} \times \Omega_h^{H_y} \times \Omega_h^{H_z}$.

We assume that the PEC boundary condition (2) is satisfied on the discrete Yee mesh. We denote the set of all grid points on the boundary of the cubic spatial domain $\Omega = [0,a] \times [0,b] \times [0,c]$ as $\partial \Omega_h^{\mathbf{E}}$. Then the discrete analogue of the PEC boundary condition, $\mathbf{n} \times \mathbf{E}_h = 0$, on the Yee grid is that the degrees of freedom of

the electric grid function $\mathbf{E}_h$ satisfy

$$
\begin{aligned}
(28) \quad & E_{x,h_{\ell+\frac{1}{2},0,k}} = E_{x,h_{\ell+\frac{1}{2},J,k}} = E_{x,h_{\ell+\frac{1}{2},j,0}} = E_{x,h_{\ell+\frac{1}{2},j,K}} = 0, \\
& E_{y,h_{0,j+\frac{1}{2},k}} = E_{y,h_{I,j+\frac{1}{2},k}} = E_{y,h_{\ell,j+\frac{1}{2},0}} = E_{y,h_{\ell,j+\frac{1}{2},K}} = 0, \\
& E_{z,h_{0,j,k+\frac{1}{2}}} = E_{z,h_{I,j,k+\frac{1}{2}}} = E_{z,h_{\ell,0,k+\frac{1}{2}}} = E_{z,h_{\ell,J,k+\frac{1}{2}}} = 0,
\end{aligned}
$$

for any $0 \le \ell \le I$, $0 \le j \le J$, $0 \le k \le K$ and for all time t.

We define the centered temporal difference operator, the discrete time averaging operator as well as the centered spatial difference operators acting on grid functions as follows. For U_h a discrete grid function approximating a smooth scalar field component $u(\mathbf{x}, t)$, we have

(29a)
$$
U^{\gamma}_{h_{\alpha,\beta,\kappa}} \approx u(\alpha\Delta x, \beta\Delta y, \kappa\Delta z, \gamma\Delta t),
$$

(29b)
$$
\delta_t U^{\gamma}_{h_{\alpha,\beta,\kappa}} := \frac{U^{\gamma+\frac{1}{2}}_{h_{\alpha,\beta,\kappa}} - U^{\gamma-\frac{1}{2}}_{h_{\alpha,\beta,\kappa}}}{\Delta t},
$$

(29c)
$$
\overline{U}^{\gamma}_{h_{\alpha,\beta,\kappa}} := \frac{U^{\gamma+\frac{1}{2}}_{h_{\alpha,\beta,\kappa}} + U^{\gamma-\frac{1}{2}}_{h_{\alpha,\beta,\kappa}}}{2},
$$

(29d)
$$
\delta_x U^{\gamma}_{h_{\alpha,\beta,\kappa}} := \frac{U^{\gamma}_{h_{\alpha+\frac{1}{2},\beta,\kappa}} - U^{\gamma}_{h_{\alpha-\frac{1}{2},\beta,\kappa}}}{\Delta x},
$$

(29e)
$$
\delta_y U^{\gamma}_{h_{\alpha,\beta,\kappa}} := \frac{U^{\gamma}_{h_{\alpha,\beta+\frac{1}{2},\kappa}} - U^{\gamma}_{h_{\alpha,\beta-\frac{1}{2},\kappa}}}{\Delta y},
$$

(29f)
$$
\delta_z U^{\gamma}_{h_{\alpha,\beta,\kappa}} := \frac{U^{\gamma}_{h_{\alpha,\beta,\kappa+\frac{1}{2}}} - U^{\gamma}_{h_{\alpha,\beta,\kappa-\frac{1}{2}}}}{\Delta z}.
$$

The discrete grid inner products are defined as follows. Let $\Delta^3 = \Delta x \Delta y \Delta z$. For any fields related to the electric field denoted as $\mathbf{F}_h, \mathbf{G}_h$, which are defined on $\Omega^{\mathbf{E}}_h$, and for magnetic fields denoted by $\mathbf{U}_h, \mathbf{V}_h$, defined on $\Omega^{\mathbf{H}}_h$, we define the inner products

$$
\begin{aligned}
(30a) \quad (\mathbf{F}_h, \mathbf{G}_h)_E = & \Delta^3 \sum_{\ell=0}^{I-1} \sum_{j=0}^{J-1} \sum_{k=0}^{K-1} \Big(F_{x,h_{\ell+\frac{1}{2},j,k}} G_{x,h_{\ell+\frac{1}{2},j,k}} \\
& + F_{y,h_{\ell,j+\frac{1}{2},k}} G_{y,h_{\ell,j+\frac{1}{2},k}} + F_{z,h_{\ell,j,k+\frac{1}{2}}} G_{z,h_{\ell,j,k+\frac{1}{2}}} \Big),
\end{aligned}
$$

$$
\begin{aligned}
(30b) \quad (\mathbf{U}_h, \mathbf{V}_h)_H = & \Delta^3 \sum_{\ell=0}^{I-1} \sum_{j=0}^{J-1} \sum_{k=0}^{K-1} \Big(U_{x,h_{\ell,j+\frac{1}{2},k+\frac{1}{2}}} V_{x,h_{\ell,j+\frac{1}{2},k+\frac{1}{2}}} \\
& + U_{y,h_{\ell+\frac{1}{2},j,k+\frac{1}{2}}} V_{y,h_{\ell+\frac{1}{2},j,k+\frac{1}{2}}} + U_{z,h_{\ell+\frac{1}{2},j+\frac{1}{2},k}} V_{z,h_{\ell+\frac{1}{2},j+\frac{1}{2},k}} \Big).
\end{aligned}
$$

The discrete norms associated to the inner products are defined as

(31a)
$$
\|\mathbf{F}_h\|_E^2 = \Delta^3 \sum_{\ell=0}^{I-1} \sum_{j=0}^{J-1} \sum_{k=0}^{K-1} \Big(|F_{x,h_{\ell+\frac{1}{2},j,k}}|^2 + |F_{y,h_{\ell,j+\frac{1}{2},k}}|^2 + |F_{z,h_{\ell,j,k+\frac{1}{2}}}|^2 \Big),
$$

(31b)
$$
\|\mathbf{U}_h\|_H^2 = \Delta^3 \sum_{\ell=0}^{I-1} \sum_{j=0}^{J-1} \sum_{k=0}^{K-1} \Big(|U_{x,h_{\ell,j+\frac{1}{2},k+\frac{1}{2}}}|^2 + |U_{y,h_{\ell+\frac{1}{2},j,k+\frac{1}{2}}}|^2 + |U_{z,h_{\ell+\frac{1}{2},j+\frac{1}{2},k}}|^2 \Big).
$$

Next, we define discrete spaces for the electric field, polarization and polarization current density. Define the spaces

(32) $\vee_h^E := \{\mathbf{F}_h = (F_{x,h}, F_{y,h}, F_{z,h}), \text{ on } \Omega_h^{\mathbf{E}}, \|\mathbf{F}_h\|_E < \infty\},$

(33) $\vee_{h,0}^E := \{\mathbf{F}_h = (F_{x,h}, F_{y,h}, F_{z,h}) \in \vee_h^E; \mathbf{n} \times \mathbf{F}_h = \mathbf{0}, \text{ on } \partial\Omega_h^{\mathbf{E}}\}.$

Similarly, we define discrete spaces for the magnetic field as

(34) $\vee_h^H := \{\mathbf{U}_h = (U_{x,h}, U_{y,h}, U_{z,h}), \text{ on } \Omega_h^{\mathbf{H}}, \|\mathbf{U}_h\|_H < \infty\}.$

The discrete curl operators, primary and dual, are then defined respectively, as

(35a) $\mathbf{curl}_h : \vee_h^E \to \vee_h^H,$

(35b) $\widetilde{\mathbf{curl}}_h : \vee_h^H \to \vee_h^E,$

such that

(36a)

$\mathbf{curl}_h \mathbf{E}_h = \Big((\delta_y E_{z,h} - \delta_z E_{y,h})_{\ell,j+\frac{1}{2},k+\frac{1}{2}}, (\delta_z E_{x,h} - \delta_x E_{z,h})_{\ell+\frac{1}{2},j,k+\frac{1}{2}},$

$$(\delta_x E_{y,h} - \delta_y E_{x,h})_{\ell+\frac{1}{2},j+\frac{1}{2},k} \Big)^T \in \vee_h^H,$$

(36b)

$\widetilde{\mathbf{curl}}_h \mathbf{H}_h = \Big((\delta_y H_{z,h} - \delta_z H_{y,h})_{\ell+\frac{1}{2},j,k}, (\delta_z H_{x,h} - \delta_x H_{z,h})_{\ell,j+\frac{1}{2},k},$

$$(\delta_x H_{y,h} - \delta_y H_{x,h})_{\ell,j,k+\frac{1}{2}} \Big)^T \in \vee_h^E.$$

Summation (discrete integration) by parts (also see [3, 11]) yields the following adjoint property of the discrete curl operator: for any $\mathbf{E}_h \in \vee_{h,0}^E$ and $\mathbf{H}_h \in \vee_h^H$, we have that

(37) $(\mathbf{curl}_h \mathbf{E}_h, \mathbf{H}_h)_H = (\mathbf{E}_h, \widetilde{\mathbf{curl}}_h \mathbf{H}_h)_E.$

The discrete curl operators (35) are represented in matrix form as [12, 9]

(38) $\widetilde{\mathbf{curl}}_h := \mathbf{curl}_h := \begin{pmatrix} 0 & -\delta_z & \delta_y \\ \delta_z & 0 & -\delta_x \\ -\delta_y & \delta_x & 0 \end{pmatrix}.$

In the next sections we construct and analyze Yee schemes for Debye, Lorentz and cold plasma models described earlier.

4. Yee Scheme for the Maxwell-Debye System

Extensions of the Yee-FDTD schemes for the 3D Maxwell-Debye model (7) should use a staggered leap-frog discretization in time and space for staggering electromagnetic field components. Using the notation developed in the previous section we can write down the scalar form of a Yee-FDTD scheme as an update of discrete electromagnetic field solutions at time $t^n = n\Delta t, n \in \mathcal{N}$ to time $t^{n+1} = (n+1)\Delta t$ as follows:

3D Yee-FDTD Maxwell-Debye Scheme (Scalar form)

$$(39a) \qquad \delta_t H^n_{x,h_{\ell,j+\frac{1}{2},k+\frac{1}{2}}} = \frac{1}{\mu_0}\left(\delta_z E^n_{y,h_{\ell,j+\frac{1}{2},k+\frac{1}{2}}} - \delta_y E^n_{z,h_{\ell,j+\frac{1}{2},k+\frac{1}{2}}}\right),$$

$$(39b) \qquad \delta_t H^n_{y,h_{\ell+\frac{1}{2},j,k+\frac{1}{2}}} = \frac{1}{\mu_0}\left(\delta_x E^n_{z,h_{\ell+\frac{1}{2},j,k+\frac{1}{2}}} - \delta_z E^n_{x,h_{\ell+\frac{1}{2},j,k+\frac{1}{2}}}\right),$$

$$(39c) \qquad \delta_t H^n_{z,h_{\ell+\frac{1}{2},j+\frac{1}{2},k}} = \frac{1}{\mu_0}\left(\delta_y E^n_{x,h_{\ell+\frac{1}{2},j+\frac{1}{2},k}} - \delta_x E^n_{y,h_{\ell+\frac{1}{2},j+\frac{1}{2},k}}\right),$$

$$(39d) \qquad \delta_t E^{n+\frac{1}{2}}_{x,h_{\ell+\frac{1}{2},j,k}} = \frac{1}{\epsilon_0\epsilon_\infty}\left(\delta_y H^{n+\frac{1}{2}}_{z,h_{\ell+\frac{1}{2},j,k}} - \delta_z H^{n+\frac{1}{2}}_{y,h_{\ell+\frac{1}{2},j,k}}\right)$$
$$- \frac{(\epsilon_q - 1)}{\tau}\overline{E}^{n+\frac{1}{2}}_{x,h_{\ell+\frac{1}{2},j,k}} + \frac{1}{\epsilon_0\epsilon_\infty\tau}\overline{P}^{n+\frac{1}{2}}_{x,h_{\ell+\frac{1}{2},j,k}},$$

$$(39e) \qquad \delta_t E^{n+\frac{1}{2}}_{y,h_{\ell,j+\frac{1}{2},k}} = \frac{1}{\epsilon_0\epsilon_\infty}\left(\delta_z H^{n+\frac{1}{2}}_{x,h_{\ell,j+\frac{1}{2},k}} - \delta_x H^{n+\frac{1}{2}}_{z,h_{\ell,j+\frac{1}{2},k}}\right)$$
$$- \frac{(\epsilon_q - 1)}{\tau}\overline{E}^{n+\frac{1}{2}}_{y,h_{\ell,j+\frac{1}{2},k}} + \frac{1}{\epsilon_0\epsilon_\infty\tau}\overline{P}^{n+\frac{1}{2}}_{y,h_{\ell,j+\frac{1}{2},k}},$$

$$(39f) \qquad \delta_t E^{n+\frac{1}{2}}_{z,h_{\ell,j,k+\frac{1}{2}}} = \frac{1}{\epsilon_0\epsilon_\infty}\left(\delta_x H^{n+\frac{1}{2}}_{y,h_{\ell,j,k+\frac{1}{2}}} - \delta_y H^{n+\frac{1}{2}}_{x,h_{\ell,j,k+\frac{1}{2}}}\right)$$
$$- \frac{(\epsilon_q - 1)}{\tau}\overline{E}^{n+\frac{1}{2}}_{z,h_{\ell,j,k+\frac{1}{2}}} + \frac{1}{\epsilon_0\epsilon_\infty\tau}\overline{P}^{n+\frac{1}{2}}_{z,h_{\ell,j,k+\frac{1}{2}}},$$

$$(39g) \qquad \delta_t P^{n+\frac{1}{2}}_{x,h_{\ell+\frac{1}{2},j,k}} = \frac{\epsilon_0\epsilon_\infty(\epsilon_q - 1)}{\tau}\overline{E}^{n+\frac{1}{2}}_{x,h_{\ell+\frac{1}{2},j,k}} - \frac{1}{\tau}\overline{P}^{n+\frac{1}{2}}_{x,h_{\ell+\frac{1}{2},j,k}},$$

$$(39h) \qquad \delta_t P^{n+\frac{1}{2}}_{y,h_{\ell,j+\frac{1}{2},k}} = \frac{\epsilon_0\epsilon_\infty(\epsilon_q - 1)}{\tau}\overline{E}^{n+\frac{1}{2}}_{y,h_{\ell,j+\frac{1}{2},k}} - \frac{1}{\tau}\overline{P}^{n+\frac{1}{2}}_{y,h_{\ell,j+\frac{1}{2},k}},$$

$$(39i) \qquad \delta_t P^{n+\frac{1}{2}}_{z,h_{\ell,j,k+\frac{1}{2}}} = \frac{\epsilon_0\epsilon_\infty(\epsilon_q - 1)}{\tau}\overline{E}^{n+\frac{1}{2}}_{z,h_{\ell,j,k+\frac{1}{2}}} - \frac{1}{\tau}\overline{P}^{n+\frac{1}{2}}_{z,h_{\ell,j,k+\frac{1}{2}}}.$$

The scheme (39) can be rewritten in vector form as

3D Yee-FDTD Maxwell-Debye Scheme (Vector form)

$$(40a) \qquad \delta_t \mathbf{H}^n_h = -\frac{1}{\mu_0}\,\mathbf{curl}_h\,\mathbf{E}^n_h,$$

$$(40b) \qquad \delta_t \mathbf{E}^{n+\frac{1}{2}}_h = \frac{1}{\epsilon_0\epsilon_\infty}\widetilde{\mathbf{curl}_h}\mathbf{H}^{n+\frac{1}{2}}_h - \frac{(\epsilon_q - 1)}{\tau}\overline{\mathbf{E}}^{n+\frac{1}{2}}_h + \frac{1}{\epsilon_0\epsilon_\infty\tau}\overline{\mathbf{P}}^{n+\frac{1}{2}}_h,$$

$$(40c) \qquad \delta_t \mathbf{P}^{n+\frac{1}{2}}_h = \frac{\epsilon_0\epsilon_\infty(\epsilon_q - 1)}{\tau}\overline{\mathbf{E}}^{n+\frac{1}{2}}_h - \frac{1}{\tau}\overline{\mathbf{P}}^{n+\frac{1}{2}}_h.$$

4.1. Stability Analysis of the Yee Scheme for Debye Media. In this section, we prove a discrete energy property for the 3D Yee-FDTD Maxwell-Debye scheme given in (40). We suppose a uniform mesh $h = \Delta x = \Delta y = \Delta z > 0$. The conditional stability of the 3D Yee-FDTD Maxwell-Debye scheme is given by the following theorem which proves the decay of discrete energy in time.

Theorem 4.1 (Yee Stability-Debye). *If the time step and uniform mesh spatial step sizes satisfy the stability condition*

$$(41) \qquad \frac{c_\infty \Delta t}{h} < \frac{1}{\sqrt{3}},$$

where $c_\infty = 1/\sqrt{\mu_0 \epsilon_0 \epsilon_\infty}$, *then the discrete solutions of the 3D Yee-FDTD scheme for the Maxwell-Debye equations* (40) *satisfy the discrete energy decay,*

$$\mathcal{E}_{h,D}^{n+1} \leq \mathcal{E}_{h,D}^n, \tag{42}$$

for all $n \geq 0$ *where the discrete energy is defined as*

$$\mathcal{E}_{h,D}^n := \left(\mu_0 \|\mathbf{H}_h^{n-\frac{1}{2}}\|_H^2 + \epsilon_0 \epsilon_\infty \|\mathbf{E}_h^n\|_E^2 + \frac{\|\mathbf{P}_h^n\|_E^2}{\epsilon_0 \epsilon_\infty (\epsilon_q - 1)} - \Delta t \left(\mathbf{curl}_h \, \mathbf{E}_h^n, \mathbf{H}_h^{n-\frac{1}{2}} \right)_H \right)^{\frac{1}{2}}. \tag{43}$$

Proof. Multiplying both sides of equation (39a) by $\Delta^3 \, \mu_0 \overline{H}_{x,h_{\ell,j+\frac{1}{2},k+\frac{1}{2}}}^n$, (39b) by $\Delta^3 \, \mu_0 \overline{H}_{y,h_{\ell+\frac{1}{2},j,k+\frac{1}{2}}}^n$, (39c) by $\Delta^3 \, \mu_0 \overline{H}_{z,h_{\ell+\frac{1}{2},j+\frac{1}{2},k}}^n$, summing each equation over all spatial nodes, and adding all the results, we obtain

$$\frac{\mu_0}{2\Delta t} \left(\|\mathbf{H}_h^{n+\frac{1}{2}}\|_H^2 - \|\mathbf{H}_h^{n-\frac{1}{2}}\|_H^2 \right) = - \left(\mathbf{curl}_h \, \mathbf{E}_h^n, \overline{\mathbf{H}_h}^n \right)_H. \tag{44}$$

Next, multiplying both sides of equation (39d) by $\Delta^3 \, \epsilon_0 \epsilon_\infty \overline{E}_{x,h_{\ell+\frac{1}{2},j,k}}^{n+\frac{1}{2}}$, (39e) by $\Delta^3 \, \epsilon_0 \epsilon_\infty \overline{E}_{y,h_{\ell,j+\frac{1}{2},k}}^{n+\frac{1}{2}}$, (39f) by $\Delta^3 \, \epsilon_0 \epsilon_\infty \overline{E}_{z,h_{\ell,j,k+\frac{1}{2}}}^{n+\frac{1}{2}}$, summing each equation over all spatial nodes, and adding all the results, we obtain

$$\frac{\epsilon_0 \epsilon_\infty}{2\Delta t} \left(\|\mathbf{E}_h^{n+1}\|_E^2 - \|\mathbf{E}_h^n\|_E^2 \right) + \frac{\epsilon_0 \epsilon_\infty (\epsilon_q - 1)}{\tau} \|\overline{\mathbf{E}_h}^{n+\frac{1}{2}}\|_E^2 - \frac{1}{\tau} \left(\overline{\mathbf{P}_h}^{n+\frac{1}{2}}, \overline{\mathbf{E}_h}^{n+\frac{1}{2}} \right)_E$$
$$= \left(\widetilde{\mathbf{curl}_h \mathbf{H}_h}^{n+\frac{1}{2}}, \overline{\mathbf{E}_h}^{n+\frac{1}{2}} \right)_E. \tag{45}$$

Finally, multiplying both sides of equation (39g) by $\dfrac{\Delta^3}{\epsilon_0 \epsilon_\infty (\epsilon_q - 1)} \overline{P}_{x,h_{\ell+\frac{1}{2},j,k}}^{n+\frac{1}{2}}$, (39h) by $\dfrac{\Delta^3}{\epsilon_0 \epsilon_\infty (\epsilon_q - 1)} \overline{P}_{y,h_{\ell,j+\frac{1}{2},k}}^{n+\frac{1}{2}}$, (39i) by $\dfrac{\Delta^3}{\epsilon_0 \epsilon_\infty (\epsilon_q - 1)} \overline{P}_{z,h_{\ell,j,k+\frac{1}{2}}}^{n+\frac{1}{2}}$, summing each equation over all spatial nodes, and adding all the results, we obtain

$$\frac{\|\mathbf{P}_h^{n+1}\|_E^2 - \|\mathbf{P}_h^n\|_E^2}{2\epsilon_0 \epsilon_\infty (\epsilon_q - 1)\Delta t} = \frac{1}{\tau} \left(\overline{\mathbf{E}_h}^{n+\frac{1}{2}}, \overline{\mathbf{P}_h}^{n+\frac{1}{2}} \right)_E - \frac{\|\overline{\mathbf{P}_h}^{n+\frac{1}{2}}\|_E^2}{\epsilon_0 \epsilon_\infty (\epsilon_q - 1)\tau}. \tag{46}$$

Adding equations (44)-(46) and using a discrete analogue of integration by parts [9], we obtain

$$\frac{\mu_0}{2\Delta t} \left(\|\mathbf{H}_h^{n+\frac{1}{2}}\|_H^2 - \|\mathbf{H}_h^{n-\frac{1}{2}}\|_H^2 \right) + \frac{\epsilon_0 \epsilon_\infty}{2\Delta t} \left(\|\mathbf{E}_h^{n+1}\|_E^2 - \|\mathbf{E}_h^n\|_E^2 \right) + \frac{\|\mathbf{P}_h^{n+1}\|_E^2 - \|\mathbf{P}_h^n\|_E^2}{2\epsilon_0 \epsilon_\infty (\epsilon_q - 1)\Delta t}$$

$$= - \left(\mathbf{curl}_h \, \mathbf{E}_h^n, \overline{\mathbf{H}_h}^n \right)_H + \left(\widetilde{\mathbf{curl}_h \mathbf{H}_h}^{n+\frac{1}{2}}, \overline{\mathbf{E}_h}^{n+\frac{1}{2}} \right)_E$$

$$\qquad - \frac{\epsilon_0 \epsilon_\infty (\epsilon_q - 1)}{\tau} \|\overline{\mathbf{E}_h}^{n+\frac{1}{2}}\|_E^2 + \frac{2}{\tau} \left(\overline{\mathbf{P}_h}^{n+\frac{1}{2}}, \overline{\mathbf{E}_h}^{n+\frac{1}{2}} \right)_E - \frac{\|\overline{\mathbf{P}_h}^{n+\frac{1}{2}}\|_E^2}{\epsilon_0 \epsilon_\infty (\epsilon_q - 1)\tau}$$

$$= - \frac{1}{2} \left(\mathbf{curl}_h \, \mathbf{E}_h^n, \mathbf{H}_h^{n-\frac{1}{2}} \right)_H + \frac{1}{2} \left(\widetilde{\mathbf{curl}_h \mathbf{H}_h}^{n+\frac{1}{2}}, \mathbf{E}_h^{n+1} \right)_E$$

$$- \frac{\|\epsilon_0 \epsilon_\infty (\epsilon_q - 1)\overline{\mathbf{E}_h}^{n+\frac{1}{2}} - \overline{\mathbf{P}_h}^{n+\frac{1}{2}}\|_E^2}{\epsilon_0 \epsilon_\infty (\epsilon_q - 1)\tau}. \tag{47}$$

We can convert equation (47) into the inequality

$$\mu_0\left(\|\mathbf{H}_h^{n+\frac{1}{2}}\|_H^2 - \|\mathbf{H}_h^{n-\frac{1}{2}}\|_H^2\right) + \epsilon_0\epsilon_\infty\left(\|\mathbf{E}_h^{n+1}\|_E^2 - \|\mathbf{E}_h^n\|_E^2\right) + \frac{\left(\|\mathbf{P}_h^{n+1}\|_E^2 - \|\mathbf{P}_h^n\|_E^2\right)}{\epsilon_0\epsilon_\infty(\epsilon_q - 1)}$$

$$\tag{48} \leq \Delta t\left(\widetilde{\mathbf{curl}_h}\mathbf{H}_h^{n+\frac{1}{2}}, \mathbf{E}_h^{n+1}\right)_E - \Delta t\left(\mathbf{curl}_h\,\mathbf{E}_h^n, \mathbf{H}_h^{n-\frac{1}{2}}\right)_H.$$

Using the definition of the discrete energy function (43), the inequality (48) becomes

$$\tag{49} \left(\mathcal{E}_{h,D}^{n+1}\right)^2 \leq \left(\mathcal{E}_{h,D}^n\right)^2,$$

which applies for all $n \geq 0$.

Of course, we need to prove that the function $\mathcal{E}_{h,D}^n$ defined in (43) defines an "energy" i.e., that it takes on positive values for all $n \geq 0$. We note that, in 3D with the PEC boundary conditions, the following inequality [19, p. 51] holds

$$\tag{50} \|\mathbf{curl}_h\,\mathbf{E}_h\|_H \leq 2\sqrt{\frac{1}{\Delta x^2} + \frac{1}{\Delta y^2} + \frac{1}{\Delta z^2}}\ \|\mathbf{E}_h\|_E.$$

Assuming a uniform mesh, inequality (50) becomes

$$\tag{51} \|\mathbf{curl}_h\,\mathbf{E}_h\|_H \leq \frac{2\sqrt{3}}{h}\|\mathbf{E}_h\|_E.$$

Using Young's inequality and the inequality (51) we have that

$$\mu_0\|\mathbf{H}_h^{n-\frac{1}{2}}\|_H^2 + \epsilon_0\epsilon_\infty\|\mathbf{E}_h^n\|_E^2 + \frac{\|\mathbf{P}_h^n\|_E^2}{\epsilon_0\epsilon_\infty(\epsilon_q - 1)} - \Delta t\left(\mathbf{curl}_h\,\mathbf{E}_h^n, \mathbf{H}_h^{n-\frac{1}{2}}\right)_H$$

$$\geq \mu_0\|\mathbf{H}_h^{n-\frac{1}{2}}\|_H^2 + \epsilon_0\epsilon_\infty\|\mathbf{E}_h^n\|_E^2 - \Delta t\left[\frac{\mu_0}{\Delta t}\|\mathbf{H}_h^{n-\frac{1}{2}}\|_H^2 + \frac{3\Delta t}{h^2\mu_0}\|\mathbf{E}_h^n\|_E^2\right]$$

$$\tag{52} \geq \epsilon_0\epsilon_\infty\left(1 - \frac{3\Delta t^2}{h^2\mu_0\epsilon_0\epsilon_\infty}\right)\|\mathbf{E}_h^n\|_E^2.$$

Assuming no trivial solutions, the discrete energy function (52) is positive when

$$\tag{53} \frac{3\Delta t^2}{h^2\mu_0\epsilon_0\epsilon_\infty} < 1 \quad \Leftrightarrow \quad \frac{3c_\infty^2\Delta t^2}{h^2} < 1.$$

Thus, under the stability condition (41) we have discrete energy decay as indicated in (49). □

Remark 4.1. *The stability condition on a nonuniform spatial mesh is given by*

$$\tag{54} c_\infty\Delta t\sqrt{\frac{1}{\Delta x^2} + \frac{1}{\Delta y^2} + \frac{1}{\Delta z^2}} < 1.$$

Remark 4.2. *The stability results based on energy decay for the 3D Yee-FDTD Maxwell-Debye scheme given in (43) in Theorem 4.1 extend the 2D results in Theorem 4.1 [7] with stability conditions that are different in 3D versus 2D. We note that the discrete energy function $\mathcal{E}_{h,D}^n$ can be expressed in two different ways.*

$$\mathcal{E}_{h,D}^n = \mu_0\|\mathbf{H}_h^{n-\frac{1}{2}}\|_H^2 + \epsilon_0\epsilon_\infty\|\mathbf{E}_h^n\|_E^2 + \frac{\|\mathbf{P}_h^n\|_E^2}{\epsilon_0\epsilon_\infty(\epsilon_q - 1)} - \Delta t\left(\mathbf{curl}_h\,\mathbf{E}_h^n, \mathbf{H}_h^{n-\frac{1}{2}}\right)_H$$

$$\tag{55} = \left(\mu_0\mathbf{H}_h^{n-\frac{1}{2}} - \Delta t\,\mathbf{curl}_h\,\mathbf{E}_h^n, \mathbf{H}_h^{n-\frac{1}{2}}\right)_H + \epsilon_0\epsilon_\infty\|\mathbf{E}_h^n\|_E^2 + \frac{\|\mathbf{P}_h^n\|_E^2}{\epsilon_0\epsilon_\infty(\epsilon_q - 1)}.$$

From equation (40a), we have $\mu_0 \left(\mathbf{H}_h^{n+\frac{1}{2}} - \mathbf{H}_h^{n-\frac{1}{2}} \right) = -\Delta t\, \mathbf{curl}_h\, \mathbf{E}_h^n$. Thus, (55) becomes

$$\mathcal{E}_{h,D}^n = \mu_0 \|\mathbf{H}_h^{n-\frac{1}{2}}\|_H^2 + \epsilon_0 \epsilon_\infty \|\mathbf{E}_h^n\|_E^2 + \frac{\|\mathbf{P}_h^n\|_E^2}{\epsilon_0 \epsilon_\infty (\epsilon_q - 1)} - \Delta t \left(\mathbf{curl}_h\, \mathbf{E}_h^n, \mathbf{H}_h^{n-\frac{1}{2}} \right)_H$$

$$(56) \qquad = \mu_0 \left(\mathbf{H}_h^{n+\frac{1}{2}}, \mathbf{H}_h^{n-\frac{1}{2}} \right)_H + \epsilon_0 \epsilon_\infty \|\mathbf{E}_h^n\|_E^2 + \frac{\|\mathbf{P}_h^n\|_E^2}{\epsilon_0 \epsilon_\infty (\epsilon_q - 1)}.$$

4.2. Error Estimates and Convergence of the Yee Scheme for the Maxwell-Debye Model.

In this section, we present a convergence analysis of the Yee scheme for the Maxwell-Debye model (40) . There are two ingredients needed for a convergence analysis; the stability analysis in the previous section and analysis of truncation errors. We first present a truncation error analysis below.

Lemma 4.1. *Suppose that the solutions to the 3D Maxwell-Debye model* (7) *satisfy the regularity conditions* $\mathbf{E}, \mathbf{H} \in C^3 \left([0,T]; [C^3\left(\overline{\Omega}\right)]^3\right)$, *and* $\mathbf{P} \in C^3 \left([0,T]; [C\left(\overline{\Omega}\right)]^3\right)$. *Let* $\xi_{w_\alpha}^m$ *be truncation errors for the Yee scheme for the 3D Maxwell-Debye model* (39) *or equivalently* (40), *where* $w \in \{H, E, P\}$, $m \in \{n, n+\frac{1}{2}\}$, *and* $\alpha \in \{x, y, z\}$. *Then for any* $\alpha \in \{x, y, z\}$,

$$(57) \qquad \max\left\{ \left|\xi_{H_\alpha}^n\right|, \left|\xi_{E_\alpha}^{n+\frac{1}{2}}\right|, \left|\xi_{P_\alpha}^{n+\frac{1}{2}}\right| \right\} \le C_D \left(\Delta x^2 + \Delta y^2 + \Delta z^2 + \Delta t^2 \right),$$

where C_D *is a constant that does not depend on the mesh sizes.*

Proof. Consider equation (39a) of the Yee scheme for the 3D Maxwell-Debye model (39) given as

(58)

$$\frac{1}{\Delta t} \left(H_{x,h_{\ell,j+\frac{1}{2},k+\frac{1}{2}}}^{n+\frac{1}{2}} - H_{x,h_{\ell,j+\frac{1}{2},k+\frac{1}{2}}}^{n-\frac{1}{2}} \right)$$

$$= \frac{1}{\mu_0 \Delta z} \left(E_{y,h_{\ell,j+\frac{1}{2},k+1}}^n - E_{y,h_{\ell,j+\frac{1}{2},k}}^n \right) - \frac{1}{\mu_0 \Delta y} \left(E_{z,h_{\ell,j+1,k+\frac{1}{2}}}^n - E_{z,h_{\ell,j,k+\frac{1}{2}}}^n \right).$$

Substituting the exact solution of the Maxwell-Debye model (7) in the above and expanding using Taylor approximations around $t^n = n\Delta t$ in time and the spatial grid point $(x_\ell, y_{j+\frac{1}{2}}, z_{k+\frac{1}{2}})$ we obtain the truncation error in the form

$$\xi_{H_{x_{\ell,j+\frac{1}{2},k+\frac{1}{2}}}}^n = \frac{\Delta t^2}{24} \, \partial_t^3 H_x(x_\ell, y_{j+\frac{1}{2}}, z_{k+\frac{1}{2}}, t_1^h) - \frac{\Delta z^2}{24\mu_0} \, \partial_z^3 E_y(x_\ell, y_{j+\frac{1}{2}}, z_1^h, t^n)$$

$$(59) \qquad + \frac{\Delta y^2}{24\mu_0} \, \partial_y^3 E_z(x_\ell, y_1^h, z_{k+\frac{1}{2}}, t^n) + \mathcal{O}(\Delta t^4 + \Delta y^4 + \Delta z^4),$$

where $t^{n-\frac{1}{2}} \le t_1^h \le t^{n+\frac{1}{2}}$, $y_{j-\frac{1}{2}} \le y_1^h \le y_{j+\frac{1}{2}}$, $z_{k-\frac{1}{2}} \le z_1^h \le z_{k+\frac{1}{2}}$. Following a similar procedure, the truncation errors of equation (39b)-(39c) are

$$\xi_{H_{y_{\ell+\frac{1}{2},j,k+\frac{1}{2}}}}^n = \frac{\Delta t^2}{24} \, \partial_t^3 H_y(x_{\ell+\frac{1}{2}}, y_j, z_{k+\frac{1}{2}}, t_2^h) - \frac{\Delta x^2}{24\mu_0} \, \partial_x^3 E_z(x_1^h, y_j, z_{k+\frac{1}{2}}, t^n)$$

$$(60) \qquad + \frac{\Delta z^2}{24\mu_0} \, \partial_z^3 E_x(x_{\ell+\frac{1}{2}}, y_j, z_2^h, t^n) + \mathcal{O}(\Delta t^4 + \Delta x^4 + \Delta z^4),$$

$$\xi_{H_{z_{\ell+\frac{1}{2},j+\frac{1}{2},k}}}^n = \frac{\Delta t^2}{24} \, \partial_t^3 H_z(x_{\ell+\frac{1}{2}}, y_{j+\frac{1}{2}}, z_k, t_3^h) - \frac{\Delta y^2}{24\mu_0} \, \partial_y^3 E_x(x_{\ell+\frac{1}{2}}, y_2^h, z_k, t^n)$$

$$(61) \qquad + \frac{\Delta x^2}{24\mu_0} \, \partial_x^3 E_y(x_2^h, y_{j+\frac{1}{2}}, z_k, t^n) + \mathcal{O}(\Delta t^4 + \Delta x^4 + \Delta y^4).$$

where $t^{n-\frac{1}{2}} \leq t_2^h, t_3^h \leq t^{n+\frac{1}{2}}$, $x_{\ell-\frac{1}{2}} \leq x_1^h, x_2^h \leq x_{\ell+\frac{1}{2}}$, $y_{j-\frac{1}{2}} \leq y_2^h \leq y_{j+\frac{1}{2}}$, $z_{k-\frac{1}{2}} \leq z_2^h \leq z_{k+\frac{1}{2}}$.

We follow a similar procedure for the other electromagnetic field components in equations (39d)-(39f) to get the truncation errors

$$
\xi_{E_{x_{\ell+\frac{1}{2},j,k}}}^{n+\frac{1}{2}} = \Delta t^2 \left[\frac{1}{24} \partial_t^3 E_x(x_{\ell+\frac{1}{2}}, y_j, z_k, t_1^e) + \frac{(\epsilon_q - 1)}{8\tau} \partial_t^2 E_x(x_{\ell+\frac{1}{2}}, y_j, z_k, t_2^e) \right.
$$
$$
\left. - \frac{1}{8\tau\epsilon_0\epsilon_\infty} \partial_t^2 P_x(x_{\ell+\frac{1}{2}}, y_j, z_k, t_3^e) \right] - \frac{\Delta y^2}{24\epsilon_0\epsilon_\infty} \partial_y^3 H_z(x_{\ell+\frac{1}{2}}, y_1^e, z_k, t^{n+\frac{1}{2}})
$$
$$
(62\text{a}) \qquad + \frac{\Delta z^2}{24\epsilon_0\epsilon_\infty} \partial_z^3 H_y(x_{\ell+\frac{1}{2}}, y_j, z_1^e, t^{n+\frac{1}{2}}) + \mathcal{O}(\Delta t^4 + \Delta y^4 + \Delta z^4),
$$

$$
\xi_{E_{y_{\ell,j+\frac{1}{2},k}}}^{n+\frac{1}{2}} = \Delta t^2 \left[\frac{1}{24} \partial_t^3 E_y(x_\ell, y_{j+\frac{1}{2}}, z_k, t_4^e) + \frac{(\epsilon_q - 1)}{8\tau} \partial_t^2 E_y(x_\ell, y_{j+\frac{1}{2}}, z_k, t_5^e) \right.
$$
$$
\left. - \frac{1}{8\tau\epsilon_0\epsilon_\infty} \partial_t^2 P_y(x_\ell, y_{j+\frac{1}{2}}, z_k, t_6^e) \right] - \frac{\Delta z^2}{24\epsilon_0\epsilon_\infty} \partial_z^3 H_x(x_\ell, y_{j+\frac{1}{2}}, z_2^e, t^{n+\frac{1}{2}})
$$
$$
(62\text{b}) \qquad + \frac{\Delta x^2}{24\epsilon_0\epsilon_\infty} \partial_x^3 H_z(x_1^e, y_{j+\frac{1}{2}}, z_k, t^{n+\frac{1}{2}}) + \mathcal{O}(\Delta t^4 + \Delta x^4 + \Delta z^4),
$$

$$
\xi_{E_{z_{\ell,j,k+\frac{1}{2}}}}^{n+\frac{1}{2}} = \Delta t^2 \left[\frac{1}{24} \partial_t^3 E_z(x_\ell, y_j, z_{k+\frac{1}{2}}, t_7^e) + \frac{(\epsilon_q - 1)}{8\tau} \partial_t^2 E_z(x_\ell, y_j, z_{k+\frac{1}{2}}, t_8^e) \right.
$$
$$
\left. - \frac{1}{8\tau\epsilon_0\epsilon_\infty} \partial_t^2 P_z(x_\ell, y_j, z_{k+\frac{1}{2}}, t_9^e) \right] - \frac{\Delta x^2}{24\epsilon_0\epsilon_\infty} \partial_x^3 H_y(x_2^e, y_j, z_{k+\frac{1}{2}}, t^{n+\frac{1}{2}})
$$
$$
(62\text{c}) \qquad + \frac{\Delta y^2}{24\epsilon_0\epsilon_\infty} \partial_y^3 H_x(x_\ell, y_2^e, z_{k+\frac{1}{2}}, t^{n+\frac{1}{2}}),
$$

and in (39g)-(39i) as

$$
\xi_{P_{x_{\ell+\frac{1}{2},j,k}}}^{n+\frac{1}{2}} = \Delta t^2 \left[\frac{1}{24} \partial_t^3 P_x(x_{\ell+\frac{1}{2}}, y_j, z_k, t_1^p) - \frac{\epsilon_0\epsilon_\infty(\epsilon_q - 1)}{8\tau} \partial_t^2 E_x(x_{\ell+\frac{1}{2}}, y_j, z_k, t_2^p) \right.
$$
$$
(63\text{a}) \qquad \left. + \frac{1}{8\tau} \partial_t^2 P_x(x_{\ell+\frac{1}{2}}, y_j, z_k, t_3^p) \right] + \mathcal{O}(\Delta t^4),
$$

$$
\xi_{P_{y_{\ell,j+\frac{1}{2},k}}}^{n+\frac{1}{2}} = \Delta t^2 \left[\frac{1}{24} \partial_t^3 P_y(x_\ell, y_{j+\frac{1}{2}}, z_k, t_4^p) - \frac{\epsilon_0\epsilon_\infty(\epsilon_q - 1)}{8\tau} \partial_t^2 E_y(x_\ell, y_{j+\frac{1}{2}}, z_k, t_5^p) \right.
$$
$$
(63\text{b}) \qquad \left. + \frac{1}{8\tau} \partial_t^2 P_y(x_\ell, y_{j+\frac{1}{2}}, z_k, t_6^p) \right] + \mathcal{O}(\Delta t^4),
$$

$$
\xi_{P_{z_{\ell,j,k+\frac{1}{2}}}}^{n+\frac{1}{2}} = \Delta t^2 \left[\frac{1}{24} \partial_t^3 P_z(x_\ell, y_j, z_{k+\frac{1}{2}}, t_7^p) - \frac{\epsilon_0\epsilon_\infty(\epsilon_q - 1)}{8\tau} \partial_t^2 E_z(x_\ell, y_j, z_{k+\frac{1}{2}}, t_8^p) \right.
$$
$$
(63\text{c}) \qquad \left. + \frac{1}{8\tau} \partial_t^2 P_z(x_\ell, y_j, z_{k+\frac{1}{2}}, t_9^p) \right] + \mathcal{O}(\Delta t^4),
$$

where $t^{n-\frac{1}{2}} \leq t_r^e, t_r^p \leq t^{n+\frac{1}{2}}$, $x_{\ell-\frac{1}{2}} \leq x_s^e \leq x_{\ell+\frac{1}{2}}$, $y_{j-\frac{1}{2}} \leq y_s^e \leq y_{j+\frac{1}{2}}$, and $z_{k-\frac{1}{2}} \leq z_s^e \leq z_{k+\frac{1}{2}}$ for $r = \{1, 2, .., 9\}$ and $s = \{1, 2\}$. From the assumed regularity of the exact solution, we can bound the truncation errors to obtain the bound in (57). $\quad\square$

To prove the convergence of the Yee scheme for the 3D Maxwell-Debye model, we first define the error functions

(64a) $$\mathcal{H}_h^n = \mathbf{H}_h^n - \mathbf{H}(t^n),$$

(64b) $$\mathcal{E}_h^n = \mathbf{E}_h^n - \mathbf{E}(t^n),$$

(64c) $$\mathcal{P}_h^n = \mathbf{P}_h^n - \mathbf{P}(t^n),$$

where $\mathbf{H}(t^n), \mathbf{E}(t^n), \mathbf{P}(t^n)$ are the exact solutions to the Maxwell-Debye model in (7), while $\mathbf{H}_h^n, \mathbf{E}_h^n, \mathbf{P}_h^n$ are the solutions to the corresponding Yee scheme in (39) or (40).

The error functions in (64) satisfy the following error equations:

(65a) $$\delta_t \mathcal{H}_h^n = -\frac{1}{\mu_0} \mathbf{curl}_h \, \mathcal{E}_h^n - \vec{\xi}_H^{\,n},$$

(65b) $$\delta_t \mathcal{E}_h^{n+\frac{1}{2}} = \frac{1}{\epsilon_0 \epsilon_\infty} \widetilde{\mathbf{curl}_h} \mathcal{H}_h^{n+\frac{1}{2}} - \frac{\epsilon_q - 1}{\tau} \overline{\mathcal{E}}_h^{n+\frac{1}{2}} + \frac{1}{\tau} \overline{\mathcal{P}}_h^{n+\frac{1}{2}} - \vec{\xi}_E^{\,n+\frac{1}{2}},$$

(65c) $$\delta_t \mathcal{P}_h^{n+\frac{1}{2}} = \frac{\epsilon_0 \epsilon_\infty (\epsilon_q - 1)}{\tau} \overline{\mathcal{E}}_h^{n+\frac{1}{2}} - \frac{1}{\tau} \overline{\mathcal{P}}_h^{n+\frac{1}{2}} - \vec{\xi}_P^{\,n+\frac{1}{2}},$$

where $\vec{\xi}_w^{\,m} = \left(\xi_{w_x}^m, \xi_{w_y}^m, \xi_{w_z}^m \right), w \in \{H, E, P\}$ and $m \in \{n, n+1/2\}$ are the local truncation errors as defined in Lemma 4.1. The convergence of the Yee scheme (39) or (40) for the 3D Maxwell-Debye model is given by the following result:

Theorem 4.2. *Suppose that the solutions to the 3D Maxwell-Debye model (7) satisfy the regularity conditions* $\mathbf{E}, \mathbf{H} \in C^3\left([0,T]; [C^3\left(\overline{\Omega}\right)]^3\right)$, *and* $\mathbf{P} \in C^3\left([0,T]; [C\left(\overline{\Omega}\right)]^3\right)$. *Let* $\xi_{w_\alpha}^n$ *or* $\xi_{w_\alpha}^{n+\frac{1}{2}}$ *be truncation errors of the Yee scheme (39) or (40) for the 3D Maxwell-Debye model where* $w \in \{H, E, P\}$ *and* $\alpha \in \{x, y, z\}$ *satisfying Lemma 4.1. If the stability condition (41) is satisfied, then for any fixed* $T > 0$ *there exists a positive constant* C *depending on the medium parameters, the Courant number* $\nu = c_\infty \Delta t / h$, *but otherwise independent of the mesh parameters, such that the energy of the error at time* $t^n = n\Delta t$, *defined by*

(66)
$$\mathcal{R}_{h,D}^n = \left(\mu_0 \| \mathcal{H}_h^{n-\frac{1}{2}} \|_H^2 + \epsilon_0 \epsilon_\infty \| \mathcal{E}_h^n \|_E^2 + \frac{\| \mathcal{P}_h^n \|_E^2}{\epsilon_0 \epsilon_\infty (\epsilon_q - 1)} - \Delta t \left(\mathbf{curl}_h \, \mathcal{E}_h^n, \mathcal{H}_h^{n-\frac{1}{2}} \right)_H \right)^{\frac{1}{2}},$$

satisfies the bound

(67) $$\mathcal{R}_{h,D}^n \leq \mathcal{R}_{h,D}^0 + CT\left(\Delta x^2 + \Delta y^2 + \Delta z^2 + \Delta t^2 \right).$$

Proof. We use the energy method and follow the proof of Theorem 4.1. Multiplying (65a) by $\Delta^3 \, \mu_0 \overline{\mathcal{H}}_h^n$, (65b) by $\Delta^3 \, \epsilon_0 \epsilon_\infty \overline{\mathcal{E}}_h^{n+\frac{1}{2}}$, and (65c) by $\frac{\Delta^3}{\epsilon_0 \epsilon_\infty (\epsilon_q - 1)} \overline{\mathcal{P}}_h^{n+\frac{1}{2}}$, summing each equation over all spatial nodes, we obtain

(68a) $$\mu_0 \left(\delta_t \mathcal{H}_h^n, \overline{\mathcal{H}}_h^n \right)_H = -\left(\mathbf{curl}_h \, \mathcal{E}_h^n, \overline{\mathcal{H}}_h^n \right)_H - \mu_0 \left(\vec{\xi}_H^{\,n}, \overline{\mathcal{H}}_h^n \right)_H,$$

$$\epsilon_0 \epsilon_\infty \left(\delta_t \mathcal{E}_h^{n+\frac{1}{2}}, \overline{\mathcal{E}}_h^{n+\frac{1}{2}} \right)_E = \left(\widetilde{\mathbf{curl}_h} \mathcal{H}_h^{n+\frac{1}{2}}, \overline{\mathcal{E}}_h^{n+\frac{1}{2}} \right)_E - \frac{\epsilon_0 \epsilon_\infty (\epsilon_q - 1)}{\tau} \| \overline{\mathcal{E}}_h^{n+\frac{1}{2}} \|_E^2$$

(68b) $$+ \frac{1}{\tau} \left(\overline{\mathcal{P}}_h^{n+\frac{1}{2}}, \overline{\mathcal{E}}_h^{n+\frac{1}{2}} \right)_E - \epsilon_0 \epsilon_\infty \left(\vec{\xi}_E^{\,n+\frac{1}{2}}, \overline{\mathcal{E}}_h^{n+\frac{1}{2}} \right)_E,$$

$$\frac{1}{\epsilon_0 \epsilon_\infty (\epsilon_q - 1)} \left(\delta_t \mathcal{P}_h^{n+\frac{1}{2}}, \overline{\mathcal{P}}_h^{n+\frac{1}{2}} \right)_E = \frac{1}{\tau} \left(\overline{\mathcal{E}}_h^{n+\frac{1}{2}}, \overline{\mathcal{P}}_h^{n+\frac{1}{2}} \right)_E - \frac{1}{\tau \epsilon_0 \epsilon_\infty (\epsilon_q - 1)} \| \overline{\mathcal{P}}_h^{n+\frac{1}{2}} \|_E^2$$

(68c) $$- \frac{1}{\epsilon_0 \epsilon_\infty (\epsilon_q - 1)} \left(\vec{\xi}_P^{\,n+\frac{1}{2}}, \overline{\mathcal{P}}_h^{n+\frac{1}{2}} \right)_E.$$

We add all the results in (68) to obtain

$$
\mu_0 \left(\delta_t \mathcal{H}_h^n, \overline{\mathcal{H}}_h^n \right)_H + \epsilon_0 \epsilon_\infty \left(\delta_t \mathcal{E}_h^{n+\frac{1}{2}}, \overline{\mathcal{E}}_h^{n+\frac{1}{2}} \right)_E + \frac{1}{\epsilon_0 \epsilon_\infty (\epsilon_q - 1)} \left(\delta_t \mathcal{P}_h^{n+\frac{1}{2}}, \overline{\mathcal{P}}_h^{n+\frac{1}{2}} \right)_E
$$

$$
= - \left(\mathbf{curl}_h \, \mathcal{E}_h^n, \overline{\mathcal{H}}_h^n \right)_H + \left(\widetilde{\mathbf{curl}_h} \mathcal{H}_h^{n+\frac{1}{2}}, \overline{\mathcal{E}}_h^{n+\frac{1}{2}} \right)_E
$$

$$
- \frac{\epsilon_0 \epsilon_\infty (\epsilon_q - 1)}{\tau} \| \overline{\mathcal{E}}_h^{n+\frac{1}{2}} \|_E^2 + \frac{2}{\tau} \left(\overline{\mathcal{E}}_h^{n+\frac{1}{2}}, \overline{\mathcal{P}}_h^{n+\frac{1}{2}} \right)_E - \frac{1}{\tau \epsilon_0 \epsilon_\infty (\epsilon_q - 1)} \| \overline{\mathcal{P}}_h^{n+\frac{1}{2}} \|_E^2
$$

$$
- \mu_0 \left(\vec{\xi}_H^n, \overline{\mathcal{H}}_h^n \right)_H - \epsilon_0 \epsilon_\infty \left(\vec{\xi}_E^{n+\frac{1}{2}}, \overline{\mathcal{E}}_h^{n+\frac{1}{2}} \right)_E - \frac{1}{\epsilon_0 \epsilon_\infty (\epsilon_q - 1)} \left(\vec{\xi}_P^{n+\frac{1}{2}}, \overline{\mathcal{P}}_h^{n+\frac{1}{2}} \right)_E
$$

$$
= - \left(\mathbf{curl}_h \, \mathcal{E}_h^n, \overline{\mathcal{H}}_h^n \right)_H + \left(\widetilde{\mathbf{curl}_h} \mathcal{H}_h^{n+\frac{1}{2}}, \overline{\mathcal{E}}_h^{n+\frac{1}{2}} \right)_E
$$

$$
- \frac{1}{\tau \epsilon_0 \epsilon_\infty (\epsilon_q - 1)} \| \epsilon_0 \epsilon_\infty (\epsilon_q - 1) \overline{\mathcal{E}}_h^{n+\frac{1}{2}} - \overline{\mathcal{P}}_h^{n+\frac{1}{2}} \|_E^2
$$

$$
- \mu_0 \left(\vec{\xi}_H^n, \overline{\mathcal{H}}_h^n \right)_H - \epsilon_0 \epsilon_\infty \left(\vec{\xi}_E^{n+\frac{1}{2}}, \overline{\mathcal{E}}_h^{n+\frac{1}{2}} \right)_E - \frac{1}{\epsilon_0 \epsilon_\infty (\epsilon_q - 1)} \left(\vec{\xi}_P^{n+\frac{1}{2}}, \overline{\mathcal{P}}_h^{n+\frac{1}{2}} \right)_E
$$

$$
\leq - \left(\mathbf{curl}_h \, \mathcal{E}_h^n, \overline{\mathcal{H}}_h^n \right)_H + \left(\widetilde{\mathbf{curl}_h} \mathcal{H}_h^{n+\frac{1}{2}}, \overline{\mathcal{E}}_h^{n+\frac{1}{2}} \right)_E
$$

(69)

$$
- \mu_0 \left(\vec{\xi}_H^n, \overline{\mathcal{H}}_h^n \right)_H - \epsilon_0 \epsilon_\infty \left(\vec{\xi}_E^{n+\frac{1}{2}}, \overline{\mathcal{E}}_h^{n+\frac{1}{2}} \right)_E - \frac{1}{\epsilon_0 \epsilon_\infty (\epsilon_q - 1)} \left(\vec{\xi}_P^{n+\frac{1}{2}}, \overline{\mathcal{P}}_h^{n+\frac{1}{2}} \right)_E.
$$

The first two terms on the right hand side in the last inequality can be rewritten as

$$
- \left(\mathbf{curl}_h \, \mathcal{E}_h^n, \overline{\mathcal{H}}_h^n \right)_H + \left(\widetilde{\mathbf{curl}_h} \mathcal{H}_h^{n+\frac{1}{2}}, \overline{\mathcal{E}}_h^{n+\frac{1}{2}} \right)_E
$$

(70)
$$
= - \left(\mathbf{curl}_h \, \mathcal{E}_h^n, \overline{\mathcal{H}}_h^n \right)_H + \left(\mathcal{H}_h^{n+\frac{1}{2}}, \mathbf{curl}_h \, \overline{\mathcal{E}}_h^{n+\frac{1}{2}} \right)_H
$$

$$
= \frac{1}{2} \left(\mathcal{H}_h^{n+\frac{1}{2}}, \mathbf{curl}_h \, \mathcal{E}_h^{n+1} \right)_H - \frac{1}{2} \left(\mathcal{H}_h^{n-\frac{1}{2}}, \mathbf{curl}_h \, \mathcal{E}_h^n \right)_H.
$$

Combining the last two steps we get

$$
\mu_0 \left(\delta_t \mathcal{H}_h^n, \overline{\mathcal{H}}_h^n \right)_H + \epsilon_0 \epsilon_\infty \left(\delta_t \mathcal{E}_h^{n+\frac{1}{2}}, \overline{\mathcal{E}}_h^{n+\frac{1}{2}} \right)_E + \frac{1}{\epsilon_0 \epsilon_\infty (\epsilon_q - 1)} \left(\delta_t \mathcal{P}_h^{n+\frac{1}{2}}, \overline{\mathcal{P}}_h^{n+\frac{1}{2}} \right)_E
$$

$$
\leq \frac{1}{2} \left(\mathcal{H}_h^{n+\frac{1}{2}}, \mathbf{curl}_h \, \mathcal{E}_h^{n+1} \right)_H - \frac{1}{2} \left(\mathcal{H}_h^{n-\frac{1}{2}}, \mathbf{curl}_h \, \mathcal{E}_h^n \right)_H
$$

(71)

$$
- \mu_0 \left(\vec{\xi}_H^n, \overline{\mathcal{H}}_h^n \right)_H - \epsilon_0 \epsilon_\infty \left(\vec{\xi}_E^{n+\frac{1}{2}}, \overline{\mathcal{E}}_h^{n+\frac{1}{2}} \right)_E - \frac{1}{\epsilon_0 \epsilon_\infty (\epsilon_q - 1)} \left(\vec{\xi}_P^{n+\frac{1}{2}}, \overline{\mathcal{P}}_h^{n+\frac{1}{2}} \right)_E.
$$

Using the definition of the energy of the error (66) in equation (71) we obtain the inequality

$$
\left(\mathcal{R}_{h,D}^{n+1} \right)^2 - \left(\mathcal{R}_{h,D}^n \right)^2
$$

$$
\leq 2 \Delta t \left| \mu_0 \left(\vec{\xi}_H^n, \overline{\mathcal{H}}_h^n \right)_H + \epsilon_0 \epsilon_\infty \left(\vec{\xi}_E^{n+\frac{1}{2}}, \overline{\mathcal{E}}_h^{n+\frac{1}{2}} \right)_E + \frac{\left(\vec{\xi}_P^{n+\frac{1}{2}}, \overline{\mathcal{P}}_h^{n+\frac{1}{2}} \right)_E}{\epsilon_0 \epsilon_\infty (\epsilon_q - 1)} \right|
$$

(72)

$$
\leq C_1 \Delta t \max \left\{ \| \vec{\xi}_H^n \|_H, \| \vec{\xi}_E^{n+\frac{1}{2}} \|_E, \| \vec{\xi}_P^{n+\frac{1}{2}} \|_E \right\} \left(\| \overline{\mathcal{H}}_h^n \|_H + \| \overline{\mathcal{E}}_h^{n+\frac{1}{2}} \|_E + \| \overline{\mathcal{P}}_h^{n+\frac{1}{2}} \|_E \right),
$$

where C_1 is a constant depending on $\mu_0, \epsilon_0, \epsilon_\infty, \epsilon_q$. Applying Young's inequality with $0 < \gamma \leq 4$, and equation (51), we obtain

$$(73) \qquad \left(\mathbf{curl}_h\, \mathcal{E}_h^n, \mathcal{H}_h^{n-\frac{1}{2}}\right)_H \leq \frac{\gamma\mu_0}{4\Delta t}\|\mathcal{H}_h^{n-\frac{1}{2}}\|_H^2 + \frac{12\Delta t}{h^2\gamma\mu_0}\|\mathcal{E}_h^n\|_E^2.$$

From the definition of the energy of the error in equation (66), we have the inequality

$$\left(\mathcal{R}_{h,D}^n\right)^2 = \mu_0\|\mathcal{H}_h^{n-\frac{1}{2}}\|_H^2 + \epsilon_0\epsilon_\infty\|\mathcal{E}_h^n\|_E^2 + \frac{\|\mathcal{P}_h^n\|_E^2}{\epsilon_0\epsilon_\infty(\epsilon_q - 1)} - \Delta t\left(\mathbf{curl}_h\, \mathcal{E}_h^n, \mathcal{H}_h^{n-\frac{1}{2}}\right)_H$$

$$(74) \qquad \geq \mu_0\left(1 - \frac{\gamma}{4}\right)\|\mathcal{H}_h^{n-\frac{1}{2}}\|_H^2 + \epsilon_0\epsilon_\infty\left(1 - \frac{12\Delta t^2}{\gamma\epsilon_0\epsilon_\infty\mu_0 h^2}\right)\|\mathcal{E}_h^n\|_E^2 + \frac{\|\mathcal{P}_h^n\|_E^2}{\epsilon_0\epsilon_\infty(\epsilon_q - 1)}.$$

If the stability condition (41), $\dfrac{c_\infty\Delta t}{h} < \dfrac{1}{\sqrt{3}}$, is satisfied, all terms on the right side (74) are nonnegative and for $n \geq 0$, we have

$$(75) \qquad \mathcal{R}_{h,D}^n \geq C_2\left(\|\mathcal{H}_h^{n-\frac{1}{2}}\|_H + \|\mathcal{E}_h^n\|_E + \|\mathcal{P}_h^n\|_E\right),$$

where $C_2 = \min\left\{\sqrt{\mu_0\left(1 - \frac{\gamma}{4}\right)}, \sqrt{\epsilon_0\epsilon_\infty\left(1 - \frac{12\Delta t^2}{\gamma\epsilon_0\epsilon_\infty\mu_0 h^2}\right)}, \frac{1}{\sqrt{\epsilon_0\epsilon_\infty(\epsilon_q - 1)}}\right\}$. From (72) and (75), we therefore obtain

$$\left(\mathcal{R}_{h,D}^{n+1}\right)^2 - \left(\mathcal{R}_{h,D}^n\right)^2$$

$$\leq C_1\Delta t \max\left\{\|\vec{\xi}_H^n\|_H, \|\vec{\xi}_E^{n+\frac{1}{2}}\|_E, \|\vec{\xi}_P^{n+\frac{1}{2}}\|_E\right\}\left(\|\overline{\mathcal{H}}_h^n\|_H + \|\overline{\mathcal{E}}_h^{n+\frac{1}{2}}\|_E + \|\overline{\mathcal{P}}_h^{n+\frac{1}{2}}\|_E\right)$$

$$(76)$$

$$\leq C_1 C_2 \Delta t \max\left\{\|\vec{\xi}_H^n\|_H, \|\vec{\xi}_E^{n+\frac{1}{2}}\|_E, \|\vec{\xi}_P^{n+\frac{1}{2}}\|_E\right\}\left(\mathcal{R}_{h,D}^{n+1} + \mathcal{R}_{h,D}^n\right).$$

Dividing by $\mathcal{R}_{h,D}^{n+1} + \mathcal{R}_{h,D}^n$ and rearranging terms in (76), we obtain

$$\mathcal{R}_{h,D}^{n+1} - \mathcal{R}_{h,D}^n \leq C\Delta t \max\left\{\|\vec{\xi}_H^n\|_H, \|\vec{\xi}_E^{n+\frac{1}{2}}\|_E, \|\vec{\xi}_P^{n+\frac{1}{2}}\|_E\right\}$$

$$(77) \qquad \leq C\Delta t\left(\Delta x^2 + \Delta y^2 + \Delta z^2 + \Delta t^2\right)$$

where $C = C_D C_1 C_2$ is a constant depending on medium parameters, the Courant number $\nu = c_\infty\Delta t/h$, and the constant γ. Recursively applying the inequality (77) from n to 0 and using the fact that $T = N\Delta t$, we have

$$\mathcal{R}_{h,D}^n - \mathcal{R}_{h,D}^0 \leq Cn\Delta t\left(\Delta x^2 + \Delta y^2 + \Delta z^2 + \Delta t^2\right)$$

$$(78) \qquad \leq CT\left(\Delta x^2 + \Delta y^2 + \Delta z^2 + \Delta t^2\right).$$

$\square$

4.3. Discrete Divergence: Yee Scheme for the Maxwell-Debye Model.

In this section, we define the discrete divergence operators and show that the electric and magnetic grid functions in the Yee scheme satisfies discrete divergence-free conditions.

We first define the vertex and cell-centered discrete meshes [9]

(79a)

$$\tau_h^{\text{div}\mathbf{E}} := \{(x_i, y_j, z_k) | 0 \leq i \leq I, 0 \leq j \leq J, 0 \leq k \leq K\},$$

(79b)

$$\tau_h^{\text{div}\mathbf{H}} := \left\{(x_{i+\frac{1}{2}}, y_{j+\frac{1}{2}}, z_{k+\frac{1}{2}}) | 0 \leq i \leq I - 1, 0 \leq j \leq J - 1, 0 \leq k \leq K - 1\right\}.$$

Let $\mathbf{F}_h = (F_{x,h}, F_{y,h}, F_{z,h})$ be an electromagnetic grid function. We define the discrete divergence operator, div_h as

$$(80) \qquad \text{div}_h \mathbf{F}_h := \delta_x F_{x,h} + \delta_y F_{y,h} + \delta_z F_{z,h}.$$

As the discrete derivative operators commute, we can show that,

$$(81) \qquad \text{div}_h(\mathbf{curl}_h \, \mathbf{F}_h) = 0.$$

Theorem 4.3. *The discrete divergence of the solutions to the Yee scheme* (39) *or* (40) *for the 3D Maxwell-Debye model is preserved at all time levels $n \geq 0$, i.e., we have the identities,*

$$(82a) \qquad div_h \mathbf{D}_h^n = div_h \mathbf{D}_h^0,$$

$$(82b) \qquad div_h \mathbf{B}_h^{n+\frac{1}{2}} = div_h \mathbf{B}_h^{\frac{1}{2}},$$

where the vector fields $\mathbf{D}_h$ and $\mathbf{B}_h$ are defined on the meshes τ_h^{divE} and τ_h^{divH}, respectively.

Proof. From the Yee scheme for the Maxwell-Debye model (40), applying the operator $\epsilon_0 \epsilon_\infty \Delta t \, \text{div}_h$ on both sides of equation (40b) and applying the operator $\Delta t \, \text{div}_h$ on both sides of equation (40c) and summing the resulting equations, we obtain

$$\text{div}_h(\epsilon_0 \epsilon_\infty \mathbf{E}_h^{n+1}) + \text{div}_h(\mathbf{P}_h^{n+1}) - \text{div}_h(\epsilon_0 \epsilon_\infty \mathbf{E}_h^n) - \text{div}_h(\mathbf{P}_h^n)$$
$$(83) \qquad = \Delta t \, \text{div}_h(\widetilde{\mathbf{curl}_h \mathbf{H}}_h^{n+\frac{1}{2}}).$$

Applying the operator $\mu_0 \Delta t \, \text{div}_h$ on both sides of the equation (40a), we obtain

$$(84) \qquad \text{div}_h(\mu_0 \mathbf{H}_h^{n+\frac{1}{2}}) - \text{div}_h(\mu_0 \mathbf{H}_h^{n-\frac{1}{2}}) = -\Delta t \, \text{div}_h(\mathbf{curl}_h \mathbf{E}_h^n).$$

As the discrete divergence operator is linear, using the identities, $\mathbf{D}_h = \epsilon_0 \epsilon_\infty \mathbf{E}_h + \mathbf{P}_h$ and $\mathbf{B}_h = \mu_0 \mathbf{H}_h$, equation (83) and equation (84) can be written as

$$(85a) \qquad \text{div}_h \mathbf{D}_h^{n+1} - \text{div}_h \mathbf{D}_h^n = 0,$$

$$(85b) \qquad \text{div}_h \mathbf{B}_h^{n+\frac{1}{2}} - \text{div}_h \mathbf{B}_h^{n-\frac{1}{2}} = 0.$$

We apply the equation (85) recursively from time level n to obtain (82a) and (82b), respectively. □

5. Yee Scheme for the Maxwell-Lorentz System

The fully discrete Yee scheme for the 3D Maxwell-Lorentz system (15) can be constructed as

$$(86a) \quad \delta_t H^n_{x,h_{\ell,j+\frac{1}{2},k+\frac{1}{2}}} = \frac{1}{\mu_0}\left(\delta_z E^n_{y,h_{\ell,j+\frac{1}{2},k+\frac{1}{2}}} - \delta_y E^n_{z,h_{\ell,j+\frac{1}{2},k+\frac{1}{2}}}\right),$$

$$(86b) \quad \delta_t H^n_{y,h_{\ell+\frac{1}{2},j,k+\frac{1}{2}}} = \frac{1}{\mu_0}\left(\delta_x E^n_{z,h_{\ell+\frac{1}{2},j,k+\frac{1}{2}}} - \delta_z E^n_{x,h_{\ell+\frac{1}{2},j,k+\frac{1}{2}}}\right),$$

$$(86c) \quad \delta_t H^n_{z,h_{\ell+\frac{1}{2},j+\frac{1}{2},k}} = \frac{1}{\mu_0}\left(\delta_y E^n_{x,h_{\ell+\frac{1}{2},j+\frac{1}{2},k}} - \delta_x E^n_{y,h_{\ell+\frac{1}{2},j+\frac{1}{2},k}}\right),$$

$$(86d) \quad \delta_t E^{n+\frac{1}{2}}_{x,h_{\ell+\frac{1}{2},j,k}} = \frac{1}{\epsilon_0\epsilon_\infty}\left(\delta_y H^{n+\frac{1}{2}}_{z,h_{\ell+\frac{1}{2},j,k}} - \delta_z H^{n+\frac{1}{2}}_{y,h_{\ell+\frac{1}{2},j,k}}\right) - \frac{1}{\epsilon_0\epsilon_\infty}\overline{J}^{n+\frac{1}{2}}_{x,h_{\ell+\frac{1}{2},j,k}},$$

$$(86e) \quad \delta_t E^{n+\frac{1}{2}}_{y,h_{\ell,j+\frac{1}{2},k}} = \frac{1}{\epsilon_0\epsilon_\infty}\left(\delta_z H^{n+\frac{1}{2}}_{x,h_{\ell,j+\frac{1}{2},k}} - \delta_x H^{n+\frac{1}{2}}_{z,h_{\ell,j+\frac{1}{2},k}}\right) - \frac{1}{\epsilon_0\epsilon_\infty}\overline{J}^{n+\frac{1}{2}}_{y,h_{\ell,j+\frac{1}{2},k}},$$

$$(86f) \quad \delta_t E^{n+\frac{1}{2}}_{z,h_{\ell,j,k+\frac{1}{2}}} = \frac{1}{\epsilon_0\epsilon_\infty}\left(\delta_x H^{n+\frac{1}{2}}_{y,h_{\ell,j,k+\frac{1}{2}}} - \delta_y H^{n+\frac{1}{2}}_{x,h_{\ell,j,k+\frac{1}{2}}}\right) - \frac{1}{\epsilon_0\epsilon_\infty}\overline{J}^{n+\frac{1}{2}}_{z,h_{\ell,j,k+\frac{1}{2}}},$$

$$(86g) \quad \delta_t J^{n+\frac{1}{2}}_{x,h_{\ell+\frac{1}{2},j,k}} = -\frac{1}{\tau}\overline{J}^{n+\frac{1}{2}}_{x,h_{\ell+\frac{1}{2},j,k}} - \omega_0^2\overline{P}^{n+\frac{1}{2}}_{x,h_{\ell+\frac{1}{2},j,k}} + \epsilon_0\omega_p^2\overline{E}^{n+\frac{1}{2}}_{x,h_{\ell+\frac{1}{2},j,k}},$$

$$(86h) \quad \delta_t J^{n+\frac{1}{2}}_{y,h_{\ell,j+\frac{1}{2},k}} = -\frac{1}{\tau}\overline{J}^{n+\frac{1}{2}}_{y,h_{\ell,j+\frac{1}{2},k}} - \omega_0^2\overline{P}^{n+\frac{1}{2}}_{y,h_{\ell,j+\frac{1}{2},k}} + \epsilon_0\omega_p^2\overline{E}^{n+\frac{1}{2}}_{y,h_{\ell,j+\frac{1}{2},k}},$$

$$(86i) \quad \delta_t J^{n+\frac{1}{2}}_{z,h_{\ell,j,k+\frac{1}{2}}} = -\frac{1}{\tau}\overline{J}^{n+\frac{1}{2}}_{z,h_{\ell,j,k+\frac{1}{2}}} - \omega_0^2\overline{P}^{n+\frac{1}{2}}_{z,h_{\ell,j,k+\frac{1}{2}}} + \epsilon_0\omega_p^2\overline{E}^{n+\frac{1}{2}}_{z,h_{\ell,j,k+\frac{1}{2}}},$$

$$(86j) \quad \delta_t P^{n+\frac{1}{2}}_{x,h_{\ell+\frac{1}{2},j,k}} = \overline{J}^{n+\frac{1}{2}}_{x,h_{\ell+\frac{1}{2},j,k}},$$

$$(86k) \quad \delta_t P^{n+\frac{1}{2}}_{y,h_{\ell,j+\frac{1}{2},k}} = \overline{J}^{n+\frac{1}{2}}_{y,h_{\ell,j+\frac{1}{2},k}},$$

$$(86l) \quad \delta_t P^{n+\frac{1}{2}}_{z,h_{\ell,j,k+\frac{1}{2}}} = \overline{J}^{n+\frac{1}{2}}_{z,h_{\ell,j,k+\frac{1}{2}}}.$$

Then the scheme (86) can be written as follows

$$(87a) \quad \delta_t \mathbf{H}^n_h = -\frac{1}{\mu_0}\operatorname{\mathbf{curl}_h}\mathbf{E}^n_h,$$

$$(87b) \quad \delta_t \mathbf{E}^{n+\frac{1}{2}}_h = \frac{1}{\epsilon_0\epsilon_\infty}\widetilde{\operatorname{\mathbf{curl}_h}}\mathbf{H}^{n+\frac{1}{2}}_h - \frac{1}{\epsilon_0\epsilon_\infty}\overline{\mathbf{J}}^{n+\frac{1}{2}}_h,$$

$$(87c) \quad \delta_t \mathbf{J}^{n+\frac{1}{2}}_h = -\frac{1}{\tau}\overline{\mathbf{J}}^{n+\frac{1}{2}}_h - \omega_0^2\overline{\mathbf{P}}^{n+\frac{1}{2}}_h + \epsilon_0\omega_p^2\overline{\mathbf{E}}^{n+\frac{1}{2}}_h,$$

$$(87d) \quad \delta_t \mathbf{P}^{n+\frac{1}{2}}_h = \overline{\mathbf{J}}^{n+\frac{1}{2}}_h.$$

5.1. The Stability Analysis of the Yee Scheme for Lorentz Media.
In this section, we show that the solution of the fully discrete scheme (86) satisfies the energy decay property by the following theorem.

Theorem 5.1. *If the time step and uniform mesh spatial step sizes satisfy the stability condition*

$$(88) \quad \frac{c_\infty \Delta t}{h} < \frac{1}{\sqrt{3}},$$

where $c_\infty = 1/\sqrt{\mu_0\epsilon_0\epsilon_\infty}$, *then the discrete solutions of the 3D Yee-FDTD scheme for the Maxwell-Lorentz equations* (87) *satisfy the discrete energy decay,*

$$(89) \qquad\qquad\qquad \mathcal{E}_{h,L}^{n+1} \le \mathcal{E}_{h,L}^n,$$

for all $n \ge 0$ *where a discrete energy is defined by*

$$\mathcal{E}_{h,L}^n = \Big(\mu_0\|\mathbf{H}_h^{n-\frac{1}{2}}\|_H^2 + \epsilon_0\epsilon_\infty\|\mathbf{E}_h^n\|_E^2 + \frac{\|\mathbf{J}_h^n\|_E^2}{\epsilon_0\omega_p{}^2} + \frac{\|\mathbf{P}_h^n\|_E^2}{\epsilon_0\epsilon_\infty(\epsilon_q-1)}$$

$$(90) \qquad\qquad - \Delta t \left(\mathbf{curl}_\mathrm{h}\,\mathbf{E}_h^n, \mathbf{H}_h^{n-\frac{1}{2}}\right)_H \Big)^{\frac{1}{2}}.$$

Proof. Multiplying (86a) by $\Delta^3\ \mu_0\overline{H}_{x,h_{\ell,j+\frac{1}{2},k+\frac{1}{2}}}^n$, (86b) by $\Delta^3\ \mu_0\overline{H}_{y,h_{\ell+\frac{1}{2},j,k+\frac{1}{2}}}^n$, (86c) by $\Delta^3\ \mu_0\overline{H}_{z,h_{\ell+\frac{1}{2},j+\frac{1}{2},k}}^n$, summing each equation over all spatial nodes, and adding all the results, we obtain

$$(91) \qquad \frac{\mu_0}{2\Delta t}\left(\|\mathbf{H}_h^{n+\frac{1}{2}}\|_H^2 - \|\mathbf{H}_h^{n-\frac{1}{2}}\|_H^2\right) = -\left(\mathbf{curl}_\mathrm{h}\,\mathbf{E}_h^n, \overline{\mathbf{H}}_h^n\right)_H.$$

Secondly, multiplying (86d) by $\Delta^3\ \epsilon_0\epsilon_\infty\overline{E}_{x,h_{\ell+\frac{1}{2},j,k}}^{n+\frac{1}{2}}$, (86e) by $\Delta^3\ \epsilon_0\epsilon_\infty\overline{E}_{y,h_{\ell,j+\frac{1}{2},k}}^{n+\frac{1}{2}}$, (86f) by $\Delta^3\ \epsilon_0\epsilon_\infty\overline{E}_{z,h_{\ell,j,k+\frac{1}{2}}}^{n+\frac{1}{2}}$, summing each equation over all spatial nodes, and adding all the results, we obtain

$$(92) \quad \frac{\epsilon_0\epsilon_\infty}{2\Delta t}\left(\|\mathbf{E}_h^{n+1}\|_E^2 - \|\mathbf{E}_h^n\|_E^2\right) = \left(\widetilde{\mathbf{curl}_\mathrm{h}}\mathbf{H}_h^{n+\frac{1}{2}}, \overline{\mathbf{E}}_h^{n+\frac{1}{2}}\right)_E - \left(\overline{\mathbf{J}}_h^{n+\frac{1}{2}}, \overline{\mathbf{E}}_h^{n+\frac{1}{2}}\right)_E.$$

Next, multiplying (86g) by $\dfrac{\Delta^3}{\epsilon_0\omega_p{}^2}\overline{J}_{x,h_{\ell+\frac{1}{2},j,k}}^{n+\frac{1}{2}}$, (86h) by $\dfrac{\Delta^3}{\epsilon_0\omega_p{}^2}\overline{J}_{y,h_{\ell,j+\frac{1}{2},k}}^{n+\frac{1}{2}}$, (86i) by $\dfrac{\Delta^3}{\epsilon_0\omega_p{}^2}\overline{J}_{z,h_{\ell,j,k+\frac{1}{2}}}^{n+\frac{1}{2}}$, summing each equation over all spatial nodes, and adding all the results, we obtain

$$(93)$$
$$\frac{\|\mathbf{J}_h^{n+1}\|_E^2 - \|\mathbf{J}_h^n\|_E^2}{2\Delta t\epsilon_0\omega_p{}^2} = -\frac{\|\overline{\mathbf{J}}_h^{n+\frac{1}{2}}\|_E^2}{\tau\epsilon_0\omega_p{}^2} - \frac{\omega_0^2}{\epsilon_0\omega_p{}^2}\left(\overline{\mathbf{P}}_h^{n+\frac{1}{2}}, \overline{\mathbf{J}}_h^{n+\frac{1}{2}}\right)_E + \left(\overline{\mathbf{E}}_h^{n+\frac{1}{2}}, \overline{\mathbf{J}}_h^{n+\frac{1}{2}}\right)_E.$$

Finally, multiplying (86j) by $\dfrac{\Delta^3\ \overline{P}_{x,h_{\ell+\frac{1}{2},j,k}}^{n+\frac{1}{2}}}{\epsilon_0\epsilon_\infty(\epsilon_q-1)}$, (86k) by $\dfrac{\Delta^3\ \overline{P}_{y,h_{\ell,j+\frac{1}{2},k}}^{n+\frac{1}{2}}}{\epsilon_0\epsilon_\infty(\epsilon_q-1)}$, and (86l) by $\dfrac{\Delta^3}{\epsilon_0\epsilon_\infty(\epsilon_q-1)}\overline{P}_{z,h_{\ell,j,k+\frac{1}{2}}}^{n+\frac{1}{2}}$, summing each equation over all spatial nodes, and finally adding all the results, we obtain

$$(94) \quad \frac{1}{2\epsilon_0\epsilon_\infty(\epsilon_q-1)\Delta t}\left(\|\mathbf{P}_h^{n+1}\|_E^2 - \|\mathbf{P}_h^n\|_E^2\right) = \frac{1}{\epsilon_0\epsilon_\infty(\epsilon_q-1)}\left(\overline{\mathbf{J}}_h^{n+\frac{1}{2}}, \overline{\mathbf{P}}_h^{n+\frac{1}{2}}\right)_E.$$

Adding all equations (91)-(94) and using a discrete analogue of integration by parts [9], we obtain

$$\frac{\mu_0}{2\Delta t}\left(\|\mathbf{H}_h^{n+\frac{1}{2}}\|_H^2 - \|\mathbf{H}_h^{n-\frac{1}{2}}\|_H^2\right) + \frac{\epsilon_0\epsilon_\infty}{2\Delta t}\left(\|\mathbf{E}_h^{n+1}\|_E^2 - \|\mathbf{E}_h^n\|_E^2\right)$$

$$+ \frac{\left(\|\mathbf{J}_h^{n+1}\|_E^2 - \|\mathbf{J}_h^n\|_E^2\right)}{2\Delta t\epsilon_0\omega_p{}^2} + \frac{\left(\|\mathbf{P}_h^{n+1}\|_E^2 - \|\mathbf{P}_h^n\|_E^2\right)}{2\epsilon_0\epsilon_\infty(\epsilon_q-1)\Delta t}$$

$$= -\left(\mathbf{curl}_h\,\mathbf{E}_h^n, \overline{\mathbf{H}}_h^n\right)_H + \left(\widetilde{\mathbf{curl}_h}\mathbf{H}_h^{n+\frac{1}{2}}, \overline{\mathbf{E}}_h^{n+\frac{1}{2}}\right)_E - \frac{1}{\tau\epsilon_0\omega_p{}^2}\|\overline{\mathbf{J}}_h^{n+\frac{1}{2}}\|_E^2$$

$$(95)\quad = -\frac{1}{2}\left(\mathbf{curl}_h\,\mathbf{E}_h^n, \mathbf{H}_h^{n-\frac{1}{2}}\right)_H + \frac{1}{2}\left(\widetilde{\mathbf{curl}_h}\mathbf{H}_h^{n+\frac{1}{2}}, \mathbf{E}_h^{n+1}\right)_E - \frac{1}{\tau\epsilon_0\omega_p{}^2}\|\overline{\mathbf{J}}_h^{n+\frac{1}{2}}\|_E^2.$$

We can convert equation (95) into the inequality

$$\mu_0\left(\|\mathbf{H}_h^{n+\frac{1}{2}}\|_H^2 - \|\mathbf{H}_h^{n-\frac{1}{2}}\|_H^2\right) + \epsilon_0\epsilon_\infty\left(\|\mathbf{E}_h^{n+1}\|_E^2 - \|\mathbf{E}_h^n\|_E^2\right)$$

$$+ \frac{\left(\|\mathbf{J}_h^{n+1}\|_E^2 - \|\mathbf{J}_h^n\|_E^2\right)}{\epsilon_0\omega_p{}^2} + \frac{\left(\|\mathbf{P}_h^{n+1}\|_E^2 - \|\mathbf{P}_h^n\|_E^2\right)}{\epsilon_0\epsilon_\infty(\epsilon_q-1)}$$

$$(96)\quad \leq \Delta t\left(\widetilde{\mathbf{curl}_h}\mathbf{H}_h^{n+\frac{1}{2}}, \mathbf{E}_h^{n+1}\right)_E - \Delta t\left(\mathbf{curl}_h\,\mathbf{E}_h^n, \mathbf{H}_h^{n-\frac{1}{2}}\right)_H.$$

Using the definition of the discrete energy function (90), the inequality (96) becomes

$$(97)\qquad\qquad \left(\mathcal{E}_{h,L}^{n+1}\right)^2 \leq \left(\mathcal{E}_{h,L}^n\right)^2,$$

which applies for all $n \geq 0$.

We follow a similar procedure to the Debye case to confirm conditional stability by showing that $\mathcal{E}_{h,L}^n$ is a discrete energy function. By the inequality (51), we have

$$\mu_0\|\mathbf{H}_h^{n-\frac{1}{2}}\|_H^2 + \epsilon_0\epsilon_\infty\|\mathbf{E}_h^n\|_E^2 + \frac{\|\mathbf{J}_h^n\|_E^2}{\epsilon_0\omega_p{}^2} + \frac{\|\mathbf{P}_h^n\|_E^2}{\epsilon_0\epsilon_\infty(\epsilon_q-1)} - \Delta t\left(\mathbf{curl}_h\,\mathbf{E}_h^n, \mathbf{H}_h^{n-\frac{1}{2}}\right)_H$$

$$(98)\qquad \geq \epsilon_0\epsilon_\infty\left(1 - \frac{3\Delta t^2}{h^2\mu_0\epsilon_0\epsilon_\infty}\right)\|\mathbf{E}_h^n\|_E^2.$$

Thus, the discrete energy function (90) is positive when

$$(99)\qquad\qquad \frac{3\Delta t^2}{h^2\mu_0\epsilon_0\epsilon_\infty} < 1 \quad\Leftrightarrow\quad \frac{3c_\infty^2\Delta t^2}{h^2} < 1,$$

so the stability condition (88) holds. $\qquad\square$

Remark 5.1. *The stability condition on nonuniform spatial meshes for the 3D Yee-FDTD Maxwell-Lorentz scheme is identical to the stability criterion in Remark 4.1.*

5.2. Error Estimates and Convergence of the Yee Scheme for the Maxwell-Lorentz Model. In this section, we first analyze the truncation errors in the Yee scheme for the Maxwell-Lorentz model and then prove convergence of the scheme.

Lemma 5.1. *Suppose that the solutions to the 3D Maxwell-Lorentz model (15) satisfy the regularity conditions* $\mathbf{E}, \mathbf{H} \in C^3\left([0,T]; [C^3\left(\overline{\Omega}\right)]^3\right)$, *and* $\mathbf{J}, \mathbf{P} \in C^3\left([0,T]; [C\left(\overline{\Omega}\right)]^3\right)$. *Let* $\psi_{w_\alpha}^m$ *be truncation errors for the Yee scheme for the 3D Maxwell-Lorentz model, (86) or equivalently (87), where* $w \in \{H, E, J, P\}$, $m \in \{n, n+\frac{1}{2}\}$, *and* $\alpha \in \{x, y, z\}$. *Then for any* $\alpha \in \{x, y, z\}$,

$$(100)\quad \max\left\{\left|\psi_{H_\alpha}^n\right|, \left|\psi_{E_\alpha}^{n+\frac{1}{2}}\right|, \left|\psi_{J_\alpha}^{n+\frac{1}{2}}\right|, \left|\psi_{P_\alpha}^{n+\frac{1}{2}}\right|\right\} \leq C_L\left(\Delta x^2 + \Delta y^2 + \Delta z^2 + \Delta t^2\right),$$

where C_L is a constant and does not depend on the mesh sizes.

Proof. From equation (86a), its scalar form is

$$(101) \quad \frac{1}{\Delta t}\left(H_{x,h_{\ell,j+\frac{1}{2},k+\frac{1}{2}}}^{n+\frac{1}{2}} - H_{x,h_{\ell,j+\frac{1}{2},k+\frac{1}{2}}}^{n-\frac{1}{2}}\right)$$
$$= \frac{1}{\mu_0\Delta z}\left(E_{y,h_{\ell,j+\frac{1}{2},k+1}}^{n} - E_{y,h_{\ell,j+\frac{1}{2},k}}^{n}\right) - \frac{1}{\mu_0\Delta y}\left(E_{z,h_{\ell,j+1,k+\frac{1}{2}}}^{n} - E_{z,h_{\ell,j,k+\frac{1}{2}}}^{n}\right).$$

We substitute in the exact solutions and perform the Taylor expansions to obtain truncation errors in the form

$$\psi_{H_{x_{\ell,j+\frac{1}{2},k+\frac{1}{2}}}}^{n} = \frac{\Delta t^2}{24}\partial_t^3 H_x(x_\ell, y_{j+\frac{1}{2}}, z_{k+\frac{1}{2}}, t_1^h) - \frac{\Delta z^2}{24\mu_0}\partial_z^3 E_y(x_\ell, y_{j+\frac{1}{2}}, z_1^h, t^n)$$
$$(102) \qquad + \frac{\Delta y^2}{24\mu_0}\partial_y^3 E_z(x_\ell, y_1^h, z_{k+\frac{1}{2}}, t^n) + \mathcal{O}(\Delta t^4 + \Delta y^4 + \Delta z^4),$$

where $t^{n-\frac{1}{2}} \le t_1^h \le t^{n+\frac{1}{2}}$, $y_{j-\frac{1}{2}} \le y_1^h \le y_{j+\frac{1}{2}}$, $z_{k-\frac{1}{2}} \le z_1^h \le z_{k+\frac{1}{2}}$. Following a similar procedure, the truncation errors of equation (86b)-(86c) are

$$\psi_{H_{y_{\ell+\frac{1}{2},j,k+\frac{1}{2}}}}^{n} = \frac{\Delta t^2}{24}\partial_t^3 H_y(x_{\ell+\frac{1}{2}}, y_j, z_{k+\frac{1}{2}}, t_2^h) - \frac{\Delta x^2}{24\mu_0}\partial_x^3 E_z(x_1^h, y_j, z_{k+\frac{1}{2}}, t^n)$$
$$(103) \qquad + \frac{\Delta z^2}{24\mu_0}\partial_z^3 E_x(x_{\ell+\frac{1}{2}}, y_j, z_2^h, t^n) + \mathcal{O}(\Delta t^4 + \Delta x^4 + \Delta z^4),$$

$$\psi_{H_{z_{\ell+\frac{1}{2},j+\frac{1}{2},k}}}^{n} = \frac{\Delta t^2}{24}\partial_t^3 H_z(x_{\ell+\frac{1}{2}}, y_{j+\frac{1}{2}}, z_k, t_3^h) - \frac{\Delta y^2}{24\mu_0}\partial_y^3 E_x(x_{\ell+\frac{1}{2}}, y_2^h, z_k, t^n)$$
$$(104) \qquad + \frac{\Delta x^2}{24\mu_0}\partial_x^3 E_y(x_2^h, y_{j+\frac{1}{2}}, z_k, t^n) + \mathcal{O}(\Delta t^4 + \Delta x^4 + \Delta y^4),$$

where $t^{n-\frac{1}{2}} \le t_2^h, t_3^h \le t^{n+\frac{1}{2}}$, $x_{\ell-\frac{1}{2}} \le x_1^h, x_2^h \le x_{\ell+\frac{1}{2}}$, $y_{j-\frac{1}{2}} \le y_2^h \le y_{j+\frac{1}{2}}$, $z_{k-\frac{1}{2}} \le z_2^h \le z_{k+\frac{1}{2}}$. We follow a similar procedure for the other electromagnetic field components in (86d)-(86f) as

$$\psi_{E_{x_{\ell+\frac{1}{2},j,k}}}^{n+\frac{1}{2}} = \Delta t^2\left[\frac{1}{24}\partial_t^3 E_x(x_{\ell+\frac{1}{2}}, y_j, z_k, t_1^e) + \frac{1}{8\epsilon_0\epsilon_\infty}\partial_t^2 J_x(x_{\ell+\frac{1}{2}}, y_j, z_k, t_2^e)\right]$$
$$- \frac{\Delta y^2}{24\epsilon_0\epsilon_\infty}\partial_y^3 H_z(x_{\ell+\frac{1}{2}}, y_1^e, z_k, t^{n+\frac{1}{2}}) + \frac{\Delta z^2}{24\epsilon_0\epsilon_\infty}\partial_z^3 H_y(x_{\ell+\frac{1}{2}}, y_j, z_1^e, t^{n+\frac{1}{2}})$$
$$(105a) \qquad + \mathcal{O}(\Delta t^4 + \Delta y^4 + \Delta z^4),$$

$$\psi_{E_{y_{\ell,j+\frac{1}{2},k}}}^{n+\frac{1}{2}} = \Delta t^2\left[\frac{1}{24}\partial_t^3 E_y(x_\ell, y_{j+\frac{1}{2}}, z_k, t_3^e) + \frac{1}{8\epsilon_0\epsilon_\infty}\partial_t^2 J_y(x_\ell, y_{j+\frac{1}{2}}, z_k, t_4^e)\right]$$
$$- \frac{\Delta z^2}{24\epsilon_0\epsilon_\infty}\partial_z^3 H_x(x_\ell, y_{j+\frac{1}{2}}, z_2^e, t^{n+\frac{1}{2}}) + \frac{\Delta x^2}{24\epsilon_0\epsilon_\infty}\partial_x^3 H_z(x_1^e, y_{j+\frac{1}{2}}, z_k, t^{n+\frac{1}{2}})$$
$$(105b) \qquad + \mathcal{O}(\Delta t^4 + \Delta x^4 + \Delta z^4),$$

$$\psi_{E_{z_{\ell,j,k+\frac{1}{2}}}}^{n+\frac{1}{2}} = \Delta t^2\left[\frac{1}{24}\partial_t^3 E_z(x_\ell, y_j, z_{k+\frac{1}{2}}, t_5^e) + \frac{1}{8\epsilon_0\epsilon_\infty}\partial_t^2 J_z(x_\ell, y_j, z_{k+\frac{1}{2}}, t_6^e)\right]$$
$$- \frac{\Delta x^2}{24\epsilon_0\epsilon_\infty}\partial_x^3 H_y(x_2^e, y_j, z_{k+\frac{1}{2}}, t^{n+\frac{1}{2}}) + \frac{\Delta y^2}{24\epsilon_0\epsilon_\infty}\partial_y^3 H_x(x_\ell, y_2^e, z_{k+\frac{1}{2}}, t^{n+\frac{1}{2}})$$
$$(105c) \qquad + \mathcal{O}(\Delta t^4 + \Delta x^4 + \Delta y^4),$$

and in (86g)-(86i) as

$$\psi_{J_{x_{\ell+\frac{1}{2},j,k}}}^{n+\frac{1}{2}} = \frac{\Delta t^2}{24}\left[\partial_t^3 J_x(x_{\ell+\frac{1}{2}},y_j,z_k,t_1^j) + 3\partial_t^2 J_x(x_{\ell+\frac{1}{2}},y_j,z_k,t_2^j)\right.$$

$$(106a) \qquad \left. + 3\omega_0^2\partial_t^2 P_x(x_{\ell+\frac{1}{2}},y_j,z_k,t_3^j) - 3\epsilon_0\omega_p{}^2 E_x(x_{\ell+\frac{1}{2}},y_j,z_k,t_4^j)\right] + \mathcal{O}(\Delta t^4),$$

$$\psi_{J_{y_{\ell,j+\frac{1}{2},k}}}^{n+\frac{1}{2}} = \frac{\Delta t^2}{24}\left[\partial_t^3 J_y(x_\ell,y_{j+\frac{1}{2}},z_k,t_5^j) + 3\partial_t^2 J_y(x_\ell,y_{j+\frac{1}{2}},z_k,t_6^j)\right.$$

$$(106b) \qquad \left. + 3\omega_0^2\partial_t^2 P_y(x_\ell,y_{j+\frac{1}{2}},z_k,t_7^j) - 3\epsilon_0\omega_p{}^2 E_y(x_\ell,y_{j+\frac{1}{2}},z_k,t_8^j)\right] + \mathcal{O}(\Delta t^4),$$

$$\psi_{J_{z_{\ell,j,k+\frac{1}{2}}}}^{n+\frac{1}{2}} = \frac{\Delta t^2}{24}\left[\partial_t^3 J_z(x_\ell,y_j,z_{k+\frac{1}{2}},t_9^j) + 3\partial_t^2 J_z(x_\ell,y_j,z_{k+\frac{1}{2}},t_{10}^j)\right.$$

$$(106c) \qquad \left. + 3\omega_0^2\partial_t^2 P_z(x_\ell,y_j,z_{k+\frac{1}{2}},t_{11}^j) - 3\epsilon_0\omega_p{}^2 E_z(x_\ell,y_j,z_{k+\frac{1}{2}},t_{12}^j)\right] + \mathcal{O}(\Delta t^4),$$

and finally in (86j)-(86l) as

(107a)
$$\psi_{P_{x_{\ell+\frac{1}{2},j,k}}}^{n+\frac{1}{2}} = \frac{\Delta t^2}{24}\left[\partial_t^3 P_x(x_{\ell+\frac{1}{2}},y_j,z_k,t_1^p) - 3\partial_t^2 J_x(x_{\ell+\frac{1}{2}},y_j,z_k,t_2^p)\right] + \mathcal{O}(\Delta t^4),$$

(107b)
$$\psi_{P_{y_{\ell,j+\frac{1}{2},k}}}^{n+\frac{1}{2}} = \frac{\Delta t^2}{24}\left[\partial_t^3 P_y(x_\ell,y_{j+\frac{1}{2}},z_k,t_3^p) - 3\partial_t^2 J_y(x_\ell,y_{j+\frac{1}{2}},z_k,t_4^p)\right] + \mathcal{O}(\Delta t^4),$$

(107c)
$$\psi_{P_{z_{\ell,j,k+\frac{1}{2}}}}^{n+\frac{1}{2}} = \frac{\Delta t^2}{24}\left[\partial_t^3 P_z(x_\ell,y_j,z_{k+\frac{1}{2}},t_5^p) - 3\partial_t^2 J_z(x_\ell,y_j,z_{k+\frac{1}{2}},t_6^p)\right] + \mathcal{O}(\Delta t^4).$$

where $t^{n-\frac{1}{2}} \leq t_r^e, t_r^j, t_r^p \leq t^{n+\frac{1}{2}}$, $x_{\ell-\frac{1}{2}} \leq x_s^e \leq x_{\ell+\frac{1}{2}}$, $y_{j-\frac{1}{2}} \leq y_s^e \leq y_{j+\frac{1}{2}}$, and $z_{k-\frac{1}{2}} \leq z_s^e \leq z_{k+\frac{1}{2}}$ for $r = \{1,2,..,12\}$ and $s = \{1,2\}$. From the assumed regularity of the exact solution, we can bound the truncation errors to obtain the bound in (100). □

To prove the convergence of the Yee scheme for the 3D Maxwell-Lorentz model, we follow a similar procedure to the convergence analysis in Theorem 4.2. We use the error functions (64) and define the additional one

$$(108) \qquad\qquad \mathcal{J}_h^n = \mathbf{J}_h^n - \mathbf{J}(t^n).$$

In combining these variables (64) and (108), we arrive at the error equations of the Yee scheme for the 3D Maxwell-Lorentz model:

$$(109a) \qquad\qquad \delta_t\mathcal{H}_h^n = -\frac{1}{\mu_0}\mathbf{curl}_h\,\mathcal{E}_h^n - \vec{\psi}_H^n,$$

$$(109b) \qquad\qquad \delta_t\mathcal{E}_h^{n+\frac{1}{2}} = \frac{1}{\epsilon_0\epsilon_\infty}\widetilde{\mathbf{curl}}_h\mathcal{H}_h^{n+\frac{1}{2}} - \frac{1}{\epsilon_0\epsilon_\infty}\overline{\mathcal{J}}_h^{n+\frac{1}{2}} - \vec{\psi}_E^{n+\frac{1}{2}},$$

$$(109c) \qquad\qquad \delta_t\mathcal{J}_h^{n+\frac{1}{2}} = -\frac{1}{\tau}\overline{\mathcal{J}}_h^{n+\frac{1}{2}} - \omega_0^2\overline{\mathcal{P}}_h^{n+\frac{1}{2}} + \epsilon_0\omega_p{}^2\overline{\mathcal{E}}_h^{n+\frac{1}{2}} - \vec{\psi}_J^{n+\frac{1}{2}},$$

$$(109d) \qquad\qquad \delta_t\mathcal{P}_h^{n+\frac{1}{2}} = \overline{\mathcal{J}}_h^{n+\frac{1}{2}} - \vec{\psi}_P^{n+\frac{1}{2}},$$

where $\vec{\psi}_w^m = \left(\psi_{w_x}^m, \psi_{w_y}^m, \psi_{w_z}^m\right)$, $w \in \{H,E,J,P\}$ and $m \in \{n,n+1/2\}$. The convergence property of the Yee scheme for the 3D Maxwell-Lorentz model is given by the following result:

Theorem 5.2. *Suppose that the solutions to the 3D Maxwell-Lorentz model* (15) *satisfy the regularity conditions* $\mathbf{E}_h, \mathbf{H}_h \in C^3\left([0,T]; [C^3\left(\overline{\Omega}\right)]^3\right)$, *and* $\mathbf{J}_h, \mathbf{P}_h \in C^3\left([0,T]; [C\left(\overline{\Omega}\right)]^3\right)$. *Let* $\psi_{w_\alpha}^n$ *or* $\psi_{w_\alpha}^{n+\frac{1}{2}}$ *be truncation errors of the Yee scheme,* (86) *or equivalently* (87), *for the 3D Maxwell-Lorentz model where* $w \in \{H, E, J, P\}$ *and* $\alpha \in \{x, y, z\}$ *satisfying Lemma 5.1. Assuming the stability condition* (88) *is satisfied and letting the Courant number* $\nu = c_\infty \Delta t / h$, *then for any fixed* $T > 0$ *there exists a positive constant* $\widetilde{C}$ *depending on the medium parameters, the Courant number, but independent of the mesh parameters, such that*

$$(110) \qquad\qquad \mathcal{R}_{h,L}^n \leq \mathcal{R}_{h,L}^0 + \widetilde{C}T\left(\Delta x^2 + \Delta y^2 + \Delta z^2 + \Delta t^2\right),$$

where the energy of the error at time $t^n = n\Delta t$ *is defined by*

$$\mathcal{R}_{h,L}^n = \Bigl(\mu_0\|\mathcal{H}_h^{n-\frac{1}{2}}\|_H^2 + \epsilon_0\epsilon_\infty\|\mathcal{E}_h^n\|_E^2 + \frac{\|\mathcal{J}_h^n\|_E^2}{\epsilon_0\omega_p^2} + \frac{\|\mathcal{P}_h^n\|_E^2}{\epsilon_0\epsilon_\infty(\epsilon_q - 1)}$$

$$(111) \qquad\qquad - \Delta t\left(\mathbf{curl}_h\,\mathcal{E}_h^n, \mathcal{H}_h^{n-\frac{1}{2}}\right)_H\Bigr)^{1/2}.$$

Proof. We again apply the energy method as has been used in the proof of Theorem 4.1 and Theorem 4.2. Multiplying (109a) by $\Delta^3\ \mu_0\overline{\mathcal{H}}_h^n$, multiplying (109b) by $\Delta^3\ \epsilon_0\epsilon_\infty\overline{\mathcal{E}}_h^{n+\frac{1}{2}}$, multiplying (109c) by $\dfrac{\Delta^3}{\epsilon_o\omega_p^2}\overline{\mathcal{J}}_h^{n+\frac{1}{2}}$, and multiplying (109d) by $\dfrac{\Delta^3}{\epsilon_0\epsilon_\infty(\epsilon_q - 1)}\ \overline{\mathcal{P}}_h^{n+\frac{1}{2}}$ and finally summing each over all spatial nodes, we obtain

$$(112a) \quad \mu_0\left(\delta_t\mathcal{H}_h^n, \overline{\mathcal{H}}_h^n\right)_H = -\left(\mathbf{curl}_h\,\mathcal{E}_h^n, \overline{\mathcal{H}}_h^n\right)_H - \mu_0\left(\vec{\psi}_H^n, \overline{\mathcal{H}}_h^n\right)_H,$$

$$\epsilon_0\epsilon_\infty\left(\delta_t\mathcal{E}_h^{n+\frac{1}{2}}, \overline{\mathcal{E}}_h^{n+\frac{1}{2}}\right)_E = \left(\widetilde{\mathbf{curl}_h}\mathcal{H}_h^{n+\frac{1}{2}}, \overline{\mathcal{E}}_h^{n+\frac{1}{2}}\right)_E - \left(\overline{\mathcal{J}}_h^{n+\frac{1}{2}}, \overline{\mathcal{E}}_h^{n+\frac{1}{2}}\right)_E$$

$$(112b) \qquad\qquad\qquad - \epsilon_0\epsilon_\infty\left(\vec{\psi}_E^{n+\frac{1}{2}}, \overline{\mathcal{E}}_h^{n+\frac{1}{2}}\right)_E,$$

$$\frac{1}{\epsilon_0\omega_p^2}\left(\delta_t\mathcal{J}_h^{n+\frac{1}{2}}, \overline{\mathcal{J}}_h^{n+\frac{1}{2}}\right)_E = -\frac{1}{\tau\epsilon_0\omega_p^2}\|\overline{\mathcal{J}}_h^{n+\frac{1}{2}}\|_E^2 - \frac{\omega_0^2}{\epsilon_0\omega_p^2}\left(\overline{\mathcal{P}}_h^{n+\frac{1}{2}}, \overline{\mathcal{J}}_h^{n+\frac{1}{2}}\right)_E$$

$$(112c) \qquad\qquad\qquad + \left(\overline{\mathcal{E}}_h^{n+\frac{1}{2}}, \overline{\mathcal{J}}_h^{n+\frac{1}{2}}\right)_E - \frac{1}{\epsilon_0\omega_p^2}\left(\vec{\psi}_J^{n+\frac{1}{2}}, \overline{\mathcal{J}}_h^{n+\frac{1}{2}}\right)_E,$$

$$(112d)$$

$$\frac{\left(\delta_t\mathcal{P}_h^{n+\frac{1}{2}}, \overline{\mathcal{P}}_h^{n+\frac{1}{2}}\right)_E}{\epsilon_0\epsilon_\infty(\epsilon_q - 1)} = \frac{1}{\epsilon_0\epsilon_\infty(\epsilon_q - 1)}\left[\left(\overline{\mathcal{J}}_h^{n+\frac{1}{2}}, \overline{\mathcal{P}}_h^{n+\frac{1}{2}}\right)_E - \left(\vec{\psi}_P^{n+\frac{1}{2}}, \overline{\mathcal{P}}_h^{n+\frac{1}{2}}\right)_E\right].$$

We add all the results in (112) to obtain

$$\mu_0\left(\delta_t\mathcal{H}_h^n, \overline{\mathcal{H}}_h^n\right)_H + \epsilon_0\epsilon_\infty\left(\delta_t\mathcal{E}_h^{n+\frac{1}{2}}, \overline{\mathcal{E}}_h^{n+\frac{1}{2}}\right)_E$$

$$+ \frac{\left(\delta_t\mathcal{J}_h^{n+\frac{1}{2}}, \overline{\mathcal{J}}_h^{n+\frac{1}{2}}\right)_E}{\epsilon_0\omega_p^2} + \frac{\left(\delta_t\mathcal{P}_h^{n+\frac{1}{2}}, \overline{\mathcal{P}}_h^{n+\frac{1}{2}}\right)_E}{\epsilon_0\epsilon_\infty(\epsilon_q - 1)}$$

$$= -\left(\mathbf{curl}_h\,\mathcal{E}_h^n, \overline{\mathcal{H}}_h^n\right)_H + \left(\widetilde{\mathbf{curl}_h}\mathcal{H}_h^{n+\frac{1}{2}}, \overline{\mathcal{E}}_h^{n+\frac{1}{2}}\right)_E - \frac{\|\overline{\mathcal{J}}_h^{n+\frac{1}{2}}\|_E^2}{\tau\epsilon_0\omega_p^2} - \mu_0\left(\vec{\psi}_H^n, \overline{\mathcal{H}}_h^n\right)_H$$

$$- \epsilon_0 \epsilon_\infty \left(\vec{\psi}_E^{n+\frac{1}{2}}, \overline{\mathcal{E}}_h^{n+\frac{1}{2}} \right)_E - \frac{\left(\vec{\psi}_J^{n+\frac{1}{2}}, \overline{\mathcal{J}}_h^{n+\frac{1}{2}} \right)_E}{\epsilon_0 \omega_p^2} - \frac{\left(\vec{\psi}_P^{n+\frac{1}{2}}, \overline{\mathcal{P}}_h^{n+\frac{1}{2}} \right)_E}{\epsilon_0 \epsilon_\infty (\epsilon_q - 1)}$$

$$\leq - \left(\mathbf{curl}_h \, \mathcal{E}_h^n, \overline{\mathcal{H}}_h^n \right)_H + \left(\widetilde{\mathbf{curl}_h \mathcal{H}_h^{n+\frac{1}{2}}}, \overline{\mathcal{E}}_h^{n+\frac{1}{2}} \right)_E$$

$$- \mu_0 \left(\vec{\psi}_H^n, \overline{\mathcal{H}}_h^n \right)_H - \epsilon_0 \epsilon_\infty \left(\vec{\psi}_E^{n+\frac{1}{2}}, \overline{\mathcal{E}}_h^{n+\frac{1}{2}} \right)_E$$

(113)
$$- \frac{\left(\vec{\psi}_J^{n+\frac{1}{2}}, \overline{\mathcal{J}}_h^{n+\frac{1}{2}} \right)_E}{\epsilon_0 \omega_p^2} - \frac{\left(\vec{\psi}_P^{n+\frac{1}{2}}, \overline{\mathcal{P}}_h^{n+\frac{1}{2}} \right)_E}{\epsilon_0 \epsilon_\infty (\epsilon_q - 1)}.$$

Using the identity (70), we get

$$\mu_0 \left(\delta_t \mathcal{H}_h^n, \overline{\mathcal{H}}_h^n \right)_H + \epsilon_0 \epsilon_\infty \left(\delta_t \mathcal{E}_h^{n+\frac{1}{2}}, \overline{\mathcal{E}}_h^{n+\frac{1}{2}} \right)_E$$

$$+ \frac{\left(\delta_t \mathcal{J}_h^{n+\frac{1}{2}}, \overline{\mathcal{J}}_h^{n+\frac{1}{2}} \right)_E}{\epsilon_0 \omega_p^2} + \frac{\left(\delta_t \mathcal{P}_h^{n+\frac{1}{2}}, \overline{\mathcal{P}}_h^{n+\frac{1}{2}} \right)_E}{\epsilon_0 \epsilon_\infty (\epsilon_q - 1)}$$

$$\leq \frac{1}{2} \left(\mathcal{H}_h^{n+\frac{1}{2}}, \mathbf{curl}_h \, \mathcal{E}_h^{n+1} \right)_H - \frac{1}{2} \left(\mathcal{H}_h^{n-\frac{1}{2}}, \mathbf{curl}_h \, \mathcal{E}_h^n \right)_H$$

$$- \mu_0 \left(\vec{\psi}_H^n, \overline{\mathcal{H}}_h^n \right)_H - \epsilon_0 \epsilon_\infty \left(\vec{\psi}_E^{n+\frac{1}{2}}, \overline{\mathcal{E}}_h^{n+\frac{1}{2}} \right)_E$$

(114)
$$- \frac{\left(\vec{\psi}_J^{n+\frac{1}{2}}, \overline{\mathcal{J}}_h^{n+\frac{1}{2}} \right)_E}{\epsilon_0 \omega_p^2} - \frac{\left(\vec{\psi}_P^{n+\frac{1}{2}}, \overline{\mathcal{P}}_h^{n+\frac{1}{2}} \right)_E}{\epsilon_0 \epsilon_\infty (\epsilon_q - 1)}.$$

Thus from equation (114) we have that

$$\left(\mathcal{R}_{h,L}^{n+1} \right)^2 - \left(\mathcal{R}_{h,L}^n \right)^2 \leq 2\Delta t \left| \mu_0 \left(\vec{\psi}_H^n, \overline{\mathcal{H}}_h^n \right)_H + \epsilon_0 \epsilon_\infty \left(\vec{\psi}_E^{n+\frac{1}{2}}, \overline{\mathcal{E}}_h^{n+\frac{1}{2}} \right)_E \right.$$

$$\left. + \frac{\left(\vec{\psi}_J^{n+\frac{1}{2}}, \overline{\mathcal{J}}_h^{n+\frac{1}{2}} \right)_E}{\epsilon_0 \omega_p^2} + \frac{\left(\vec{\psi}_P^{n+\frac{1}{2}}, \overline{\mathcal{P}}_h^{n+\frac{1}{2}} \right)_E}{\epsilon_0 \epsilon_\infty (\epsilon_q - 1)} \right|$$

$$\leq \widetilde{C}_1 \Delta t \max \left\{ \|\vec{\psi}_H^n\|_H, \|\vec{\psi}_E^{n+\frac{1}{2}}\|_E, \|\vec{\psi}_J^{n+\frac{1}{2}}\|_E, \|\vec{\psi}_P^{n+\frac{1}{2}}\|_E \right\}$$

(115)
$$\cdot \left(\|\overline{\mathcal{H}}_h^n\|_H + \|\overline{\mathcal{E}}_h^{n+\frac{1}{2}}\|_E + \|\overline{\mathcal{J}}_h^{n+\frac{1}{2}}\|_E + \|\overline{\mathcal{P}}_h^{n+\frac{1}{2}}\|_E \right),$$

where $\widetilde{C}_1$ is a constant depending on $\mu_0, \epsilon_0, \epsilon_\infty, \epsilon_q$. Applying Young's inequality and equation (51), for $\gamma > 0$, we obtain

(116)
$$\left(\mathbf{curl}_h \, \mathcal{E}_h^n, \mathcal{H}_h^{n-\frac{1}{2}} \right)_H \leq \frac{\gamma \mu_0}{4\Delta t} \|\mathcal{H}_h^{n-\frac{1}{2}}\|_H^2 + \frac{12\Delta t}{h^2 \gamma \mu_0} \|\mathcal{E}_h^n\|_E^2.$$

From the definition of the energy of the error given in (111), we have

$$\mu_0 \|\mathcal{H}_h^{n-\frac{1}{2}}\|_H^2 + \epsilon_0 \epsilon_\infty \|\mathcal{E}_h^n\|_E^2 + \frac{\|\mathcal{J}_h^n\|_E^2}{\epsilon_0 \omega_p^2}$$

$$+ \frac{\|\mathcal{P}_h^n\|_E^2}{\epsilon_0 \epsilon_\infty (\epsilon_q - 1)} - \Delta t \left(\mathbf{curl}_h \, \mathcal{E}_h^n, \mathcal{H}_h^{n-\frac{1}{2}} \right)_H$$

$$\geq \mu_0 \left(1 - \frac{\gamma}{4} \right) \|\mathcal{H}_h^{n-\frac{1}{2}}\|_H^2 + \epsilon_0 \epsilon_\infty \left(1 - \frac{12\Delta t^2}{\gamma \epsilon_0 \epsilon_\infty \mu_0 h^2} \right) \|\mathcal{E}_h^n\|_E^2$$

(117)
$$+ \frac{\|\mathcal{J}_h^n\|_E^2}{\epsilon_0 \omega_p^2} + \frac{\|\mathcal{P}_h^n\|_E^2}{\epsilon_0 \epsilon_\infty (\epsilon_q - 1)}.$$

If the stability condition (88) is satisfied, then for some $\gamma \leq 4$, all terms on the right side (117) are nonnegative, and for $n \geq 0$ we have

$$(118) \qquad \mathcal{R}_{h,L}^n \geq \widetilde{C}_2 \left(\|\mathcal{H}_h^{n-\frac{1}{2}}\|_H + \|\mathcal{E}_h^n\|_E + \|\mathcal{J}_h^n\|_E + \|\mathcal{P}_h^n\|_E \right)$$

where $\widetilde{C}_2 = \min \left\{ \sqrt{\mu_0 \left(1 - \frac{\gamma}{4}\right)}, \sqrt{\epsilon_0 \epsilon_\infty \left(1 - \frac{12\Delta t^2}{\gamma \epsilon_0 \epsilon_\infty \mu_0 h^2}\right)}, \frac{1}{\sqrt{\epsilon_0 \omega_p^2}}, \frac{1}{\sqrt{\epsilon_0 \epsilon_\infty (\epsilon_q - 1)}} \right\}$.
From (115) and (118), we therefore obtain

$$\left(\mathcal{R}_{h,L}^{n+1} \right)^2 - \left(\mathcal{R}_{h,L}^n \right)^2$$

$$(119)$$

$$\leq \widetilde{C}_1 \widetilde{C}_2 \Delta t \max \left\{ \|\vec{\psi}_H^n\|_H, \|\vec{\psi}_E^{n+\frac{1}{2}}\|_E, \|\vec{\psi}_J^{n+\frac{1}{2}}\|_E, \|\vec{\psi}_P^{n+\frac{1}{2}}\|_E \right\} \left(\mathcal{R}_{h,L}^{n+1} + \mathcal{R}_{h,L}^n \right).$$

Dividing by $\mathcal{R}_{h,L}^{n+1} + \mathcal{R}_{h,L}^n$ and rearranging terms in (119), we obtain

$$\mathcal{R}_{h,L}^{n+1} - \mathcal{R}_{h,L}^n \leq \widetilde{C} \Delta t \max \left\{ \|\vec{\psi}_H^n\|_H, \|\vec{\psi}_E^{n+\frac{1}{2}}\|_E, \|\vec{\psi}_J^{n+\frac{1}{2}}\|_E, \|\vec{\psi}_P^{n+\frac{1}{2}}\|_E \right\}$$

$$(120) \qquad\qquad \leq \widetilde{C} \Delta t \left(\Delta x^2 + \Delta y^2 + \Delta z^2 + \Delta t^2 \right)$$

where $\widetilde{C} = C_L \widetilde{C}_1 \widetilde{C}_2$ is a constant depending on medium parameters, the Courant number $\nu = c_\infty \Delta t / h$, and the constant γ. Recursively applying the inequality (120) from n to 0 and using the fact that $T = N\Delta t$, we have

$$\mathcal{R}_{h,L}^n - \mathcal{R}_{h,L}^0 \leq \widetilde{C} n \Delta t \left(\Delta x^2 + \Delta y^2 + \Delta z^2 + \Delta t^2 \right)$$

$$(121) \qquad\qquad \leq \widetilde{C} T \left(\Delta x^2 + \Delta y^2 + \Delta z^2 + \Delta t^2 \right).$$

$\square$

5.3. Discrete Divergence Constraints of the Yee Scheme for the Maxwell-Lorentz Model.
As a result of divergence-conserved property of the Maxwell-Debye model, in this section we show that the similar property holds for the Maxwell-Lorentz model.

Theorem 5.3. *Suppose that the solutions to the 3D Maxwell-Lorentz model (15) are as given in Theorem 5.2. Then discrete divergence of the Yee scheme for the 3D Maxwell-Lorentz model, (86) or equivalently (87), is preserved for all time levels $n \geq 0$, i.e., satisfies the identities*

$$(122a) \qquad\qquad \text{div}_h \mathbf{D}_h^n = \text{div}_h \mathbf{D}_h^0,$$

$$(122b) \qquad\qquad \text{div}_h \mathbf{B}_h^{n+\frac{1}{2}} = \text{div}_h \mathbf{B}_h^{\frac{1}{2}},$$

where the vector fields $\mathbf{D}_h$ and $\mathbf{B}_h$ are defined on the meshes $\tau_h^{\text{div}\mathbf{E}}$ and $\tau_h^{\text{div}\mathbf{H}}$, respectively.

Proof. The proof of this theorem is the same as the proof of Theorem 4.3 for the case of the Debye medium. $\square$

6. Development of the Yee Scheme for the Maxwell-Cold Plasma System

The fully discrete Yee scheme applied to the the 3D Maxwell-Cold Plasma systems reads

$$(123a) \qquad \delta_t H^n_{x,h_{\ell,j+\frac{1}{2},k+\frac{1}{2}}} = \frac{1}{\mu_0}\left(\delta_z E^n_{y,h_{\ell,j+\frac{1}{2},k+\frac{1}{2}}} - \delta_y E^n_{z,h_{\ell,j+\frac{1}{2},k+\frac{1}{2}}}\right),$$

$$(123b) \qquad \delta_t H^n_{y,h_{\ell+\frac{1}{2},j,k+\frac{1}{2}}} = \frac{1}{\mu_0}\left(\delta_x E^n_{z,h_{\ell+\frac{1}{2},j,k+\frac{1}{2}}} - \delta_z E^n_{x,h_{\ell+\frac{1}{2},j,k+\frac{1}{2}}}\right),$$

$$(123c) \qquad \delta_t H^n_{z,h_{\ell+\frac{1}{2},j+\frac{1}{2},k}} = \frac{1}{\mu_0}\left(\delta_y E^n_{x,h_{\ell+\frac{1}{2},j+\frac{1}{2},k}} - \delta_x E^n_{y,h_{\ell+\frac{1}{2},j+\frac{1}{2},k}}\right),$$

$$(123d) \qquad \delta_t E^{n+\frac{1}{2}}_{x,h_{\ell+\frac{1}{2},j,k}} = \frac{1}{\epsilon_0}\left(\delta_y H^{n+\frac{1}{2}}_{z,h_{\ell+\frac{1}{2},j,k}} - \delta_z H^{n+\frac{1}{2}}_{y,h_{\ell+\frac{1}{2},j,k}}\right) - \frac{1}{\epsilon_0}\overline{J}^{n+\frac{1}{2}}_{x,h_{\ell+\frac{1}{2},j,k}},$$

$$(123e) \qquad \delta_t E^{n+\frac{1}{2}}_{y,h_{\ell,j+\frac{1}{2},k}} = \frac{1}{\epsilon_0}\left(\delta_z H^{n+\frac{1}{2}}_{x,h_{\ell,j+\frac{1}{2},k}} - \delta_x H^{n+\frac{1}{2}}_{z,h_{\ell,j+\frac{1}{2},k}}\right) - \frac{1}{\epsilon_0}\overline{J}^{n+\frac{1}{2}}_{y,h_{\ell,j+\frac{1}{2},k}},$$

$$(123f) \qquad \delta_t E^{n+\frac{1}{2}}_{z,h_{\ell,j,k+\frac{1}{2}}} = \frac{1}{\epsilon_0}\left(\delta_x H^{n+\frac{1}{2}}_{y,h_{\ell,j,k+\frac{1}{2}}} - \delta_y H^{n+\frac{1}{2}}_{x,h_{\ell,j,k+\frac{1}{2}}}\right) - \frac{1}{\epsilon_0}\overline{J}^{n+\frac{1}{2}}_{z,h_{\ell,j,k+\frac{1}{2}}},$$

$$(123g) \qquad \delta_t J^{n+\frac{1}{2}}_{x,h_{\ell+\frac{1}{2},j,k}} = -\nu_c \overline{J}^{n+\frac{1}{2}}_{x,h_{\ell+\frac{1}{2},j,k}} + \epsilon_0\omega_p^2 \overline{E}^{n+\frac{1}{2}}_{x,h_{\ell+\frac{1}{2},j,k}},$$

$$(123h) \qquad \delta_t J^{n+\frac{1}{2}}_{y,h_{\ell,j+\frac{1}{2},k}} = -\nu_c \overline{J}^{n+\frac{1}{2}}_{y,h_{\ell,j+\frac{1}{2},k}} + \epsilon_0\omega_p^2 \overline{E}^{n+\frac{1}{2}}_{y,h_{\ell,j+\frac{1}{2},k}},$$

$$(123i) \qquad \delta_t J^{n+\frac{1}{2}}_{z,h_{\ell,j,k+\frac{1}{2}}} = -\nu_c \overline{J}^{n+\frac{1}{2}}_{z,h_{\ell,j,k+\frac{1}{2}}} + \epsilon_0\omega_p^2 \overline{E}^{n+\frac{1}{2}}_{z,h_{\ell,j,k+\frac{1}{2}}}.$$

Then the scheme (123) can be written as follows

$$(124a) \qquad \delta_t \mathbf{H}^n_h = -\frac{1}{\mu_0}\,\mathbf{curl}_h\,\mathbf{E}^n_h,$$

$$(124b) \qquad \delta_t \mathbf{E}^{n+\frac{1}{2}}_h = \frac{1}{\epsilon_0}\widetilde{\mathbf{curl}_h}\mathbf{H}^{n+\frac{1}{2}}_h - \frac{1}{\epsilon_0}\overline{\mathbf{J}}^{n+\frac{1}{2}}_h,$$

$$(124c) \qquad \delta_t \mathbf{J}^{n+\frac{1}{2}}_h = -\nu_c \overline{\mathbf{J}}^{n+\frac{1}{2}}_h + \epsilon_0\omega_p^2 \overline{\mathbf{E}}^{n+\frac{1}{2}}_h.$$

6.1. The Stability Analysis of the Yee Scheme for Cold Plasma Media.
In this section, we show that the solution of the fully discrete scheme (123) satisfies the energy decay property by the following theorem.

Theorem 6.1. *If the time step and uniform mesh spatial step sizes satisfy the stability condition*

$$(125) \qquad \frac{c_\infty \Delta t}{h} < \frac{1}{\sqrt{3}},$$

where $c_\infty = 1/\sqrt{\mu_0\epsilon_0}$, then the discrete solutions of the 3D Yee -FDTD Maxwell-Cold Plasma equations satisfy the discrete energy decay,

$$(126) \qquad \mathcal{E}^{n+1}_{h,C} \leq \mathcal{E}^n_{h,C},$$

for all $n \geq 0$ where a discrete energy is defined by

$$(127) \quad \mathcal{E}^n_{h,C} = \left(\mu_0\|\mathbf{H}^{n-\frac{1}{2}}_h\|_H^2 + \epsilon_0\|\mathbf{E}^n_h\|_E^2 + \frac{\|\mathbf{J}^n_h\|_E^2}{\epsilon_0\omega_p^2} - \Delta t\left(\mathbf{curl}_h\,\mathbf{E}^n_h, \mathbf{H}^{n-\frac{1}{2}}_h\right)_H\right)^{\frac{1}{2}}.$$

Proof. Multiplying (123a) by $\Delta^3 \mu_0 \overline{H}^n_{x,h_{\ell,j+\frac{1}{2},k+\frac{1}{2}}}$, multiplying (123b) by $\Delta^3 \mu_0 \overline{H}^n_{y,h_{\ell+\frac{1}{2},j,k+\frac{1}{2}}}$, multiplying (123c) by $\Delta^3 \mu_0 \overline{H}^n_{z,h_{\ell+\frac{1}{2},j+\frac{1}{2},k}}$ and finally summing each over all spatial nodes, and adding all the results, we obtain

$$(128) \qquad \frac{\mu_0}{2\Delta t} \left(\|\mathbf{H}_h^{n+\frac{1}{2}}\|_H^2 - \|\mathbf{H}_h^{n-\frac{1}{2}}\|_H^2 \right) = - \left(\mathbf{curl}_{\mathrm{h}} \, \mathbf{E}_h^n, \overline{\mathbf{H}}_h^n \right)_H.$$

Next, multiplying (123d), (123e) and (123f) by $\Delta^3 \epsilon_0 \overline{E}^{n+\frac{1}{2}}_{x,h_{\ell+\frac{1}{2},j,k}}$, $\Delta^3 \epsilon_0 \overline{E}^{n+\frac{1}{2}}_{y,h_{\ell,j+\frac{1}{2},k}}$ and $\Delta^3 \epsilon_0 \overline{E}^{n+\frac{1}{2}}_{z,h_{\ell,j,k+\frac{1}{2}}}$ respectively, and finally summing each over all spatial nodes, and adding all the results, we obtain

$$(129) \qquad \frac{\epsilon_0}{2\Delta t} \left(\|\mathbf{E}_h^{n+1}\|_E^2 - \|\mathbf{E}_h^n\|_E^2 \right) = \left(\widetilde{\mathbf{curl}_{\mathrm{h}}} \mathbf{H}_h^{n+\frac{1}{2}}, \overline{\mathbf{E}}_h^{n+\frac{1}{2}} \right)_E - \left(\overline{\mathbf{J}}_h^{n+\frac{1}{2}}, \overline{\mathbf{E}}_h^{n+\frac{1}{2}} \right)_E.$$

Finally, multiplying (123g), (123h) and (123i) by $\dfrac{\Delta^3}{\epsilon_0 \omega_p^2} \overline{J}^{n+\frac{1}{2}}_{x,h_{\ell+\frac{1}{2},j,k}}$, $\dfrac{\Delta^3}{\epsilon_0 \omega_p^2} \overline{J}^{n+\frac{1}{2}}_{y,h_{\ell,j+\frac{1}{2},k}}$ and $\dfrac{\Delta^3}{\epsilon_0 \omega_p^2} \overline{J}^{n+\frac{1}{2}}_{z,h_{\ell,j,k+\frac{1}{2}}}$ and finally summing each over all spatial nodes, and adding all the results, we obtain

$$(130) \qquad \frac{1}{2\Delta t \epsilon_0 \omega_p^2} \left(\|\mathbf{J}_h^{n+1}\|_E^2 - \|\mathbf{J}_h^n\|_E^2 \right) = - \frac{\nu_c}{\epsilon_0 \omega_p^2} \|\overline{\mathbf{J}}_h^{n+\frac{1}{2}}\|_E^2 + \left(\overline{\mathbf{E}}_h^{n+\frac{1}{2}}, \overline{\mathbf{J}}_h^{n+\frac{1}{2}} \right)_E.$$

Adding all equations (128)-(130) and using a discrete analogue of integration by parts [9], we obtain

$$\frac{\mu_0}{2\Delta t} \left(\|\mathbf{H}_h^{n+\frac{1}{2}}\|_H^2 - \|\mathbf{H}_h^{n-\frac{1}{2}}\|_H^2 \right) + \frac{\epsilon_0}{2\Delta t} \left(\|\mathbf{E}_h^{n+1}\|_E^2 - \|\mathbf{E}_h^n\|_E^2 \right) + \frac{\left(\|\mathbf{J}_h^{n+1}\|_E^2 - \|\mathbf{J}_h^n\|_E^2 \right)}{2\Delta t \epsilon_0 \omega_p^2}$$

$$= - \left(\mathbf{curl}_{\mathrm{h}} \, \mathbf{E}_h^n, \overline{\mathbf{H}}_h^n \right)_H + \left(\widetilde{\mathbf{curl}_{\mathrm{h}}} \mathbf{H}_h^{n+\frac{1}{2}}, \overline{\mathbf{E}}_h^{n+\frac{1}{2}} \right)_E - \frac{\nu_c}{\epsilon_0 \omega_p^2} \|\overline{\mathbf{J}}_h^{n+\frac{1}{2}}\|_E^2$$

$$(131)$$

$$= -\frac{1}{2} \left(\mathbf{curl}_{\mathrm{h}} \, \mathbf{E}_h^n, \mathbf{H}_h^{n-\frac{1}{2}} \right)_H + \frac{1}{2} \left(\widetilde{\mathbf{curl}_{\mathrm{h}}} \mathbf{H}_h^{n+\frac{1}{2}}, \mathbf{E}_h^{n+1} \right)_E - \frac{\nu_c}{\epsilon_0 \omega_p^2} \|\overline{\mathbf{J}}_h^{n+\frac{1}{2}}\|_E^2.$$

We convert equation (131) into an inequality

$$\mu_0 \left(\|\mathbf{H}_h^{n+\frac{1}{2}}\|_H^2 - \|\mathbf{H}_h^{n-\frac{1}{2}}\|_H^2 \right) + \epsilon_0 \left(\|\mathbf{E}_h^{n+1}\|_E^2 - \|\mathbf{E}_h^n\|_E^2 \right) + \frac{\left(\|\mathbf{J}_h^{n+1}\|_E^2 - \|\mathbf{J}_h^n\|_E^2 \right)}{\epsilon_0 \omega_p^2}$$

$$(132) \qquad \leq \Delta t \left(\widetilde{\mathbf{curl}_{\mathrm{h}}} \mathbf{H}_h^{n+\frac{1}{2}}, \mathbf{E}_h^{n+1} \right)_E - \Delta t \left(\mathbf{curl}_{\mathrm{h}} \, \mathbf{E}_h^n, \mathbf{H}_h^{n-\frac{1}{2}} \right)_H.$$

We follow a similar procedure to the Debye case to confirm conditional stability by showing that $\mathcal{E}_{h,C}^n$ is a discrete energy function. By the inequality (51), we have

$$\mu_0 \|\mathbf{H}_h^{n-\frac{1}{2}}\|_H^2 + \epsilon_0 \|\mathbf{E}_h^n\|_E^2 + \frac{\|\mathbf{J}_h^n\|_E^2}{\epsilon_0 \omega_p^2} - \Delta t \left(\mathbf{curl}_{\mathrm{h}} \, \mathbf{E}_h^n, \mathbf{H}_h^{n-\frac{1}{2}} \right)_H$$

$$(133) \qquad \geq \epsilon_0 \epsilon_\infty \left(1 - \frac{3\Delta t^2}{h^2 \mu_0 \epsilon_0} \right) \|\mathbf{E}_h^n\|_E^2.$$

Thus, the discrete energy function (127) is positive when

$$(134) \qquad \frac{3\Delta t^2}{h^2 \mu_0 \epsilon_0} < 1 \quad \Leftrightarrow \quad \frac{3c_\infty^2 \Delta t^2}{h^2} < 1,$$

so the stability condition (125) holds. $\qquad\square$

6.2. Error Estimates and Convergence of the Yee Scheme for the Maxwell-Cold Plasma Model.

In this section, we first analyze the truncation errors in the Yee scheme for the Maxwell-Cold Plasma model and prove convergence of the scheme.

Lemma 6.1. *Suppose that the solutions to the Maxwell-Cold Plasma model* (22) *satisfies the regularity conditions* $\mathbf{E}, \mathbf{H} \in C^3\left([0,T]; [C^3\left(\overline{\Omega}\right)]^3\right)$, *and* $\mathbf{J} \in C^3\left([0,T]; [C\left(\overline{\Omega}\right)]^3\right)$. *Let* $\phi_{w_\alpha}^m$ *be truncation errors for the Yee scheme for the Maxwell-Cold Plasma model,* (123) *or equivalently* (124), *where* $w \in \{H, E, J\}$, $m \in \{n, n+\frac{1}{2}\}$, *and* $\alpha \in \{x, y, z\}$. *Then for any* $\alpha \in \{x, y, z\}$,

$$(135) \qquad \max\left\{\left|\phi_{H_\alpha}^n\right|, \left|\phi_{E_\alpha}^{n+\frac{1}{2}}\right|, \left|\phi_{J_\alpha}^{n+\frac{1}{2}}\right|\right\} \leq C_C\left(\Delta x^2 + \Delta y^2 + \Delta z^2 + \Delta t^2\right),$$

where C_C *is a constant and does not depend on the mesh sizes.*

Proof. We follow a similar procedure to Lemma 5.1. □

To prove the convergence of the Yee scheme for the 3D Maxwell-Cold Plasma model, we follow the similar procedure to the convergence analysis in Theorem 5.2.

In combining variables (64) and (108), we arrive at the error equations of the Yee scheme for the 3D Maxwell-Cold Plasma model:

$$(136a) \qquad \delta_t \mathcal{H}_h^n = -\frac{1}{\mu_0} \mathbf{curl}_h \mathcal{E}_h^n - \vec{\phi}_H^n,$$

$$(136b) \qquad \delta_t \mathcal{E}_h^{n+\frac{1}{2}} = \frac{1}{\epsilon_0} \widetilde{\mathbf{curl}_h} \mathcal{H}_h^{n+\frac{1}{2}} - \frac{1}{\epsilon_0}\overline{\mathcal{J}}_h^{n+\frac{1}{2}} - \vec{\phi}_E^{n+\frac{1}{2}},$$

$$(136c) \qquad \delta_t \mathcal{J}_h^{n+\frac{1}{2}} = -\nu_c \overline{\mathcal{J}}_h^{n+\frac{1}{2}} + \epsilon_0 \omega_p^2 \overline{\mathcal{E}}_h^{n+\frac{1}{2}} - \vec{\phi}_J^{n+\frac{1}{2}},$$

where $\vec{\phi}_w^m = \left(\phi_{w_x}^m, \phi_{w_y}^m, \phi_{w_z}^m\right), w \in \{H, E, J\}$ and $m \in \{n, n+1/2\}$. The convergence property of the Yee scheme for the Maxwell-Cold Plasma model is given by the following result.

Theorem 6.2. *Suppose that the solutions to the Maxwell-Cold Plasma model* (22) *satisfy the regularity conditions* $\mathbf{E}_h, \mathbf{H}_h \in C^3\left([0,T]; [C^3\left(\overline{\Omega}\right)]^3\right)$, *and* $\mathbf{J}_h \in C^3\left([0,T]; [C\left(\overline{\Omega}\right)]^3\right)$. *Let* $\phi_{w_\alpha}^m$ *be truncation errors of the Yee scheme for the Maxwell-Cold Plasma model,* (123) *or equivalently* (124), *where* $w \in \{H, E, J\}$, $m \in \{n, n+\frac{1}{2}\}$, *and* $\alpha \in \{x, y, z\}$ *satisfying Lemma 6.1. Assuming the stability condition* (125) *is satisfied and letting the Courant number* $\nu = c_\infty \Delta t/h$, *then for any fixed* $T > 0$ *there exists a positive constant* $\widehat{C}$ *depending on the medium parameters, the Courant number, but independent of the mesh parameters, such that*

$$(137) \qquad \mathcal{R}_{h,C}^n \leq \mathcal{R}_{h,C}^0 + \widehat{C}T\left(\Delta x^2 + \Delta y^2 + \Delta z^2 + \Delta t^2\right),$$

where the energy of the error at time $t^n = n\Delta t$ *is defined by*

$$(138) \quad \mathcal{R}_{h,C}^n = \left(\mu_0\|\mathcal{H}_h^{n-\frac{1}{2}}\|_H^2 + \epsilon_0\|\mathcal{E}_h^n\|_E^2 + \frac{\|\mathcal{J}_h^n\|_E^2}{\epsilon_0\omega_p^2} - \Delta t\left(\mathbf{curl}_h \mathcal{E}_h^n, \mathcal{H}_h^{n-\frac{1}{2}}\right)_H\right)^{1/2}.$$

Proof. We follow a similar process, the energy method, that has been used in the proof of Theorem 5.2. Multiplying (136a) by $\Delta^3 \, \mu_0 \overline{\mathcal{H}}_h^n$ and summing overall spatial nodes, multiplying (136b) by $\Delta^3 \, \epsilon_0 \overline{\mathcal{E}}_h^{n+\frac{1}{2}}$, multiplying (136c) by $\dfrac{\Delta^3}{\epsilon_0\omega_p^2}\overline{\mathcal{J}}_h^{n+\frac{1}{2}}$ and

summing overall spatial nodes, we obtain

$$(139\text{a}) \qquad \mu_0 \left(\delta_t \mathcal{H}_h^n, \overline{\mathcal{H}}_h^n \right)_H = - \left(\mathbf{curl}_\text{h}\, \mathcal{E}_h^n, \overline{\mathcal{H}}_h^n \right)_H - \mu_0 \left(\vec{\phi}_H^n, \overline{\mathcal{H}}_h^n \right)_H,$$

$$\epsilon_0 \left(\delta_t \mathcal{E}_h^{n+\frac{1}{2}}, \overline{\mathcal{E}}_h^{n+\frac{1}{2}} \right)_E = \left(\widetilde{\mathbf{curl}_\text{h}} \mathcal{H}_h^{n+\frac{1}{2}}, \overline{\mathcal{E}}_h^{n+\frac{1}{2}} \right)_E$$

$$(139\text{b}) \qquad\qquad - \left(\overline{\mathcal{J}}_h^{n+\frac{1}{2}}, \overline{\mathcal{E}}_h^{n+\frac{1}{2}} \right)_E - \epsilon_0 \left(\vec{\phi}_E^{n+\frac{1}{2}}, \overline{\mathcal{E}}_h^{n+\frac{1}{2}} \right)_E,$$

$$\frac{1}{\epsilon_0 \omega_p^2} \left(\delta_t \mathcal{J}_h^{n+\frac{1}{2}}, \overline{\mathcal{J}}_h^{n+\frac{1}{2}} \right)_E = - \frac{\nu_c}{\epsilon_0 \omega_p^2} \| \overline{\mathcal{J}}_h^{n+\frac{1}{2}} \|_E^2$$

$$(139\text{c}) \qquad\qquad + \left(\overline{\mathcal{E}}_h^{n+\frac{1}{2}}, \overline{\mathcal{J}}_h^{n+\frac{1}{2}} \right)_E - \frac{1}{\epsilon_0 \omega_p^2} \left(\vec{\phi}_J^{n+\frac{1}{2}}, \overline{\mathcal{J}}_h^{n+\frac{1}{2}} \right)_E.$$

We add all the results in (139) to obtain

$$\mu_0 \left(\delta_t \mathcal{H}_h^n, \overline{\mathcal{H}}_h^n \right)_H + \epsilon_0 \left(\delta_t \mathcal{E}_h^{n+\frac{1}{2}}, \overline{\mathcal{E}}_h^{n+\frac{1}{2}} \right)_E + \frac{\left(\delta_t \mathcal{J}_h^{n+\frac{1}{2}}, \overline{\mathcal{J}}_h^{n+\frac{1}{2}} \right)_E}{\epsilon_0 \omega_p^2}$$

$$= - \left(\mathbf{curl}_\text{h}\, \mathcal{E}_h^n, \overline{\mathcal{H}}_h^n \right)_H + \left(\widetilde{\mathbf{curl}_\text{h}} \mathcal{H}_h^{n+\frac{1}{2}}, \overline{\mathcal{E}}_h^{n+\frac{1}{2}} \right)_E - \frac{\nu_c}{\epsilon_0 \omega_p^2} \| \overline{\mathcal{J}}_h^{n+\frac{1}{2}} \|_E^2$$

$$- \mu_0 \left(\vec{\phi}_H^n, \overline{\mathcal{H}}_h^n \right)_H - \epsilon_0 \left(\vec{\phi}_E^{n+\frac{1}{2}}, \overline{\mathcal{E}}_h^{n+\frac{1}{2}} \right)_E - \frac{\left(\vec{\phi}_J^{n+\frac{1}{2}}, \overline{\mathcal{J}}_h^{n+\frac{1}{2}} \right)_E}{\epsilon_0 \omega_p^2}$$

$$\leq - \left(\mathbf{curl}_\text{h}\, \mathcal{E}_h^n, \overline{\mathcal{H}}_h^n \right)_H + \left(\widetilde{\mathbf{curl}_\text{h}} \mathcal{H}_h^{n+\frac{1}{2}}, \overline{\mathcal{E}}_h^{n+\frac{1}{2}} \right)_E$$

$$(140) \qquad - \mu_0 \left(\vec{\phi}_H^n, \overline{\mathcal{H}}_h^n \right)_H - \epsilon_0 \left(\vec{\phi}_E^{n+\frac{1}{2}}, \overline{\mathcal{E}}_h^{n+\frac{1}{2}} \right)_E - \frac{\left(\vec{\phi}_J^{n+\frac{1}{2}}, \overline{\mathcal{J}}_h^{n+\frac{1}{2}} \right)_E}{\epsilon_0 \omega_p^2}.$$

Using the identity (70), we get

$$\mu_0 \left(\delta_t \mathcal{H}_h^n, \overline{\mathcal{H}}_h^n \right)_H + \epsilon_0 \left(\delta_t \mathcal{E}_h^{n+\frac{1}{2}}, \overline{\mathcal{E}}_h^{n+\frac{1}{2}} \right)_E + \frac{\left(\delta_t \mathcal{J}_h^{n+\frac{1}{2}}, \overline{\mathcal{J}}_h^{n+\frac{1}{2}} \right)_E}{\epsilon_0 \omega_p^2}$$

$$\leq \frac{1}{2} \left(\mathcal{H}_h^{n+\frac{1}{2}}, \mathbf{curl}_\text{h}\, \mathcal{E}_h^{n+1} \right)_H - \frac{1}{2} \left(\mathcal{H}_h^{n-\frac{1}{2}}, \mathbf{curl}_\text{h}\, \mathcal{E}_h^n \right)_H$$

$$(141) \qquad - \mu_0 \left(\vec{\phi}_H^n, \overline{\mathcal{H}}_h^n \right)_H - \epsilon_0 \left(\vec{\phi}_E^{n+\frac{1}{2}}, \overline{\mathcal{E}}_h^{n+\frac{1}{2}} \right)_E - \frac{\left(\vec{\phi}_J^{n+\frac{1}{2}}, \overline{\mathcal{J}}_h^{n+\frac{1}{2}} \right)_E}{\epsilon_0 \omega_p^2}.$$

Thus from equation (141) we have that

$$\left(\mathcal{R}_{h,C}^{n+1} \right)^2 - \left(\mathcal{R}_{h,C}^n \right)^2$$

$$\leq 2\Delta t \left| \mu_0 \left(\vec{\phi}_H^n, \overline{\mathcal{H}}_h^n \right)_H + \epsilon_0 \left(\vec{\phi}_E^{n+\frac{1}{2}}, \overline{\mathcal{E}}_h^{n+\frac{1}{2}} \right)_E + \frac{\left(\vec{\phi}_J^{n+\frac{1}{2}}, \overline{\mathcal{J}}_h^{n+\frac{1}{2}} \right)_E}{\epsilon_0 \omega_p^2} \right|$$

$$\leq \widehat{C}_1 \Delta t \max \left\{ \| \vec{\phi}_H^n \|_H, \| \vec{\phi}_E^{n+\frac{1}{2}} \|_E, \| \vec{\phi}_J^{n+\frac{1}{2}} \|_E \right\}$$

$$(142) \qquad \cdot \left(\| \overline{\mathcal{H}}_h^n \|_H + \| \overline{\mathcal{E}}_h^{n+\frac{1}{2}} \|_E + \| \overline{\mathcal{J}}_h^{n+\frac{1}{2}} \|_E \right),$$

where $\widehat{C}_1$ is a constant depending on $\mu_0, \epsilon_0, \epsilon_q$. Applying Young's inequality and equation (51), for $\gamma > 0$, we obtain

$$(143) \qquad \left(\mathbf{curl}_{\mathrm{h}} \, \mathcal{E}_h^n, \mathcal{H}_h^{n-\frac{1}{2}}\right)_H \leq \frac{\gamma\mu_0}{4\Delta t}\|\mathcal{H}_h^{n-\frac{1}{2}}\|_H^2 + \frac{12\Delta t}{h^2\gamma\mu_0}\|\mathcal{E}_h^n\|_E^2.$$

The the definition of the energy of the error given in (138), we have

$$\left(\mathcal{R}_{h,C}^n\right)^2 = \mu_0\|\mathcal{H}_h^{n-\frac{1}{2}}\|_H^2 + \epsilon_0\|\mathcal{E}_h^n\|_E^2 + \frac{\|\mathcal{J}_h^n\|_E^2}{\epsilon_0\omega_p^2} - \Delta t\left(\mathbf{curl}_{\mathrm{h}} \, \mathcal{E}_h^n, \mathcal{H}_h^{n-\frac{1}{2}}\right)_H$$

$$(144) \qquad \geq \mu_0\left(1 - \frac{\gamma}{4}\right)\|\mathcal{H}_h^{n-\frac{1}{2}}\|_H^2 + \epsilon_0\left(1 - \frac{12\Delta t^2}{\gamma\epsilon_0\mu_0 h^2}\right)\|\mathcal{E}_h^n\|_E^2 + \frac{\|\mathcal{J}_h^n\|_E^2}{\epsilon_0\omega_p^2}.$$

If the stability condition (125) is satisfied, then for some $\gamma \leq 4$, all terms on the right side (144) are nonnegative, and for $n \geq 0$ we have

$$(145) \qquad \mathcal{R}_{h,C}^n \geq \widehat{C}_2\left(\|\mathcal{H}_h^{n-\frac{1}{2}}\|_H + \|\mathcal{E}_h^n\|_E + \|\mathcal{J}_h^n\|_E\right)$$

where $\widehat{C}_2 = \min\left\{\sqrt{\mu_0\left(1 - \frac{\gamma}{4}\right)}, \sqrt{\epsilon_0\left(1 - \frac{12\Delta t^2}{\gamma\epsilon_0\mu_0 h^2}\right)}, \frac{1}{\sqrt{\epsilon_0\omega_p^2}}, \frac{1}{\sqrt{\epsilon_0(\epsilon_q-1)}}\right\}$. From (142) and (145), we therefore obtain

$$\left(\mathcal{R}_{h,C}^{n+1}\right)^2 - \left(\mathcal{R}_{h,C}^n\right)^2$$

$$(146) \qquad \leq \widehat{C}_1\widehat{C}_2\Delta t \max\left\{\|\vec{\phi}_H^n\|_H, \|\vec{\phi}_E^{n+\frac{1}{2}}\|_E, \|\vec{\phi}_J^{n+\frac{1}{2}}\|_E\right\}\left(\mathcal{R}_{h,C}^{n+1} + \mathcal{R}_{h,C}^n\right).$$

Dividing by $\mathcal{R}_{h,C}^{n+1} + \mathcal{R}_{h,C}^n$ and rearranging terms in (146), we obtain

$$\mathcal{R}_{h,C}^{n+1} - \mathcal{R}_{h,C}^n \leq \widehat{C}_1\widehat{C}_2\Delta t \max\left\{\|\vec{\phi}_H^n\|_H, \|\vec{\phi}_E^{n+\frac{1}{2}}\|_E, \|\vec{\phi}_J^{n+\frac{1}{2}}\|_E\right\}$$

$$(147) \qquad\qquad\qquad \leq \widehat{C}\Delta t\left(\Delta x^2 + \Delta y^2 + \Delta z^2 + \Delta t^2\right)$$

where $\widehat{C} = C_c\widehat{C}_1\widehat{C}_2$ is a constant depending on medium parameters, the Courant number $\nu = c_\infty\Delta t/h$, and the constant γ. Recursively applying the inequality (120) from n to 0 and using the fact that $T = N\Delta t$, we have

$$(148)$$
$$\mathcal{R}_{h,C}^n - \mathcal{R}_{h,C}^0 \leq \widehat{C}n\Delta t\left(\Delta x^2 + \Delta y^2 + \Delta z^2 + \Delta t^2\right) \leq \widehat{C}T\left(\Delta x^2 + \Delta y^2 + \Delta z^2 + \Delta t^2\right).$$

$\square$

6.3. Discrete Divergence Constraints of the Yee Scheme for the Maxwell-Cold Plasma Model.

In this section we analyze the properties of the discrete divergence for the 3D Yee-FDTD Maxwell-Cold Plasma equations. Due to lack of information about the polarization, the divergence of the electric flux density is not well defined. We now consider only the divergence of the magnetic flux density in the following theorem.

Theorem 6.3. *Suppose that the solutions to the 3D Maxwell-Cold Plasma model (22) are as given in Theorem 6.2. Then discrete divergence of the magnetic flux density in the Yee scheme for the 3D Maxwell-Cold Plasma model, (123) or equivalently (124), is preserved for all time levels $n \geq 0$, i.e., satisfies the identity*

$$(149) \qquad\qquad div_h\mathbf{B}_h^{n+\frac{1}{2}} = div_h\mathbf{B}_h^{\frac{1}{2}}$$

where the vector field $\mathbf{B}_h$ is defined on the mesh $\tau_h^{div\mathbf{H}}$.

Proof. The proof of this theorem is the same as the proof of Theorem 4.3 for the case of the Debye medium. $\square$

7.   Numerical Experiments

In this section, we numerically investigate the Yee scheme for the three different linear dispersive media presented in the paper. To numerically demonstrate the convergence of our Yee schemes, we consider the domain $\Omega = [0,1] \times [0,1] \times [0,1]$ with the PEC boundary conditions (28). We demonstrate our convergence results on a uniform mesh, $\Delta x = \Delta y = \Delta z = h$. The parameters of the linear model are chosen as $\mu_0 = 1, \epsilon_0 = 1, \epsilon_\infty = 1, \omega_0 = 1, \tau = 1, \epsilon_q = 2$, and $T = 1$. By considering exact solutions and relative errors for different wave numbers $\mathbf{k} = (k_x, k_y, k_z)^T$ be a wave vector, with corresponding wave number, $|\mathbf{k}| = \sqrt{k_x^2 + k_y^2 + k_z^2}$, where $(k_x, k_y, k_z)^T = \pi(\widetilde{k}_x, \widetilde{k}_y, \widetilde{k}_z)^T$ and $\widetilde{k}_x, \widetilde{k}_y, \widetilde{k}_z$ are integer constants.

We also numerically demonstrate the satisfaction of the discrete divergence property of the magnetic induction.

7.1. Yee Scheme for the Maxwell-Debye Model.

In this section, we present numerical results for the Yee scheme for the 3D Maxwell-Debye system (39).

We consider an exact solution of the 3D Maxwell-Debye system (7) given in the form

$$(150a) \qquad H_x(x,y,z;t) = \frac{|\mathbf{k}|^2}{\pi} e^{-\theta t} \sin(k_x x) \cos(k_y y) \cos(k_z z),$$

$$(150b) \qquad H_y(x,y,z;t) = \frac{|\mathbf{k}|^2}{\pi} e^{-\theta t} \cos(k_x x) \sin(k_y y) \cos(k_z z),$$

$$(150c) \qquad H_z(x,y,z;t) = \frac{|\mathbf{k}|^2}{\pi} e^{-\theta t} \cos(k_x x) \cos(k_y y) \sin(k_z z),$$

$$(150d) \qquad E_x(x,y,z;t) = -\frac{\theta}{\pi}(k_y - k_z) e^{-\theta t} \cos(k_x x) \sin(k_y y) \sin(k_z z),$$

$$(150e) \qquad E_y(x,y,z;t) = -\frac{\theta}{\pi}(k_z - k_x) e^{-\theta t} \sin(k_x x) \cos(k_y y) \sin(k_z z),$$

$$(150f) \qquad E_z(x,y,z;t) = -\frac{\theta}{\pi}(k_x - k_y) e^{-\theta t} \sin(k_x x) \sin(k_y y) \cos(k_z z),$$

$$(150g) \qquad P_x(x,y,z;t) = -\frac{\beta_D(\theta, |\mathbf{k}|)}{\pi}(k_y - k_z) e^{-\theta t} \cos(k_x x) \sin(k_y y) \sin(k_z z),$$

$$(150h) \qquad P_y(x,y,z;t) = -\frac{\beta_D(\theta, |\mathbf{k}|)}{\pi}(k_z - k_x) e^{-\theta t} \sin(k_x x) \cos(k_y y) \sin(k_z z),$$

$$(150i) \qquad P_z(x,y,z;t) = -\frac{\beta_D(\theta, |\mathbf{k}|)}{\pi}(k_x - k_y) e^{-\theta t} \sin(k_x x) \sin(k_y y) \cos(k_z z),$$

where the function $\beta_D(\theta, |\mathbf{k}|) := \epsilon_0 \epsilon_\infty(\epsilon_q - 1)\theta - \epsilon_0 \epsilon_\infty \tau \theta^2 - \tau |\mathbf{k}|^2$ and θ is a real number. The relationship between the wave number $\mathbf{k}$ and the parameter θ can be represented by the equation

$$(151) \qquad \epsilon_0 \epsilon_\infty \tau^2 \theta^3 - \epsilon_0 \epsilon_\infty \epsilon_q \tau \theta^2 + \tau^2 |\mathbf{k}|^2 \theta - \tau |\mathbf{k}|^2 = 0.$$

In particular, for $\mathbf{k} = \pi(1, 2, -3)^T$, $\theta \approx 1.007289596494$, and for $\mathbf{k} = 2\pi(1, 2, -3)^T$, $\theta \approx 1.001812580410$. Here the exact solution (150) satisfies the PEC boundary conditions on the boundary of the domain Ω for the wave vectors as chosen in Table 1.

7.1.1. Computation of Energy Errors. The energy of the exact solution (150) as defined in Theorem 2.1 can be computed to be

$$(152) \qquad \mathcal{E}_D(t) = \frac{|\mathbf{k}|}{2\pi} e^{-\theta t} \sqrt{\frac{3}{2} \left(|\mathbf{k}|^2 + \theta^2 - \beta_D^2(\theta, |\mathbf{k}|) \right)}.$$

The values of the Courant number ν, and the wave vector $\mathbf{k}$ that are used in our numerical experiments are given in Table 1. We compute numerical errors in the discrete solution by computing relative energy error defined as

$$(153) \qquad \text{Error}_D(h) = \max_{0 \le n \le N} \left\{ \frac{\mathcal{R}_{h,D}^n}{\mathcal{E}_D(t^n)} \right\},$$

with $\mathcal{R}_{h,D}^n$ as defined in Theorem 4.2.

Table 1 gives the discrete energy error for the Yee scheme for the 3D Maxwell-Debye model for various cases. We test our schemes for different Courant numbers and different wave vectors $\mathbf{k}$. The largest time step used is $\Delta t = 0.02$, and this value is successively decreased by half to run four simulations. Figure 1 illustrates that the convergence errors are all second order. This is consistent with the conclusion in Theorem 4.2.
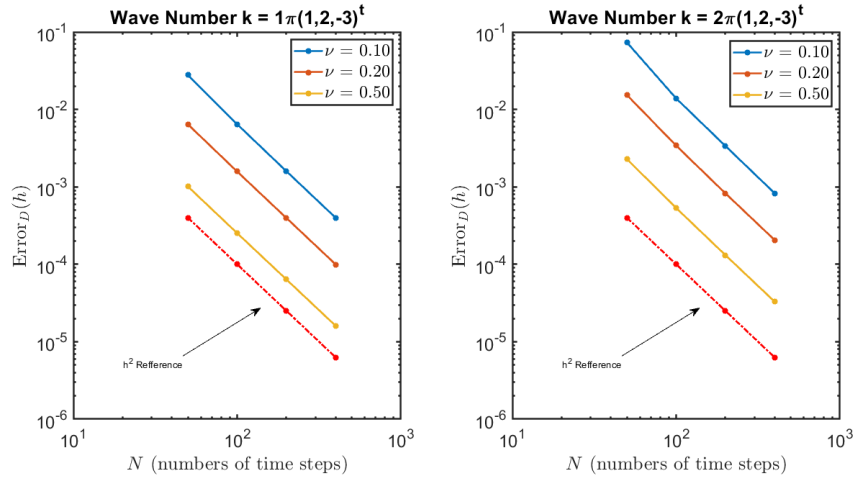
FIGURE 1. Discrete energy errors for the 3D Yee-FDTD Maxwell-Debye scheme with varying CFL number.

7.1.2. Convergence of Discrete Divergence. We show that the discrete divergence of both the electric flux density, $\mathbf{D}_h$, and magnetic flux density, $\mathbf{B}_h$, in the Yee scheme for the 3D Maxwell-Debye model is preserved. We compute the error in the discrete divergence as

$$(154a) \qquad \text{Err}(\text{div}_h D) = \max_{0 \le n \le N} \| \text{div}_h \mathbf{D}_h^n - \text{div}_h \mathbf{D}_h^0 \|_E,$$

$$(154b) \qquad \text{Err}(\text{div}_h B) = \max_{0 \le n \le N-1} \| \text{div}_h \mathbf{B}_h^{n+\frac{1}{2}} - \text{div}_h \mathbf{B}_h^{\frac{1}{2}} \|_H.$$

The errors (154) in the discrete divergence of solutions for the Maxwell-Debye model are given in Table 2. We see that the errors presented are all negligible compared to the discrete energy errors.

TABLE 1. Discrete energy errors for the Maxwell-Debye model.

Wave Vector $\mathbf{k} = \pi(1, 2, -3)^T$						
N	$\nu = 0.1$		$\nu = 0.2$		$\nu = 0.5$	
	Error$_D$	Rate	Error$_D$	Rate	Error$_D$	Rate
50	2.789×10^{-2}	-	6.422×10^{-3}	-	1.012×10^{-3}	-
100	6.432×10^{-3}	-2.117	1.576×10^{-3}	-2.027	2.524×10^{-4}	-2.003
200	1.588×10^{-3}	-2.018	3.953×10^{-4}	-1.996	6.357×10^{-5}	-1.989
400	3.971×10^{-4}	-2.000	9.924×10^{-5}	-1.994	1.598×10^{-5}	-1.992
Wave Vector $\mathbf{k} = 2\pi(1, 2, -3)^T$						
N	$\nu = 0.1$		$\nu = 0.2$		$\nu = 0.5$	
	Error$_D$	Rate	Error$_D$	Rate	Error$_D$	Rate
50	7.347×10^{-2}	-	1.540×10^{-2}	-	2.285×10^{-3}	-
100	1.387×10^{-2}	-2.405	3.405×10^{-3}	-2.177	5.337×10^{-4}	-2.098
200	3.367×10^{-3}	-2.043	8.238×10^{-4}	-2.047	1.312×10^{-4}	-2.024
400	8.240×10^{-4}	-2.031	2.049×10^{-4}	-2.007	3.279×10^{-5}	-2.001

TABLE 2. Discrete divergence errors for the Maxwell-Debye model.

Wave Vector $\mathbf{k} = \pi(1, 2, -3)^T$						
N	$\nu = 0.1$		$\nu = 0.2$		$\nu = 0.5$	
	Err(div$_h D$)	Err(div$_h B$)	Err(div$_h D$)	Err(div$_h B$)	Err(div$_h D$)	Err(div$_h B$)
50	5.02×10^{-13}	5.84×10^{-14}	1.33×10^{-12}	1.22×10^{-13}	3.24×10^{-12}	2.89×10^{-13}
100	2.05×10^{-12}	1.71×10^{-13}	3.56×10^{-12}	3.41×10^{-13}	9.46×10^{-12}	8.25×10^{-13}
200	4.70×10^{-12}	4.71×10^{-13}	1.08×10^{-11}	9.38×10^{-13}	2.70×10^{-11}	2.35×10^{-12}
400	1.51×10^{-11}	1.33×10^{-12}	3.08×10^{-11}	2.66×10^{-12}	7.75×10^{-11}	6.66×10^{-12}
Wave Vector $\mathbf{k} = 2\pi(1, 2, -3)^T$						
N	$\nu = 0.1$		$\nu = 0.2$		$\nu = 0.5$	
	Err(div$_h D$)	Err(div$_h B$)	Err(div$_h D$)	Err(div$_h B$)	Err(div$_h D$)	Err(div$_h B$)
50	5.88×10^{-12}	4.76×10^{-13}	1.00×10^{-11}	5.35×10^{-13}	2.66×10^{-11}	1.19×10^{-12}
100	1.21×10^{-11}	7.16×10^{-13}	3.00×10^{-11}	1.39×10^{-12}	7.53×10^{-11}	3.33×10^{-12}
200	4.33×10^{-11}	1.95×10^{-12}	7.90×10^{-11}	3.80×10^{-12}	2.13×10^{-10}	9.40×10^{-12}
400	1.19×10^{-10}	5.38×10^{-12}	2.45×10^{-10}	1.07×10^{-11}	6.15×10^{-10}	2.67×10^{-11}

7.1.3. Example of Yee Scheme for the Maxwell-Debye Model with the Non-uniform Mesh. For non-uniform meshes, we use the same parameters as the linear model for the Yee scheme for the 3D Maxwell-Debye system. Here we start using the following mesh parameters

(155) $$\Delta t = 0.02, \ \Delta x = 0.2, \ \Delta y = 0.1, \ \Delta z = 0.25,$$

and these values are successively decreased by half to run four simulations. The stability condition based on these parameters satisfies equation (54). The discrete energy error for the Maxwell-Debye model is given in Table 3 and Figure 2. We let λ_h represent the scaling of the number of intervals in the mesh. Figure 2 illustrates

that the convergence errors for the non-uniform mesh are of second order, which agrees with the conclusion in Theorem 4.2.

TABLE 3. Discrete energy errors for the Maxwell-Debye model with non-uniform meshes.

Δt	Δx	Δy	Δz	$\mathbf{k} = \pi(1,2,-3)^T$		$\mathbf{k} = 2\pi(1,2,-3)^T$	
				Error	**Rate**	**Error**	**Rate**
0.02	0.2	0.1	0.25	5.274×10^{-2}	-	1.872×10^{-1}	-
0.01	0.1	0.05	0.125	1.143×10^{-2}	-2.21	4.033×10^{-2}	-2.22
0.005	0.05	0.025	0.0625	2.782×10^{-3}	-2.04	9.868×10^{-3}	-2.03
0.0025	0.025	0.0125	0.03125	6.932×10^{-4}	-2.01	2.380×10^{-3}	-2.05
0.00125	0.0125	0.00625	0.015625	1.734×10^{-4}	-2.00	5.891×10^{-4}	-2.01
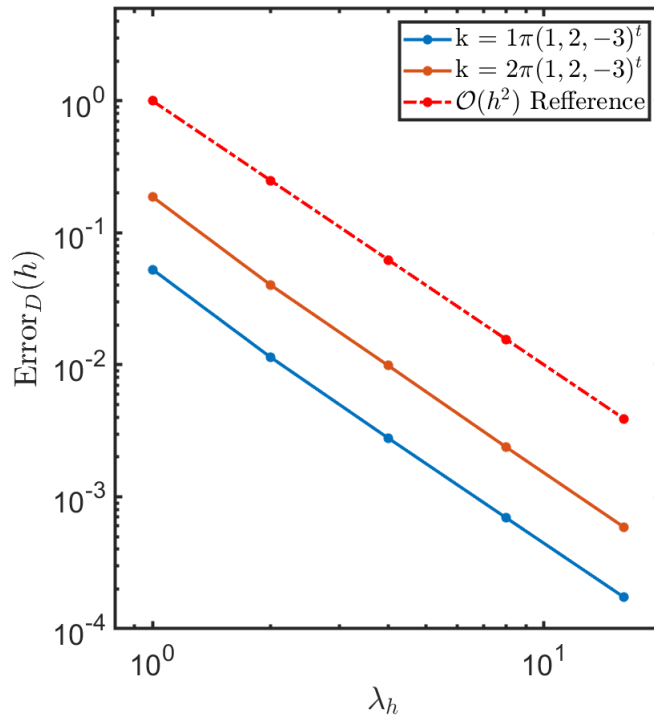
FIGURE 2. Discrete energy errors for the Maxwell-Debye model with non-uniform meshes where λ_h represents a multiple of mesh sizes.

Moreover, the discrete divergence of both electric flux density for the Maxwell-Debye model are given in Table 4 which also supports our theoretical result in (4.29).

7.2. Yee Scheme for the Maxwell-Lorentz Model. In this section, we test the proposed Yee scheme for the Maxwell-Lorentz system (86). The experiment is performed by using a uniform mesh on the domain $\Omega = [0,1] \times [0,1] \times [0,1]$ with

TABLE 4. Discrete divergence errors for the Maxwell-Debye model with non-uniform meshes.

Δt	Δx	Δy	Δz	$\mathbf{k} = \pi(1, 2, -3)^T$		$\mathbf{k} = 2\pi(1, 2, -3)^T$	
				$\mathbf{Err(div}_h D)$	$\mathbf{Err(div}_h B)$	$\mathbf{Err(div}_h D)$	$\mathbf{Err(div}_h B)$
0.02	0.2	0.1	0.25	5.69×10^{-13}	9.71×10^{-14}	1.37×10^{-11}	6.34×10^{-13}
0.01	0.1	0.05	0.125	3.13×10^{-12}	2.12×10^{-13}	2.10×10^{-11}	1.07×10^{-12}
0.005	0.05	0.025	0.0625	7.45×10^{-12}	6.48×10^{-13}	5.69×10^{-11}	2.67×10^{-12}
0.0025	0.025	0.0125	0.03125	2.25×10^{-11}	1.83×10^{-12}	1.82×10^{-10}	7.43×10^{-12}
0.00125	0.0125	0.00625	0.015625	6.32×10^{-11}	5.12×10^{-12}	4.87×10^{-10}	2.08×10^{-11}

the PEC boundary conditions (28). The parameters in this section are chosen by $\mu_0 = 1, \epsilon_0 = 1, \epsilon_\infty = 1, \omega_0 = 1, \tau = 0.4, \epsilon_q = 2$, and $T = 1$.

The analytic solutions of the 3D Maxwell-Lorentz system (15) are

$$(156a) \qquad H_x(x, y, z; t) = \frac{|\mathbf{k}|^2}{\pi} e^{-\theta t} \sin(k_x x) \cos(k_y y) \cos(k_z z),$$

$$(156b) \qquad H_y(x, y, z; t) = \frac{|\mathbf{k}|^2}{\pi} e^{-\theta t} \cos(k_x x) \sin(k_y y) \cos(k_z z),$$

$$(156c) \qquad H_z(x, y, z; t) = \frac{|\mathbf{k}|^2}{\pi} e^{-\theta t} \cos(k_x x) \cos(k_y y) \sin(k_z z),$$

$$(156d) \qquad E_x(x, y, z; t) = -\frac{\theta}{\pi}(k_y - k_z) e^{-\theta t} \cos(k_x x) \sin(k_y y) \sin(k_z z),$$

$$(156e) \qquad E_y(x, y, z; t) = -\frac{\theta}{\pi}(k_z - k_x) e^{-\theta t} \sin(k_x x) \cos(k_y y) \sin(k_z z),$$

$$(156f) \qquad E_z(x, y, z; t) = -\frac{\theta}{\pi}(k_x - k_y) e^{-\theta t} \sin(k_x x) \sin(k_y y) \cos(k_z z),$$

$$(156g) \qquad P_x(x, y, z; t) = -\frac{\alpha_L(\theta, |\mathbf{k}|)}{\pi}(k_y - k_z) e^{-\theta t} \cos(k_x x) \sin(k_y y) \sin(k_z z),$$

$$(156h) \qquad P_y(x, y, z; t) = -\frac{\alpha_L(\theta, |\mathbf{k}|)}{\pi}(k_z - k_x) e^{-\theta t} \sin(k_x x) \cos(k_y y) \sin(k_z z),$$

$$(156i) \qquad P_z(x, y, z; t) = -\frac{\alpha_L(\theta, |\mathbf{k}|)}{\pi}(k_x - k_y) e^{-\theta t} \sin(k_x x) \sin(k_y y) \cos(k_z z),$$

$$(156j) \qquad J_x(x, y, z; t) = -\frac{\beta_L(\theta, |\mathbf{k}|)}{\pi}(k_y - k_z) e^{-\theta t} \cos(k_x x) \sin(k_y y) \sin(k_z z),$$

$$(156k) \qquad J_y(x, y, z; t) = -\frac{\beta_L(\theta, |\mathbf{k}|)}{\pi}(k_z - k_x) e^{-\theta t} \sin(k_x x) \cos(k_y y) \sin(k_z z),$$

$$(156l) \qquad J_z(x, y, z; t) = -\frac{\beta_L(\theta, |\mathbf{k}|)}{\pi}(k_x - k_y) e^{-\theta t} \sin(k_x x) \sin(k_y y) \cos(k_z z),$$

where the function $\alpha_L(\theta, |\mathbf{k}|) := \left(\epsilon_0\epsilon_\infty \theta^3 - \frac{\epsilon_0\epsilon_\infty}{\tau}\theta^2 + (\epsilon_0\omega_p{}^2 + |\mathbf{k}|^2)\theta - \frac{|\mathbf{k}|^2}{\tau} \right)/\omega_0^2$ and $\beta_L(\theta, |\mathbf{k}|) := \epsilon_0\epsilon_\infty\theta^2 + |\mathbf{k}|^2$, and θ is a real number. The relationship between the wave number $|\mathbf{k}|^2$ and the parameter θ can be expressed as follows

$$(157) \qquad \epsilon_0\epsilon_\infty\theta^4 - \frac{\epsilon_0\epsilon_\infty}{\tau}\theta^3 + \left(\epsilon_0\epsilon_\infty\omega_0^2 + |\mathbf{k}|^2 + \epsilon_0\omega_p{}^2\right)\theta^2 - \frac{|\mathbf{k}|^2}{\tau}\theta + \omega_0^2|\mathbf{k}|^2 = 0.$$

In particular, for $\mathbf{k} = \pi(1, 2, -3)^T$ with the corresponding parameter $\theta \approx 0.5012108$, and for $\mathbf{k} = 2\pi(1, 2, -3)^T$ with the corresponding parameter $\theta \approx 0.500301839402$. Here the exact solution (156) satisfies the PEC boundary conditions on the boundary of the domain Ω provided that the wave vector is chosen as above.

7.2.1. Computation of Energy Errors. The exact energy, defined in Theorem 2.2, for the solutions (156) can be calculated to be

$$(158) \qquad \mathcal{E}_L(t) = \frac{|\mathbf{k}|}{2\pi} e^{-\theta t} \sqrt{\frac{3}{2} \left[|\mathbf{k}|^2 + \theta^2 + \beta_L^2 \left(1 + \frac{1}{\theta^2} \right) \right]}.$$

We compute numerical errors for the discrete solution by defining the numerical error as

$$(159) \qquad \text{Error}_L(h) = \max_{0 \leq n \leq N} \left\{ \frac{\mathcal{R}_{h,L}^n}{\mathcal{E}_L(t^n)} \right\}$$

where $\mathcal{R}_{h,L}^n$ is defined in Theorem 111.

The results of the discrete energy error for the 3D Maxwell-Lorentz model are given in Figure 3 and Table 5. Similarly to the numerical simulation in Section 7.1 with different values of wave vectors $\mathbf{k}$, we take the largest time step sizes to be $\Delta t = 0.02$, and these values are successively decreased by half to run four simulations. In Table 5, it is obvious that the discrete energy errors decay for several values of the Courant number ν and the wave vector $\mathbf{k}$. Figure 3 and Table 5 also confirm the energy decay property of the Yee scheme by showing that convergence rates are all of second order, which is in agreement with the conclusion in Theorem 5.2. Moreover, if the Courant number is increasing, then it improves the error of the scheme but the order of accuracy remains the same.
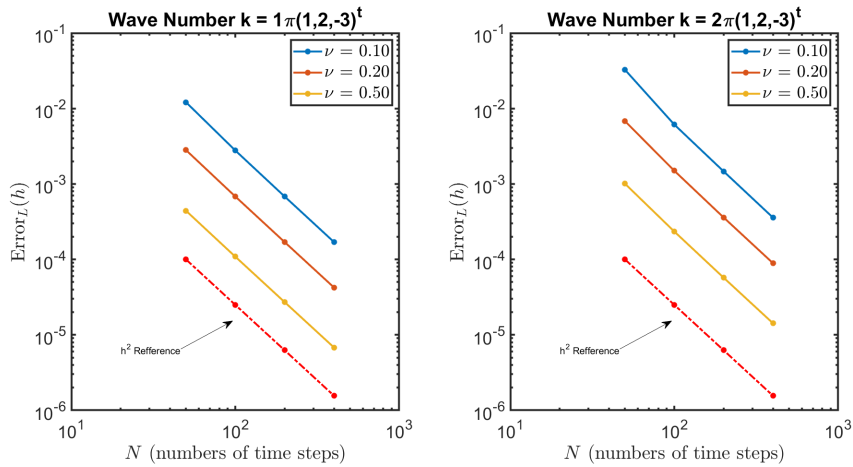
FIGURE 3. A comparison of the errors for the Yee scheme in the Lorentz medium with varying CFL conditions.

7.2.2. Convergence of Discrete Divergence. We determine the numerical discrete divergence properties for both the electric $\mathbf{D}_h$ and the magnetic $\mathbf{B}_h$ flux densities by calculating the formula defined in (154). Table 6 presents the discrete divergence errors of solutions to the Yee scheme for the 3D Maxwell-Lorentz model. All errors are relatively small.

7.3. Yee Scheme for the Maxwell-Cold Plasma Model. In this section, we test the proposed Yee scheme for the Maxwell-Cold Plasma system (123). The experiment is performed by using a uniform mesh on the domain $\Omega = [0,1] \times [0,1] \times [0,1]$ with the PEC boundary conditions (28). The parameters in this section are

TABLE 5. Discrete energy errors for the Maxwell-Lorentz model.

Wave Vector $\mathbf{k} = \pi(1, 2, -3)^T$						
N	$\nu = 0.1$		$\nu = 0.2$		$\nu = 0.5$	
	Error	**Rate**	**Error**	**Rate**	**Error**	**Rate**
50	1.213×10^{-2}	-	2.814×10^{-3}	-	4.422×10^{-4}	-
100	2.780×10^{-3}	-2.125	6.823×10^{-4}	-2.044	1.088×10^{-4}	-2.023
200	6.821×10^{-4}	-2.027	1.700×10^{-4}	-2.007	2.719×10^{-5}	-2.001
400	1.701×10^{-4}	-2.004	4.248×10^{-5}	-1.999	6.808×10^{-6}	-1.998
Wave Vector $\mathbf{k} = 2\pi(1, 2, -3)^T$						
N	$\nu = 0.1$		$\nu = 0.2$		$\nu = 0.5$	
	Error	**Rate**	**Error**	**Rate**	**Error**	**Rate**
50	3.265×10^{-2}	-	6.812×10^{-3}	-	1.009×10^{-3}	-
100	6.128×10^{-3}	-2.414	1.497×10^{-3}	-2.186	2.343×10^{-4}	-2.106
200	1.468×10^{-3}	-2.062	3.597×10^{-4}	-2.057	5.727×10^{-5}	-2.033
400	3.583×10^{-4}	-2.035	8.914×10^{-5}	-2.013	1.425×10^{-5}	-2.007

TABLE 6. Discrete divergence errors for the Maxwell-Lorentz model.

Wave Vector $\mathbf{k} = \pi(1, 2, -3)^T$						
N	$\nu = 0.1$		$\nu = 0.2$		$\nu = 0.5$	
	Err($\mathrm{div}_h D$)	Err($\mathrm{div}_h B$)	Err($\mathrm{div}_h D$)	Err($\mathrm{div}_h B$)	Err($\mathrm{div}_h D$)	Err($\mathrm{div}_h B$)
50	7.43×10^{-13}	7.38×10^{-14}	2.05×10^{-12}	1.52×10^{-13}	6.07×10^{-12}	3.52×10^{-13}
100	3.10×10^{-12}	1.95×10^{-13}	6.87×10^{-12}	4.01×10^{-13}	1.62×10^{-11}	1.00×10^{-12}
200	8.76×10^{-12}	5.70×10^{-13}	1.87×10^{-11}	1.13×10^{-12}	4.67×10^{-11}	2.83×10^{-12}
400	2.52×10^{-11}	1.61×10^{-12}	5.22×10^{-11}	3.22×10^{-12}	1.33×10^{-10}	8.03×10^{-12}
Wave Vector $\mathbf{k} = 2\pi(1, 2, -3)^T$						
N	$\nu = 0.1$		$\nu = 0.2$		$\nu = 0.5$	
	Err($\mathrm{div}_h D$)	Err($\mathrm{div}_h B$)	Err($\mathrm{div}_h D$)	Err($\mathrm{div}_h B$)	Err($\mathrm{div}_h D$)	Err($\mathrm{div}_h B$)
50	9.40×10^{-12}	4.67×10^{-13}	1.40×10^{-11}	6.64×10^{-13}	4.65×10^{-11}	1.44×10^{-12}
100	3.26×10^{-11}	1.00×10^{-12}	5.61×10^{-11}	1.70×10^{-12}	1.27×10^{-10}	4.04×10^{-12}
200	5.70×10^{-11}	2.32×10^{-12}	1.40×10^{-10}	4.56×10^{-12}	3.75×10^{-10}	1.13×10^{-11}
400	1.92×10^{-10}	6.48×10^{-12}	4.02×10^{-10}	1.29×10^{-11}	1.05×10^{-9}	3.21×10^{-11}

chosen similarly to the case of Maxwell-Lorentz model i.e. $\mu_0 = 1, \epsilon_0 = 1, \epsilon_\infty = 1, \omega_0 = 1, \nu_c = 2.5, \epsilon_q = 2$, and $T = 1$. The following analytic solutions of the 3D

Maxwell-Cold Plasma system (22) are

$$H_x(x, y, z; t) = \frac{|\mathbf{k}|^2}{\pi} e^{-\theta t} \sin(k_x x) \cos(k_y y) \cos(k_z z), \tag{160a}$$

$$H_y(x, y, z; t) = \frac{|\mathbf{k}|^2}{\pi} e^{-\theta t} \cos(k_x x) \sin(k_y y) \cos(k_z z), \tag{160b}$$

$$H_z(x, y, z; t) = \frac{|\mathbf{k}|^2}{\pi} e^{-\theta t} \cos(k_x x) \cos(k_y y) \sin(k_z z), \tag{160c}$$

$$E_x(x, y, z; t) = -\frac{\theta}{\pi}(k_y - k_z) e^{-\theta t} \cos(k_x x) \sin(k_y y) \sin(k_z z), \tag{160d}$$

$$E_y(x, y, z; t) = -\frac{\theta}{\pi}(k_z - k_x) e^{-\theta t} \sin(k_x x) \cos(k_y y) \sin(k_z z), \tag{160e}$$

$$E_z(x, y, z; t) = -\frac{\theta}{\pi}(k_x - k_y) e^{-\theta t} \sin(k_x x) \sin(k_y y) \cos(k_z z), \tag{160f}$$

$$J_x(x, y, z; t) = -\frac{\beta_C(\theta, |\mathbf{k}|)}{\pi}(k_y - k_z) e^{-\theta t} \cos(k_x x) \sin(k_y y) \sin(k_z z), \tag{160g}$$

$$J_y(x, y, z; t) = -\frac{\beta_C(\theta, |\mathbf{k}|)}{\pi}(k_z - k_x) e^{-\theta t} \sin(k_x x) \cos(k_y y) \sin(k_z z), \tag{160h}$$

$$J_z(x, y, z; t) = -\frac{\beta_C(\theta, |\mathbf{k}|)}{\pi}(k_x - k_y) e^{-\theta t} \sin(k_x x) \sin(k_y y) \cos(k_z z), \tag{160i}$$

where the function $\beta_C(\theta, |\mathbf{k}|) := \epsilon_0 \theta^2 + |\mathbf{k}|^2$, and θ is a real number. The relationship between the wave number $|\mathbf{k}|$ and the parameter θ can be expressed as follows

$$\epsilon_0 \theta^3 - \epsilon_0 \nu_c \theta^2 + \left(\epsilon_0 \omega_p^2 + |\mathbf{k}|^2\right) \theta - |\mathbf{k}|^2 \nu_c = 0. \tag{161}$$

In particular, for $\mathbf{k} = \pi(1, 2, -3)^T$ with the corresponding parameter $\theta \approx 2.4827988$, and for $\mathbf{k} = 2\pi(1, 2, -3)^T$ with the corresponding parameter $\theta \approx 2.495535120632$. Here the exact solution (160) satisfies the PEC boundary conditions on the boundary of the domain Ω provided that the wave vector is chosen as above.

7.3.1. Computation of Energy Errors. The exact energy (160) defined in Theorem 2.3 can be calculated to be

$$\mathcal{E}_C(t) = \frac{|\mathbf{k}|}{2\pi} e^{-\theta t} \sqrt{\frac{3}{2} [|\mathbf{k}|^2 + \theta^2 + \beta_C^2]}. \tag{162}$$

We compute numerical errors for the discrete solution by defining the numerical error as

$$\text{Error}_C(h) = \max_{0 \leq n \leq N} \left\{ \frac{\mathcal{R}_{h,C}^n}{\mathcal{E}_C(t^n)} \right\}, \tag{163}$$

where $\mathcal{R}_{h,C}^n$ is defined in Theorem 6.2.

The results of the discrete energy error for the Yee scheme for the 3D Maxwell-Cold Plasma model are given in Figure 4 and Table 7. Similarly to the numerical simulation in Section 7.1 we take the largest time step sizes to be $\Delta t = 0.02$, and these values are successively decreased by half to run four simulations. In Table 7, it is obvious that the discrete energy errors decay for several values of the Courant number ν and the wave vector $\mathbf{k}$. Figure 4 and Table 7 also confirm the energy decay property of the Yee scheme by showing that convergence errors of the energy-decayed finite-difference time-domain scheme for different space and time sizes are all of second order, which is in agreement with the conclusion in Theorem 6.2. Moreover, if the Courant number is increasing, then it improves the error of the scheme but the order of accuracy remains the same, which exhibits the second order of the Yee scheme with respect to a $\mathcal{O}(h^2)$ reference.
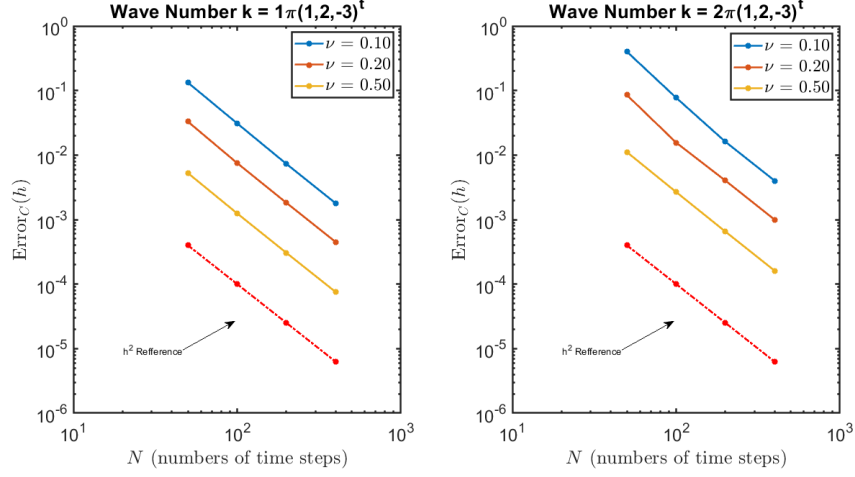
FIGURE 4. A comparison of the discrete energy errors for the Yee scheme in a Cold Plasma medium with varying CFL conditions.

TABLE 7. Discrete energy errors for the Maxwell-Cold Plasma model.

N	$\nu = 0.1$		$\nu = 0.2$		$\nu = 0.5$	
	Error	**Rate**	**Error**	**Rate**	**Error**	**Rate**
50	1.329×10^{-1}	-	3.298×10^{-2}	-	5.260×10^{-3}	-
100	3.095×10^{-2}	-2.102	7.509×10^{-3}	-2.136	1.247×10^{-3}	-2.076
200	7.277×10^{-3}	-2.089	1.815×10^{-3}	-2.049	3.043×10^{-4}	-2.035
400	1.782×10^{-3}	-2.030	4.476×10^{-4}	-2.020	7.517×10^{-5}	-2.017

Wave Vector $\mathbf{k} = \pi(1, 2, -3)^T$ appears as the title row above.

N	$\nu = 0.1$		$\nu = 0.2$		$\nu = 0.5$	
	Error	**Rate**	**Error**	**Rate**	**Error**	**Rate**
50	4.004×10^{-1}	-	8.515×10^{-2}	-	1.113×10^{-2}	-
100	7.727×10^{-2}	-2.373	1.559×10^{-2}	-2.450	2.671×10^{-3}	-2.059
200	1.602×10^{-2}	-2.270	4.007×10^{-3}	-1.960	6.497×10^{-4}	-2.039
400	3.985×10^{-3}	-2.001	9.922×10^{-4}	-2.014	1.605×10^{-4}	-2.017

The second part has title row: Wave Vector $\mathbf{k} = 2\pi(1, 2, -3)^T$.

7.3.2. Convergence of Discrete Divergence. We determine the numerical discrete divergence properties for the magnetic $\mathbf{B}_h$ flux densities by calculating the formula defined in (154). Table 8 presents the discrete divergence errors of solutions to the Yee scheme for the 3D Maxwell-Cold Plasma model. All errors are relatively small.

7.4. Comparison of Discrete Divergence across all Models. In this section, we compare the discrete divergence of the Maxwell's equations in all linearly dispersive media over the long time computation. Here we focus on the discrete divergence of the magnetic flux density and set $T = 200$ and $\Delta t = 0.02$. For each the CFL number ν and the wave vector $\mathbf{k}$, we compute the norm of the discrete divergence of the magnetic field, $\|\text{div}_h B^{n+\frac{1}{2}}\|_H$, plotted against the time level n.

TABLE 8. Discrete divergence errors for the Maxwell-Cold Plasma model where $\mathbf{k}_1 = \pi(1, 2, -3)^T$ and $\mathbf{k}_2 = 2\pi(1, 2, -3)^T$.

	$\mathrm{Err}(\mathrm{div}_h B)$					
N	$\nu = 0.1$		$\nu = 0.2$		$\nu = 0.5$	
	$\mathbf{k}_1$	$\mathbf{k}_2$	$\mathbf{k}_1$	$\mathbf{k}_2$	$\mathbf{k}_1$	$\mathbf{k}_2$
50	$5.87{\times}10^{-14}$	$3.47{\times}10^{-13}$	$8.34{\times}10^{-14}$	$3.99{\times}10^{-13}$	$1.95{\times}10^{-13}$	$7.98{\times}10^{-13}$
100	$1.10{\times}10^{-13}$	$5.47{\times}10^{-13}$	$2.30{\times}10^{-13}$	$9.29{\times}10^{-13}$	$5.60{\times}10^{-13}$	$2.24{\times}10^{-12}$
200	$3.12{\times}10^{-13}$	$1.29{\times}10^{-12}$	$6.34{\times}10^{-13}$	$2.55{\times}10^{-12}$	$1.60{\times}10^{-12}$	$6.37{\times}10^{-12}$
400	$9.04{\times}10^{-13}$	$3.58{\times}10^{-12}$	$1.81{\times}10^{-12}$	$7.21{\times}10^{-12}$	$4.55{\times}10^{-12}$	$1.81{\times}10^{-11}$

Figure 5 shows that the discrete divergence is proportional to the wave number squared. Moreover, when the CFL number increases, the discrete divergence grows rapidly, but will be controlled under 2×10^{-12} for both cases of wave vectors. However, the discrete divergence for the Debye model grows linearly when the CFL number is small, while the others grow slowly and are controlled. This means that the convergence of discrete divergence for all models confirms our theoretical analysis when the CFL number is large enough, while the divergence is overestimated in our theoretical analysis when the CFL number is small, at least for long time computation.
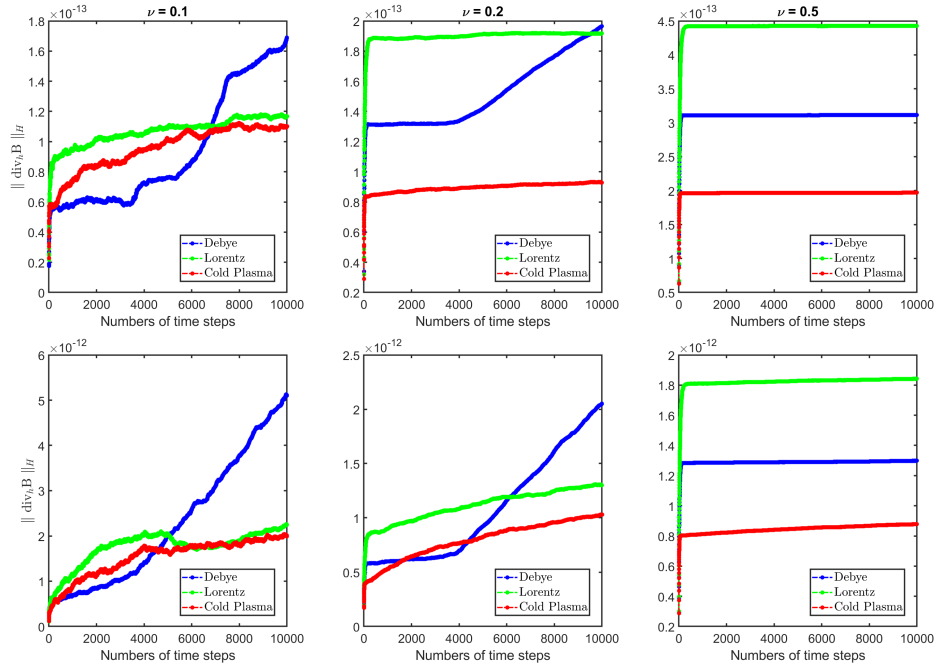

FIGURE 5. A comparison of the discrete divergence for the Yee scheme in all medium with varying CFL conditions. First row: the wave vector $\mathbf{k} = \pi(1, 2, -3)^T$; Second row: the wave vector $\mathbf{k} = 2\pi(1, 2, -3)^T$. First column: $\nu = 0.1$; Second column: $\nu = 0.2$; Third column: $\nu = 0.5$.

8.   Conclusions

In this paper, we have constructed and analyzed finite difference time domain (FDTD) methods coupled to Debye, Lorentz and cold isotropic plasma linear dispersive media based on the Yee scheme for the time-dependent Maxwell's equations in three-dimensional space. We began with the model formulation, followed by construction of the weak formulations of Maxwell's equations in the linear dispersive media and energy estimates for the continuous models. Based on the energy method, we have presented accuracy, stability and convergence analysis of the Yee scheme for each of the three linear dispersive models considered in this paper. It was shown that the Yee scheme are conditionally stable under the same condition as that of the classical Yee scheme for 3D Maxwell's equations in a non-dispersive dielectric. Our convergence analysis indicated that the fully discrete schemes are of second order accuracy in both time and space. In addition, the discrete divergence of the scheme is also studied and it is proved that the Yee scheme satisfies the discrete divergence-free conditions in the numerical grid, an important aspect of any numerical approximation for Maxwell's equations. Finally, numerical experiments are presented that demonstrate our theoretical results. We construct exact solutions for each of the three linear dispersive media with the PEC boundary conditions and confirm the energy decay properties, second order accuracy and discrete analogues of the divergence free nature of the magnetic flux density.

Acknowledgments

References

[1] Aziz, M. M. Sub-nanosecond electromagnetic-micromagnetic dynamic simulations using the finite-difference time-domain method. Progress In Electromagnetics Research, 15 (2009), 1–29.

[2] Banks, H. T., Buksas, M. W., and Lin, T. Electromagnetic Material Interrogation Using Conductive Interfaces and Acoustic Wavefronts, vol. 21. Society for Industrial Mathematics (SIAM), 2000.

[3] Bécache, E., and Joly, P. On the analysis of Bérenger's perfectly matched layers for Maxwell's equations. Mathematical Modelling and Numerical Analysis, 36, 1 (2002), 87–119.

[4] Bidégaray-Fesquet, B. Stability of FD–TD schemes for Maxwell–Debye and Maxwell–Lorentz equations. SIAM Journal on Numerical Analysis, 46, 5 (2008), 2551–2566.

[5] Bokil, V. A., Cheng, Y., Jiang, Y., Li, F., and Sakkaplangkul, P. High spatial order energy stable FDTD methods for Maxwell's equations in nonlinear optical media in one dimension. Journal of Scientific Computing, 77 (2018), 330–371.

[6] Bokil, V. A., and Gibson, N. L. Analysis of Spatial High-Order Finite Difference Methods for Maxwell's Equations in Dispersive Media. IMA Journal of Numerical Analysis 32, 3 (2012), 926–956.

[7] Bokil, V. A., and Gibson, N. L. Convergence analysis of Yee schemes for Maxwell's equations in Debye and Lorentz dispersive media. International Journal of Numerical Analysis and Modeling, 11, 4 (2014), 657–687.

[8] Bokil, V. A., Keefer, O., and Leung, A.-Y. Operator splitting methods for Maxwell's equations in dispersive media with orientational polarization. Journal of Computational and Applied Mathematics, 263 (2014), 160–188.

[9] Bokil, V. A., and Sakkaplangkul, P. Construction and analysis of weighted sequential splitting FDTD methods for the 3D Maxwell's equations. International Journal of Numerical Analysis and Modeling, 15, 6 (2018), 747–784.

[10] Causley, M. F., Petropoulos, P. G., and Jiang, S. Incorporating the Havriliak–Negami dielectric model in the FD-TD method. Journal of Computational Physics, 230, 10 (2011), 3884–3899.

[11] Chen, W., Li, X., and Liang, D. Energy-conserved splitting FDTD methods for Maxwell's equations. Numerische Mathematik, 108, 3 (2008), 445–485.

[12] Chen, W., Li, X., and Liang, D. Energy-conserved splitting finite-difference time-domain methods for Maxwell's equations in three dimensions. SIAM Journal on Numerical Analysis, 48, 4 (2010), 1530–1554.

[13] Cole, K. S., and Cole, R. H. Dispersion and absorption in dielectrics i. alternating current characteristics. Journal of Chemical Physics, 9 (1941), 341–351.

[14] Cummer, S. A. An analysis of new and existing FDTD methods for isotropic cold plasma and a method for improving their accuracy. IEEE Transactions on Antennas and Propagation, 45, 3 (1997), 392–400.

[15] Da Silva, F., Pinto, M. C., Després, B., and Heuraux, S. Stable explicit coupling of the yee scheme with a linear current model in fluctuating magnetized plasmas. Journal of Computational Physics, 295 (2015), 24–45.

[16] Debye, P. J. W. Polar Molecules. Dover New York, 1929.

[17] Gansen, A., El Hachemi, M., Belouettar, S., Hassan, O., and Morgan, K. A 3D Unstructured Mesh FDTD Scheme for EM Modelling. Archives of Computational Methods in Engineering, (2020), 1–33.

[18] Gao, L., and Zhang, B. Stability and superconvergence analysis of the FDTD scheme for the 2D Maxwell equations in a lossy medium. Science China Mathematics, 54, 12 (2011), 2693–2712.

[19] Gedney, S. D. Introduction to the finite-difference time-domain (fdtd) method for electromagnetics. Synthesis Lectures on Computational Electromagnetics, 6, 1 (2011), 1–250.

[20] Gilles, L., Hagness, S., and Vázquez, L. Comparison between staggered and unstaggered finite-difference time-domain grids for few-cycle temporal optical soliton propagation. Journal of Computational Physics, 161, 2 (2000), 379–400.

[21] Hao, Y., and Mittra, R. FDTD modeling of metamaterials: Theory and applications. Artech house, 2008.

[22] Huang, Y., Li, J., and Yang, W. Interior penalty DG methods for Maxwell's equations in dispersive media. Journal of Computational Physics, 230, 12 (2011), 4559–4570.

[23] Jackson, J. D. Classical electrodynamics. John Wiley & Sons, 2007.

[24] James, R. Wait, electromagnetic waves in stratified media. Oxford: Pergmon Press, 2 (1962), 17.

[25] Jiang, Y., Sakkaplangkul, P., Bokil, V. A., Cheng, Y., and Li, F. Dispersion analysis of finite difference and discontinuous Galerkin schemes for Maxwell's equations in linear Lorentz media. Journal of Computational Physics, 394 (2019), 100–135.

[26] Joseph, R. M., Hagness, S. C., and Taflove, A. Direct time integration of Maxwell's equations in linear dispersive media with absorption for scattering and propagation of femtosecond electromagnetic pulses. Optics Letters, 16, 18 (1991), 1412–1414.

[27] Kashiwa, T., and Fukai, I. A treatment by the FD-TD method of the dispersive characteristics associated with electronic polarization. Microwave and Optical Technology Letters, 3, 6 (1990), 203–205.

[28] Kashiwa, T., Yoshida, N., and Fukai, I. A treatment by the finite-difference time domain method of the dispersive characteristics associated with orientational polarization. IEEE Trans. IEICE, 73, 8 (1990), 1326–1328.

[29] Lanteri, S., and Scheid, C. Convergence of a discontinuous Galerkin scheme for the mixed time-domain Maxwell's equations in dispersive media. IMA Journal of Numerical Analysis, 33, 2 (2013), 432–459.

[30] Li, J. Numerical convergence and physical fidelity analysis for Maxwell's equations in metamaterials. Computer Methods in Applied Mechanics and Engineering, 198, 37 (2009), 3161–3172.

[31] Li, J. Unified analysis of leap-frog methods for solving time-domain Maxwell's equations in dispersive media. Journal of Scientific Computing, 47, 1 (2011), 1–26.

[32] Li, J., and Huang, Y. Time-domain finite element methods for Maxwell's equations in metamaterials, vol. 43. Springer, 2013.

[33] Li, J., Huang, Y., and Lin, Y. Developing finite element methods for Maxwell's equations in a Cole-Cole dispersive medium. SIAM Journal on Scientific Computing, 33, 6 (2011), 3153–3174.

[34] Li, J., and Shields, S. Superconvergence analysis of yee scheme for metamaterial maxwells equations on non-uniform rectangular meshes. Numerische Mathematik, 134, 4 (2016), 741–781.

[35] Li, W., and Liang, D. The energy conservative splitting FDTD scheme and its energy iden-
tities for metamaterial electromagnetic lorentz system. Computer Physics Communications,
239 (2019), 94–111.

[36] Liang, D., and Yuan, Q. The spatial fourth-order energy-conserved S-FDTD scheme for
Maxwells equations. Journal of Computational Physics, 243 (2013), 344–364.

[37] Lu, T., Zhang, P., and Cai, W. Discontinuous Galerkin methods for dispersive and lossy
Maxwell's equations and PML boundary conditions. Journal of Computational Physics, 200,
2 (2004), 549–580.

[38] Luebbers, R., Hunsberger, F. P., Kunz, K. S., Standler, R. B., and Schneider, M.
A frequency-dependent finite-difference time-domain formulation for dispersive materials.
IEEE Transactions on Electromagnetic Compatibility, 32, 3 (1990), 222–227.

[39] Luebbers, R. J., Hunsberger, F., and Kunz, K. S. A frequency-dependent finite-difference
time-domain formulation for transient propagation in plasma. IEEE Transactions on Anten-
nas and Propagation, 39, 1 (1991), 29–34.

[40] Monk, P., and Süli, E. A convergence analysis of Yee's scheme on nonuniform grids. SIAM
Journal on Numerical Analysis, 31, 2 (1994), 393–412.

[41] Monk, P., and Suli, E. Error estimates for yee's method on non-uniform grids. IEEE Trans-
actions on Magnetics, 30, 5 (1994), 3200–3203.

[42] Oughstun, K. E., and Sherman, G. C. Uniform asymptotic description of electromagnetic
pulse propagation in a linear dispersive medium with absorption (the Lorentz medium).
Journal of the Optical Society of America A, 6, 9 (1989), 1394–1420.

[43] Petropoulos, P. G. Stability and phase error analysis of FDTD in dispersive dielectrics.
Antennas and Propagation, IEEE Transactions on, 42, 1 (1994), 62–69.

[44] Stix, T. Waves in Plasmas. American Institute of Physics, 1992.

[45] Sun, J., Collino, F., Monk, P., and Wang, L. An eddy-current and micromagnetism model
with applications to disk write heads. International Journal for Numerical Methods in En-
gineering, 60, 10 (2004), 1673–1698.

[46] Swanson, D. G. Plasma waves. Elsevier, 2012.

[47] Taflove, A., and Hagness, S. C. Computational electrodynamics: The Finite-Difference
Time-Domain method, 3rd ed. Artech House, Norwood, MA, 2005.

[48] Wang, B., Xie, Z., and Zhang, Z. Error analysis of a discontinuous Galerkin method for
Maxwell equations in dispersive media. Journal of Computational Physics, 229, 22 (2010),
8552–8563.

[49] Xie, J., Liang, D., and Zhang, Z. Energy-preserving local mesh-refined splitting FDTD
schemes for two dimensional Maxwell's equations. Journal of Computational Physics, 425
(2021), 109896.

[50] Yee, K. Numerical solution of initial boundary value problems involving Maxwell's equations
in isotropic media. Antennas and Propagation, IEEE Transactions on, 14, 3 (1966), 302–307.

[51] Young, J. A full finite difference time domain implementation for radio wave propagation in
a plasma. Radio Science, 29, 6 (1994), 1513–1522.

[52] Young, J. A higher order FDTD method for EM propagation in a collisionless cold plasma.
IEEE Antennas and Propagation Magazine, 44, 9 (1996), 1283–1289.

[53] Young, J. L., and Nelson, R. O. A Summary and Systematic Analysis of FDTD Algorithms
for Linearly Dispersive Media. IEEE Antennas and Propagation Magazine, 43 (2001), 61–77.

Department of Mathematics, Faculty of Science, King Mongkut's Institute of Technology Lad-
krabang, Ladkrabang, Bangkok 10520, Thailand.
  E-mail: `puttha.sa@kmitl.ac.th`

Department of Mathematics, Oregon State University, Corvallis, OR 97331 U.S.A.
  E-mail: `bokilv@math.oregonstate.edu`
  URL: `http://sites.science.oregonstate.edu/∼bokilv/`